Session 4

Case Studies

A MACROSCOPIC FINITE ELEMENT BASED COMPUTER MODEL FOR EVALUATING THE FIRE RESPONSE OF FRP-STRENGTHENED REINFORCED CONCRETE BEAMS

Ahmed, A.[a], Kodur, V.K.R.[b]

[a] Principal Structural Engineer, Directorate of Design & Consultancy, Pakistan
[b] Professor, Department of Civil and Environmental Engineering, Michigan State University, USA

INTRODUCTION

Fiber Reinforced Polymers (FRP) are widely used to strengthen and rehabilitate structural members mainly due to its high strength, light weight, durability, cost effectiveness and ease of application. In buildings, externally bonded FRP is effectively applied to increase the flexural capacity of existing reinforced concrete (RC) structures. When used in buildings, performance of FRP under fire exposure remains a major concern. However, there have been only limited experimental and numerical studies on fire resistance of FRP-strengthened RC beams. Thus, there is very little guidance available in codes and standards for the fire design of FRP-strengthened RC beams.

In recent years, limited fire tests have been conducted to study the fire performance of FRP-strengthened RC members and most of these were aimed at developing fire resistance ratings. However, the behavior of FRP-strengthened RC beams has not been studied under realistic fire, loading, restraint and bond conditions. In the case of numerical modeling, only thermal response has been studied under standard fire exposure, without giving any due consideration to overall structural response, effect of fire induced bond degradation and axial restraint force. Thus, the absences of reliable numerical models, and relatively high cost of fire tests are the two main reasons for lack of rational fire design provisions in codes and standards. To overcome this, a macroscopic finite element model has been developed for evaluating fire response of FRP-strengthened RC members. The proposed model accounts for high temperature properties for concrete, steel, FRP and insulation to capture the fire response of FRP-RC beams under realistic fire, loading and restraint scenarios. The, model also accounts for FRP-concrete substrate bond slippage in the analysis. A summary of the model features, together with its validation and case studies is presented in this paper.

1   COMPUTR PROGRAM

1.1   Calculation Procedure

A macroscopic finite element (FE) based computer model that utilizes moment-curvature relationships is developed to trace the response of FRP-strengthened RC beams under fire conditions (Ahmed 2010). In the analysis, the beam is idealized by dividing it into a number of segments along its length and the mid-section of each segment is assumed to represent the overall behavior of the segment. This mid-section is discretized into a number of elements as shown in Fig. 1.

In the analysis, the total fire exposure time is divided into number of time steps and at each time step, the response of the beam is traced through the following steps:
- Establishing temperatures due to fire exposure (standard and design fires).
- Conducting heat transfer analysis to determine temperature distribution in segmental cross-section.
- Calculating the slip (ε_{slip}) at the interface of FRP and concrete.
- Generating moment curvature $(M - \kappa)$ relationships for each beam segment and performing beam analysis to compute internal forces and deflections.

The various steps involved in the fire resistance analysis are illustrated in the flow chart (see Fig. 2). At each time step, thermal analysis is carried out to determine the temperature distribution within

the cross-section of each segment utilizing high temperature thermal properties of constitutive materials. The computed cross sectional temperatures form the input to strength analysis, wherein, time dependent $M-\kappa$ relationships are generated for each beam segment. For evaluating these $M-\kappa$ relations, various strain components in each element of concrete, steel and FRP are added to obtain effective mechanical strains, and then stresses are evaluated using relevant high temperature stress-strain relationships. The initial strain (ε_{bi}) in FRP is evaluated based on dead loads at the time of retrofitting, while bond-slip (ε_{slip}) along the length of the beam segment is calculated as described in the Reference (Ahmed and Kodur 2011).
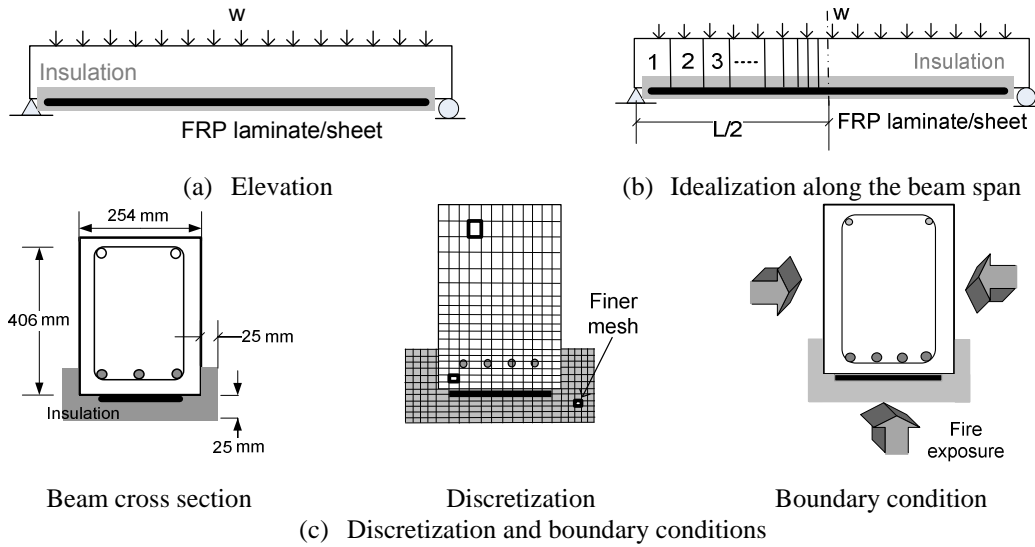

Fig. 1: Layout of typical FRP-strengthened RC beam, its idealization and discretization for analysis

At each time step, the computed forces are used to check force equilibrium. For an assumed total strain at the top layer of concrete $(\varepsilon_{c,T})$, curvature (κ) is iterated until force equilibrium is satisfied.

This iterative procedure is repeated till equilibrium, compatibility and convergence criterion are satisfied. Once these conditions are satisfied, moment and curvature corresponding to that strain is computed. Through this approach, various points on the moment-curvature curve are generated for each time step.

Following the generation of $M-\kappa$ relationships, an iterative procedure described by Cambell and Kodur (1990) is employed to evaluate deflections of the beam at each time step. In this approach, the stiffness matrix and the loading vector are computed for each longitudinal beam segment, assembled in the form of a nonlinear global stiffness equation, and solved to compute deflections at that time step:

$$[K_g]\ [\delta]=[P] \tag{1}$$

where: K_g = global stiffness matrix, δ = nodal displacements, $P = P_f + P_s$ where P_f = equivalent load vector due to applied loading and P_s = equivalent nodal vector due to $P-\delta$ effect.

The model generates various output parameters, such as cross sectional temperatures, stresses, strains, deflections and moment capacity for each time increment. These parameters are checked against pre-designated failure criterion, which include thermal and structural considerations. The time increment continues until one of the limiting criteria is reached. At this time step, the beam is said to have failed. The time duration to reach this failure point is the fire resistance of the beam. Full details on the development of the computer model, including the evaluation of various strains, stresses, bond-slip and forces are given by Kodur and Ahmed (2010).

In the model, any or all of the following limiting criteria can be applied to evaluate failure of the FRP-strengthened RC beam:-

• The moment due to applied load exceeds the strength capacity of the beam.
• The temperature in reinforcing steel (tension reinforcement) exceeds $593^{o}C$.

- The deflection of the beam exceeds $L/20$, where L is the length of the beam, at any fire exposure time.
- The rate of deflection exceeds the limit $L^2/9000d$ (mm/min) where L is the length of the beam (mm); and d, effective depth of the beam (mm).
- The temperature in FRP layer exceeds glass transition temperature (T_g) of FRP.

It should be noted that the user has the option to specify any (or all) of the five limit states to define failure.

1.2 High Temperature Material Properties

For modeling the response of FRP-strengthened beams, high temperature properties of concrete, steel reinforcement, FRP, adhesive and insulation are required. These properties include thermal, mechanical and deformation properties which vary as a function of temperature. In literature, there is reliable data on high temperature properties of concrete and steel. However, knowledge is limited on high temperature properties of FRP, adhesive and insulation. For concrete and steel, the properties suggested by ASCE Manual (Lie 1992) and for FRP and insulation, semi-empirical relationships suggested by Bisby (2003), have been incorporated into the model. To account for bond-slip at the interface of FRP-concrete, bond stress-slip curves presented by Leone et al. (2009) have been included in the model. These curves provide data for shear modulus (G) as function of temperature to compute bond-slip (ε_{slip}) at interface of FRP-concrete. For adhesive and insulation, properties available in the literature are utilized (Ahmed 2010).
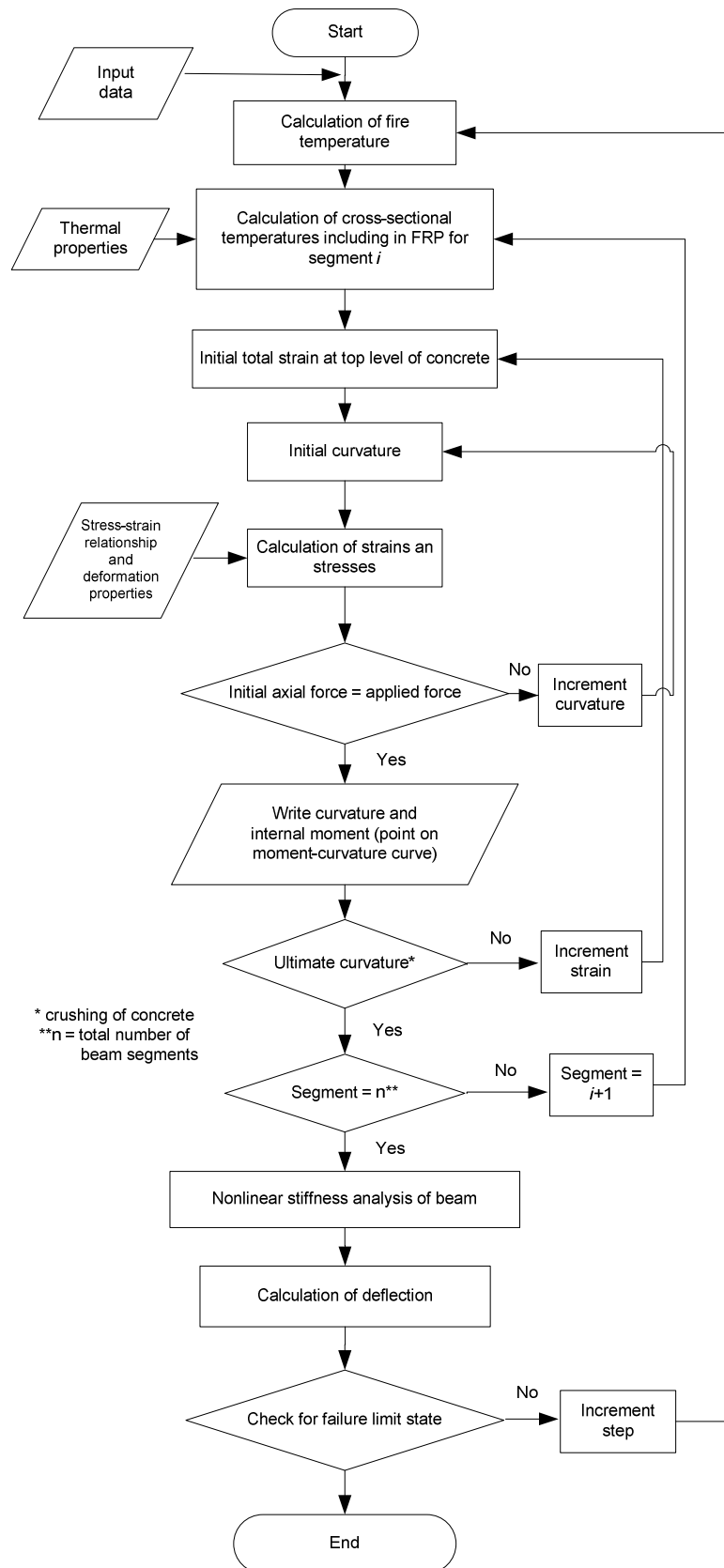

Fig. 2: Flow chart of analysis procedure used in computer program

241

2 VALIDATION OF MODEL

The above computer program is verified by comparing predictions from the model with measured data on a number of FRP-strengthened RC beams tested in Canada, USA and Europe. This paper presents validation on four FRP-RC beams (designated as Beams B1 to B4), tested as part of research at Michigan State University (Ahmed and Kodur 2010). Full details on the test beams are given by Ahmed (2010).

The thermal validation on one of the four tested FRP-RC beams (Beam B1) is presented here. Fig. 3 shows a comparison of temperatures at FRP/concrete and FRP/insulation interfaces, and at three different locations (TC5, TC6 and TC9) in the beam cross section. TC5 represent temperature in compression reinforcement, TC6 represent corner rebar temperature (flexural reinforcement) while TC9 is at mid-depth of beam cross section (203 mm). It can be seen (refer to Fig. 3 (a)) that the measured and predicted temperatures are in good agreement throughout the fire duration.

Fig. 3 (b) provides a comparison between predicted and measured temperatures at FRP/concrete and FRP/insulation (VG) interfaces. These temperatures are critical indicators of the performance of FRP under elevated temperatures. The model predicts temperature fairly well up to 40 minutes of fire exposure time. Beyond this, the model under predicts temperature at FRP/insulation interface and over predicts FRP/concrete interface temperatures. This could be attributed to the fact that measured temperature at FRP/insulation interface increase rapidly after 40 minutes due to localized burning of epoxy as a result of crack propagation in insulation. Due to this localized burning, measured temperatures are higher as compared to that predicted by the model. On the contrary, increase in temperatures recorded at FRP/concrete interface is slightly lower than predicted by the model. The possible reason for this temperature lag could be due to the formation of char layer as a result of thermal decomposition of epoxy (pyrolysis process) that acts as a thermal barrier and restricts heat flow to inner interface. The analysis of various other FRP-RC beams showed that the model predicts temperature progression reasonably well Ahmed (2010).
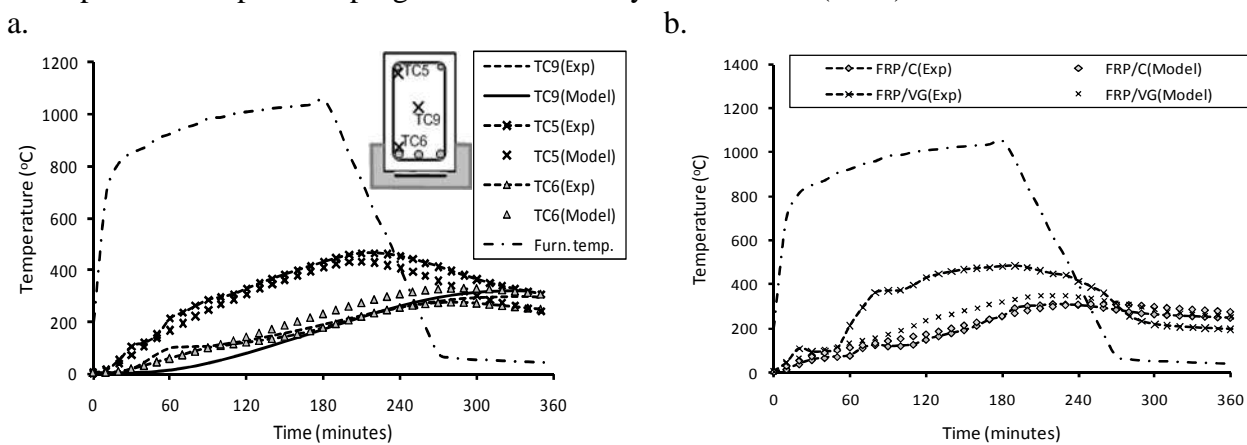
a.
b.

Fig. 3: Measured and predicted temperatures for FRP-RC Beam 1

The predicted and measured mid-span deflections for four tested FRP-RC beams are compared in Fig. 4(a). There is a good agreement between measured and predicted deflections for all four beams. Compared to observed time of FRP debonding at about 20-25 minutes, the model predicts it around 30 minutes. This variation can be attributed to the discrepancy between measured and predicted temperatures at interface of FRP as discussed above. For axially restraint beam B4, the result of predicted and measured axial restraint force is in good agreement for entire duration of the test (refer to Fig. 4(b)). Overall, the model provides reasonable estimates of cross-sectional temperatures, deflections and restraining force.

A comparison of fire resistance of FRP-RC beams as predicted in model and seen in tests is tabulated in Table 1. The time to reach failure is defined as the fire resistance of the structural member. All four FRP-strengthened RC beams sustained load during the entire fire tests (more than 3 hours). The results from the analysis show that the beams met the rebar temperature criterion and strength failure criteria specified in codes and standards. Analysis of the tests data showed that glass transition temperature of FRP exceeded in about 20-25 minutes which resulted in FRP debonding.

However, no strength failure occurred in FRP-strengthened beams. Thus, glass transition temperature failure criterion is overly conservative for insulated FRP-strengthened RC beams.
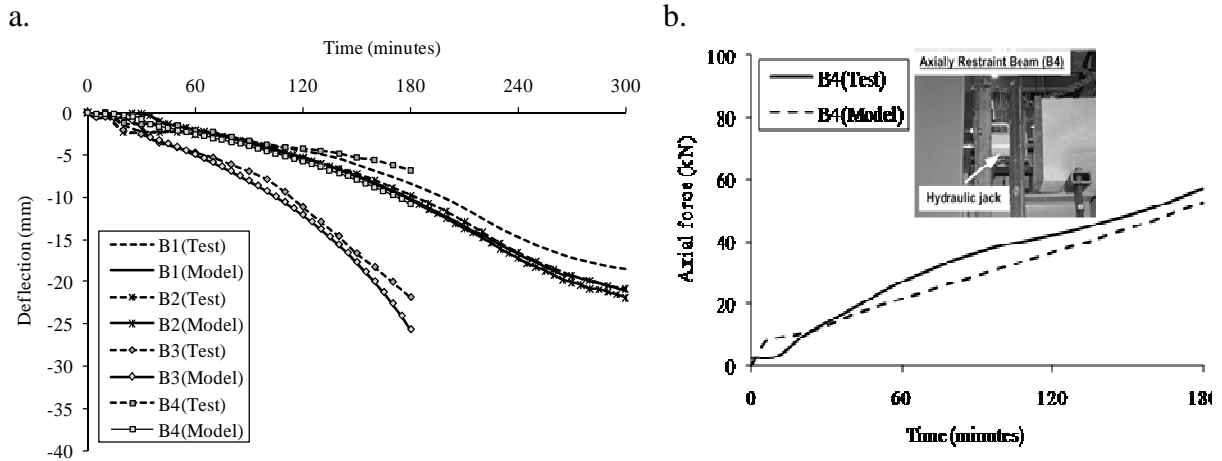
a.   b.

Fig. 4: Measured and predicted mid-span deflections and axial restraint force

Table 1 Summary of test parameters and of tested beams

Beam	CFRP strengthening	Insulation type	Insulation thickness (mm)		Fire scenario	Support condition	Load (kN)	Failure time (min)
			VG	EI-R				
B1		Tyfo® WR AFP-Type A	25	0.1	Design fire	SS	70	NF*
B2	2 layers of 203 mm wide	Tyfo® WR AFP-Type B	25	0.1	Design fire	SS	70	NF*
B3		Tyfo® WR AFP-Type A	25	0.1	ASTM E119	SS**	70	NF*
B4		Tyfo® WR AFP-Type A	25	0.1	ASTM E119	AR***	70	NF*

* NF – No failure   ** Simply supported   *** Axially restrained

3   CASE STUDY

The above developed computer program can be applied for evaluating fire response of FRP-strengthened RC beams and also for developing effective insulation schemes for achieving optimum fire resistance levels. This is illustrated through a numerical example. The selected beam (6.7 m in length and a cross section of 380×610 mm) is made with concrete of compressive strength $f_c' = 38\,MPa$, yield strength of steel $f_y = 414\,MPa$. The beam is strengthened in flexure by providing three layers of unidirectional CFRP at the tension face of the beam. These CFRP layers are applied at full width (380 mm) of the beam cross section. For fire protection, Tyfo® VG (vermiculite gypsum) insulation is applied at the bottom of the beam that extends 105 mm on two sides of the beam cross section. The thickness of insulation is kept 20 mm (constant) except when specified. The fire resistance of this beam was evaluated based on thermal, strength, and deflection failure criteria. Full details of analysis, including discretization and material properties, are given in Reference (Ahmed 2010).

3.1   Insulation Layout

In FRP-strengthened RC members, insulation layout is an important consideration for achieving fire resistance. The fire insulation helps to keep overall beam cross sectional temperatures low. Therefore, proper detailing of insulation can help to keep the temperatures low not only in FRP but also in tension steel reinforcement and help in achieving optimum insulation levels. An optimum geometric insulation configuration was developed to achieve good fire resistance in FRP-strengthened RC beams (Ahmed 2010).

The five insulation schemes that can be adopted for FRP-strengthened RC beam with rectangular beam cross section are shown in Fig. 4 (Ahmed 2010). It has been established that externally

bonded FRP without fire protection is not appropriate for FRP-strengthened RC beams (Gamage et al. 2006). Therefore, FRP without supplemental insulation is not recommended (refer to Fig. 4(a)). The two insulation configurations shown in Fig. 4(b) and (c) do not lead to optimum protection since rebar temperatures will not be kept for sufficient time to yield good fire resistance. From the parametric studies and fire tests, it was found that extending the insulation to two time the depth of concrete cover ($2C_c$) from bottom of the beam cross section (on either side) is required to achieve optimum fire resistance (Ahmed 2010). Based on these results, the two recommended insulation configurations are shown in Fig. 4(d) and (e). Both these insulation configurations can provide effective fire protection to overall beam cross section. However, the insulation scheme shown in Fig. 4(d) is the most preferred option, as compared to the one shown in Fig. 4(e), since applying insulation along complete exposed surfaces of the beam cross section is not practical and is an expensive proposition. A similar insulation schemes was also developed for FRP-strengthened T-beams (Ahmed 2010).

| (a) Not recommended | (b) Not recommended | (c) Not preferred | (d) Recommended option | (e) Workable but can be expensive |
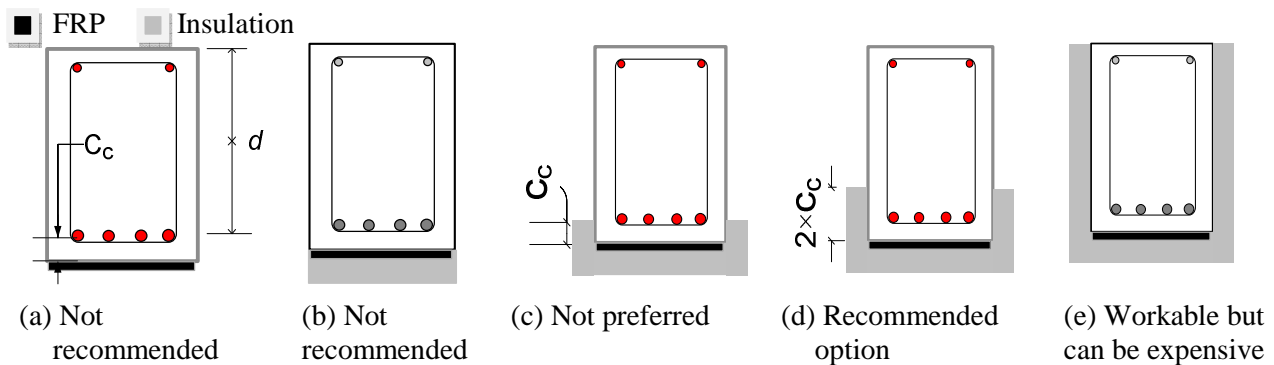
Fig. 4: Proposed geometric configuration schemes for fire insulation in FRP-strengthened RC beams

3.2   Insulation Thickness

Apart from the geometric configuration, insulation thickness is another key factor that governs fire resistance of FRP-strengthened RC beams. The effectiveness of insulation on fire resistance mainly depends on the thickness, specific heat and thermal conductivity properties of fire insulation. The fire resistance of FRP-strengthened RC beams increases with insulation thickness. However, there is a certain level of thickness beyond which any further increase in the thickness is not beneficial. This level of insulation thickness is referred to as "*optimum insulation thickness*".

Corner rebar temp. and yield strength ratio as a function of insulation thickness for 3-hour of fire exposure time

Insulation thickness for 2 hours of fire resistance

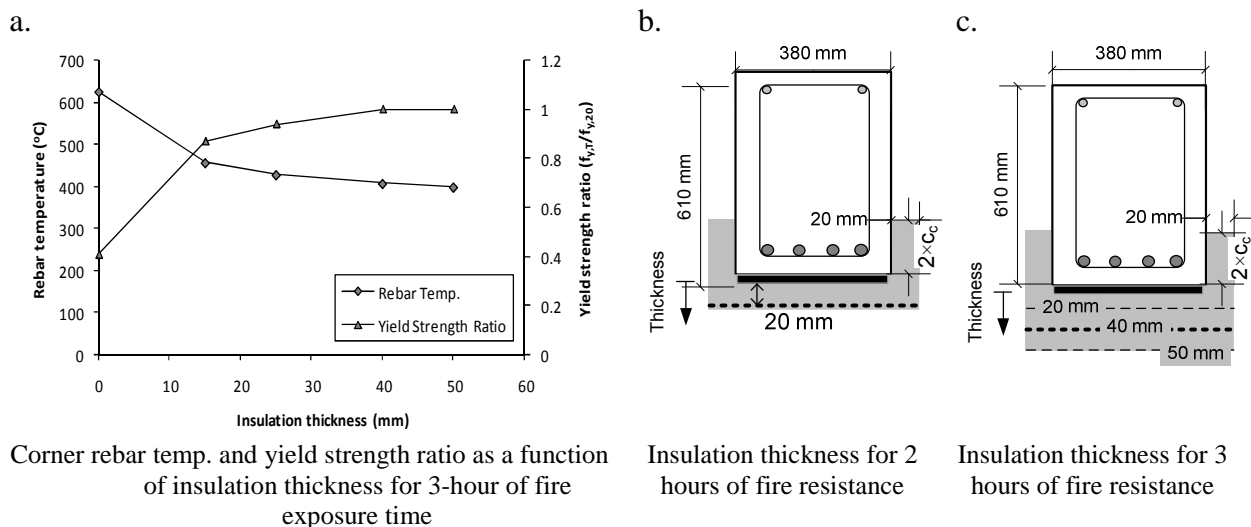Insulation thickness for 3 hours of fire resistance

Fig. 5 Proposed optimum thickness for fire insulation in FRP-strengthened RC beams

For flexural members such as beams, it is not desirable to have insulation thickness beyond an optimum value since it adds to weight of the structures and accelerate insulation fall off under increased dead weight, especially when beam deflections increase under fire conditions. The insulation also limits the temperature rise in steel reinforcement and this in turn helps to achieve

higher moment capacity at a given fire exposure time. However, beyond optimum insulation thickness, at which steel rebar temperatures reaches about 400^oC, any further reduction in steel reinforcement temperature does not result in higher tension force or capacity of the beam, as shown in Fig. 5(a) (Eurocode 2 2004). Figs. 5(b) and (c) shows the optimum insulation thicknesses recommended for FRP-strengthened RC beam and these thicknesses were derived through parametric studies for an insulation that has thermal conductivity of 0.12 W/m-^oK (Ahmed 2010). An optimum insulation thickness of 40 mm is required to achieve 3 hours of fire resistance while a minimum of 20 mm thickness is needed to achieve a fire resistance up to 2 hours.

SUMMARY

The proposed macroscopic finite element based computer model, is capable of predicting the fire response of FRP-strengthened RC beams under wide range of design scenarios. The model accounts for high temperature material properties of constitutive materials, fire induced bond degradation, axial restraint force, and different strain components. The computer model can be applied to quantify the influence of various parameters (such as insulation schemes) on the fire response of FRP-strengthened RC beams and recommend broad guidelines for enhancing fire resistance. Such fire design guidelines, like the ones presented in this paper, will facilitate the wider use of FRP in strengthening of concrete members in buildings and other structures, where fire safety is one of the crucial issues.

ACKNOWLEDGEMENTS

REFERENCES

Ahmed, A. (2010). "Behavior of FRP-strengthened Reinforced Concrete Beams under Fire Conditions," Doctoral Thesis, Michigan State University, East Lansing, USA.

Ahmed, A., and Kodur, V. K. R. (2010). "Performance of FRP-strengthened Reinforced Concrete Beams under Design Fire Exposure." Proceedings of Sixth International Conference on Structures in Fire, East Lansing, Michigan.

Ahmed, A., and Kodur, V. K. R. (2011). "Effect of bond degradation on fire resistance of FRP-strengthened reinforced concrete beams." Composites Part B: Engineering, 42(2), 226-237.

Bisby, L. A. (2003). "Fire behavior of fibre-reinforced polymer (FRP) reinforced or confined concrete," Doctoral Thesis, Queen's University, Kingston, Canada.

Campbell, T. I., and Kodur, V. K. R. (1990). "Deformation controlled nonlinear analysis of prestressed concrete continuous beams." PCI Journal, 35(5), 42-90.

Eurocode 2. (2004). "EN 1992-1-2: Design of concrete structures. Part 1-2: General rules - Structural fire design." European Committee for Standardization, Brussels, Belgium.

Kodur, V. K. R., and Ahmed, A. (2010). "A Numerical Model for Tracing the Response of FRP Strengthened Reinforced Concrete Beams Exposed to Fire." Journal of Composites for Construction, 14(6), 85.

Leone, M., Matthys, S., and Aiello, M. A. (2009). "Effect of elevated service temperature on bond between FRP EBR systems and concrete." Composites Part B, 40(1), 85-93.

Lie, T. T. (1992). "Structural fire protection." ASCE Committee on Fire Protection, Structural Division, American Society of Civil Engineers, New York,NY, 225-229.

FIRE PROTECTION OF STEEL STRUCTURES USING AUTOMATINC WATER EXTINQUISHING SYSTEM

Jyri Outinen [a]

[a] Rautaruukki Corporation, Vantaa, Finland

INTRODUCTION

A continuation to a previous research program [1] has been carried out in Finland in order to study further the cooling effect of water extinguishing system in fire situation to steel structures. The objective was to study how the temperatures of the load-bearing structures including steel trusses, columns, bracing and corrugated sheeting develop in fire situation, when there's a sprinkler system present and acting. Possibility to use unprotected steel structures within certain limits when a specified sprinkler network is installed was investigated in this research.

The research is based on experimental fire tests and numerical simulation [2,3] carried out by VTT, Technical Research Centre of Finland. On the basis of these researches a national product approval [4] was achieved. Also a European product approval is applied for the system.

1   BACKGROUND

It is very common to have a 60-120 minutes fire resistance requirement to load-bearing structures in typical buildings in Finland and also in other European countries. Normally quite expensive passive fire protection, e.g. fire protection paint, gypsum boards, rock wool or other material to cover and protect the structure is needed to fulfil this requirement for steel structures. These are naturally simple ways of achieving the fire resistance, but there are also some problems with these solutions and high costs.

The objective of this research was to study whether the cooling effect of quite effective sprinkler systems ensure the fire protection of steel structures with no need for passive fire protection. It is known that automatic water suppression also keeps the fire local in most cases when functioning properly [5].

The fire protection is always expensive whether it is done by passive or active measures. That is why there's also a financial benefit when either of these can be totally or partly left out. The sprinkler system is more important when talking about protecting the people, which of course is more essential than the building itself. Naturally in some cases the passive protection is still more reasonable than using active measures.

When automatic water suppression is required to a building for common fire safety reasons, the use of it also as structural fire protection can be very cost-effective. With this system the structural fire resistance can be achieved simultaneously ensuring the life safety of the occupants or users of the building. When the fire sprinkler system is designed, installed and maintained properly, the risk that it won't work is very little [5]. As it is known the sprinkler systems are required in certain types of buildings with certain criteria. This differs from country to another, even within EU countries [6].

In some countries the structural fire resistance can be lowered when the fire sprinklers are present. Almost in every country some other benefits in fire safety design can be gained, e.g. bigger fire-compartments, compromises in smoke extraction etc. This is also the case in Finland and especially the fire-compartment size is a normal compensation.

The Authorities can then decide whether the water suppression system can also be used to lower e.g. the structural fire resistance requirements.

2   TESTING FACILITIES

2.1 Test arrangements

The previous fire tests were conducted in Finland in 2009. A small steel framed hall was constructed, the sprinkler system was installed to the ceiling and the studied steel trusses, beams and columns and other parts of the building were equipped with temperature detectors. The outer walls were left enough open from the bottom so that there would be enough oxygen for the fire. In Figure 1 the basic geometry and the sprinkler locations of the tested system are presented. The outer walls were constructed from sandwich panels and the roof was built from load-bearing corrugated steel sheets with insulations above it. Temperatures were measured also from the corrugated steel sheeting.
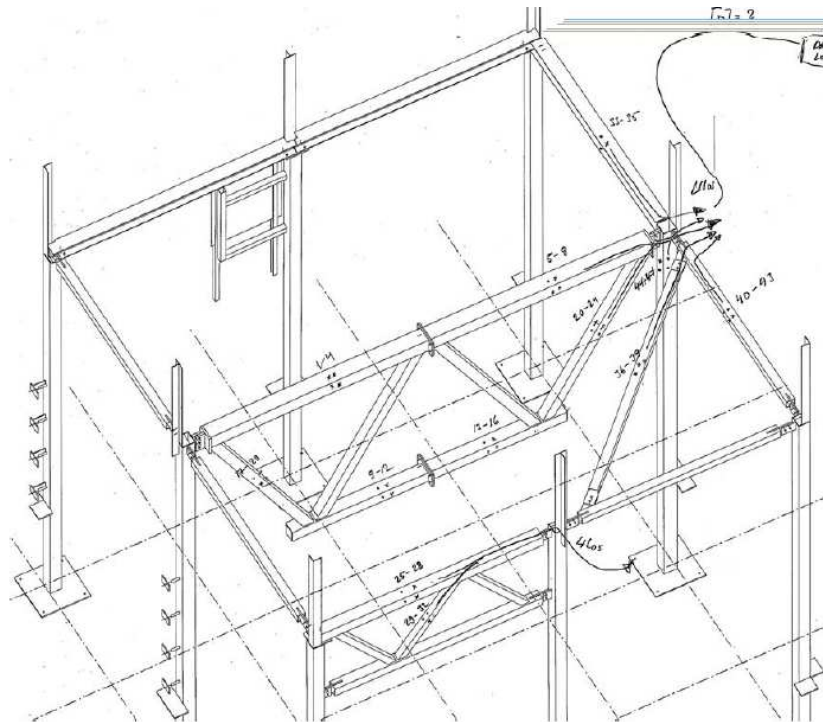
Fig. 1. Skeleton of the structures

2.2 Fire scenario

The system was tested against standard ISO-fire. The fire load was produced by heptan-spray burner, which was situated centrally under the studied structures spreading the fire with three nozzles. The test was run so far as to get enough information about the temperature development in the test room and in the structures to get the needed data for the product approval of the system.

2.3 Tested structures

The temperatures were measured from tubular steel trusses, beams and columns. Also the temperatures from the connections, bracing and steel sheeting were measured. The height of the steel truss was about 1,5m and it was built from different sized cross-sections. The temperatures were measured from different parts of the truss. The other structures were also selected so that they represented the smaller sized structures normally used, in order to widen the use of the results to bigger sections.

2.4 Water extinguishers

In the tests, three kind of sprinkler nozzle types were tested, ESFR (early suppression fast response), normal spray-nozzles and also conventional sprinklers. The water flow was set to a normal value used in building design. The pressure was set to quite low level. In ESFR tests only half of the nozzles could be used because of the huge amount of water produced by the system.

The sprinklers produce an umbrella shaped water flow. The watering is determined mainly to put down or at least restrict the fire from spreading around. At the same time water cools down the structures directly and very effectively as was found out in the research. Different sprinkler heads, or nozzles are presented in the following figure.

| Installation | ESFR | Conventional | Spray |

Fig. 2 Sprinkler nozzle types
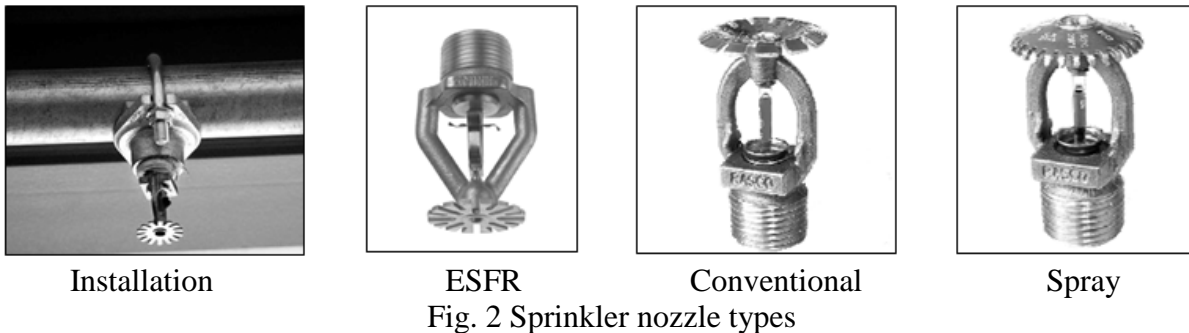
2.5 Simulations

The fire test was also simulated using FDS (Fire Dynamics Simulator). The heating of the structures was studied. In the picture below the system is in use in a real commercial building in Finland. E.G this kind of system was simulated in fire situation.

Simulating sprinkler's effect is quite complicated, but the tools in FDS are being developed all the time. A separate 3-year project was carried out in Finland in 2008-2010. Ruukki was financing and participating to this research. The project "Fire Suppression" was carried out by VTT and the final report will be published soon.
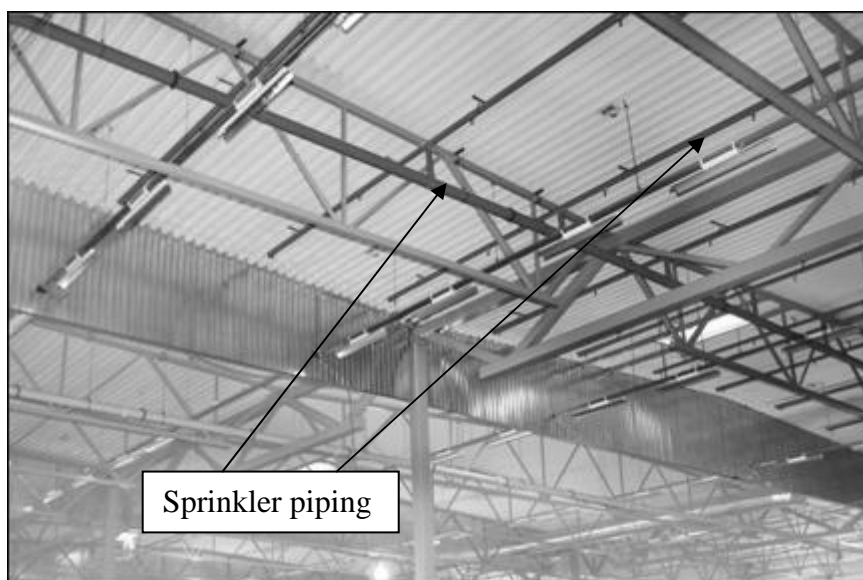
Fig. 3 Steel structures, sprinkler piping and nozzles

3   RESULTS

In the fire tests a standard fire exposure was set by using heptan-spray burners underneath the structure system. Temperatures from the installed structures were measured during the test. For the defined set of cross-sections, the temperatures of the steel structures did not raise above critical level in standard fire exposure. This can be noted from the figures 3 and 4.
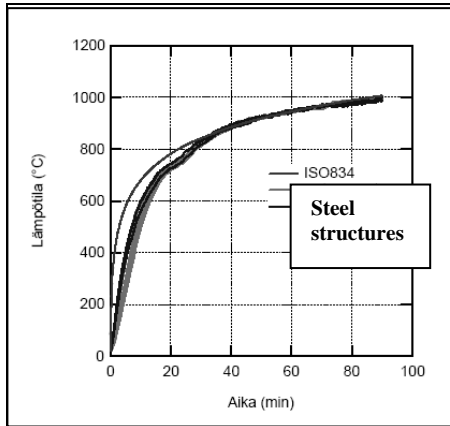
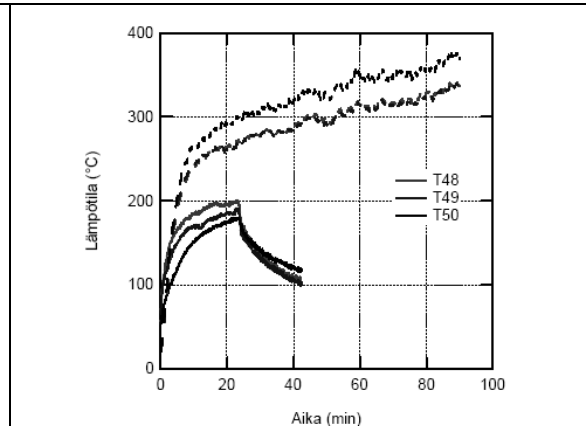| Fig. 4 Temperatures of the steel structures in free burn test. No sprinklers	Fig. 5 Temperatures of the steel sheeting in sprinkler test. Dotted lines from simulation, solid lines from tests.

All in all the temperatures of the structures stayed at adequate level. On the basis of these tests product approval for 90 minutes fire rating was got to the systems. The tests went well and the measurements and simulations were carried out successfully.

On the basis of the tests a short design guide for structural design and also for the design of the water sprinkler system was introduced. In these instructions the limitations to the structures, cross-sections, structures' dimensions are set. For the water sprinklers the design principles concerning the water flow, number and location of the sprinkler nozzles are instructed.

4   SUMMARY

A research concerning the fire protection of steel structures in standard fire exposure was carried out in Finland. Structural fire protection of steel structures was studied using automatic water extinguishing systems. Several different sprinkler types were used to study the temperatures in selected steel structures. The research was carried out with fire tests and also simulations.

The aim was to study the possible fire resistance rating to the system and according to he research results; fire rating of R90 was accomplished. The temperatures of the steel structures stayed at very low level so that there is no need for additional fire protection in this kind of case.

This kind of systems will be used typically in 1-2 storey building at the moment, but the field of application will be widened in the future.

More research is planned to investigate different scenarios and structural systems.

REFERENCES

Outinen, Kansa, Fire protection of steel structures using water sprinklers, ASFE conference, Prague, 2009.

Fire protection of steel structures using sprinkler systems", VTT Research report VTT-R-1871-10.

Fire protection of steel structures using sprinkler systems", VTT Research report, VTT-R 7226-10

Steel structure with a water sprinkler system fire-protection, VTT Certificate VTT-C-4921-10, 2011.

Hietaniemi, J., Cajot, L.-G., Pierre, M., Fraser-Mitchell, J. Joyeux, D. & Papaioannou, K. Risk-Based Fire Resistance Requirements. Final Report. Luxembourg: Office for Official Publications of the European Communities 2005.

European sprinkler organisation homepage, www.eurosprinkler.org

ROLE OF CFD IN THE QUANTITATIVE ASSESSMENT OF STRUCTURAL PERFORMANCE IN FIRE SCENARIOS

Filippo Gentili, Luca Grossi, Franco Bontempi

Sapienza University of Rome, School of Engineering, Rome, Italy

INTRODUCTION

The quantitative assessment of the structural performance is based on a multiphysics analysis. In the process of calculating the structural behaviour, three essential models can be identified: a fire model, a heat transfer model and a structural model (Buchanan, 2002).

Computational fluid dynamics (CFD) simulation plays an important role in fire research. It allows evaluating the fire development and provides a new, efficient, reliable and economic path for fire investigations. As a consequence, it is considered nowadays an important fire research tool (Yeoh and Yuen, 2008). With the wide adoption of performance-based fire safety design, CFD simulation is becoming a routine practice for obtaining the necessary fire design information. With new developments in modelling techniques, fast increase of computing power, and quick drop of hardware price, it is expected that CFD simulation will keep gaining popularity in the fire research community. A CFD model permits a quite realistic representation of fire scenarios, because it takes into account the distribution of fuel, the geometry and the occupancy of individual compartments in a structure.

In this paper, an industrial hall has been considered as a case study. The development of fire of wooden pallets has been studied by means of a CFD code, FDS (McGrattan et al, 2009), considering different positions of the combustible material and different ventilation conditions. The adiabatic surface temperature (AST), (Duthinh et al, 2008), solves the heat transfer model and creates a link with FE codes in order to assess the structural performances.

1 CASE STUDY

The industrial hall considered as a case study is shown in Fig. 1. This structure has been previously investigated by Vassart et al. (2004). The system is composed by 5 frames, joined by means of purlins. The length of the main slightly inclined beams is 20 m, and the height of the 15 columns is 5 m.
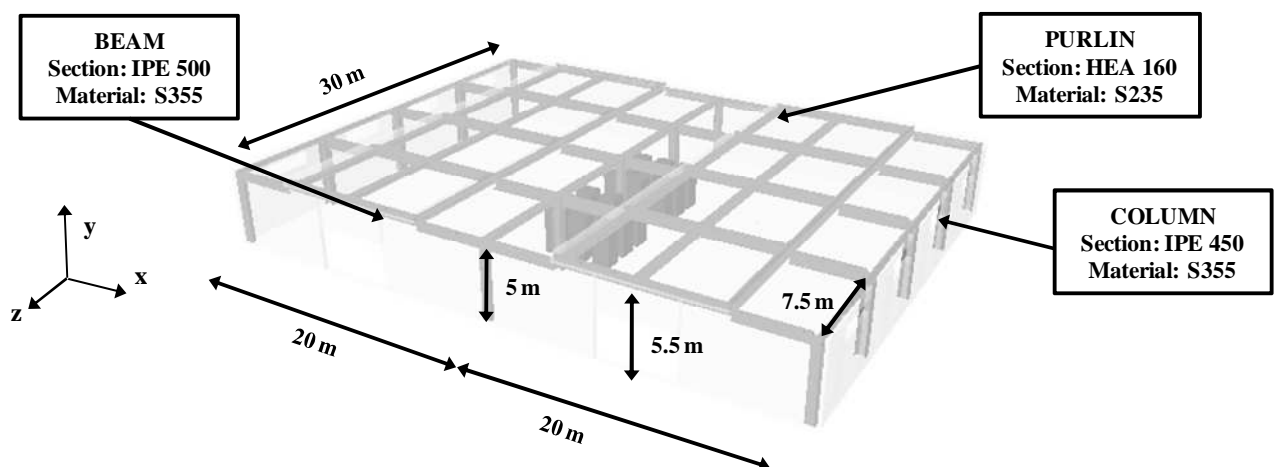

Fig. 1. Structure taken as case-study.

Due to the doors located on the longest building facade with an area of 30 m², and due to the windows located on the shortest sides with an area of 28 m², the opening factor of the structure is

equal to 0.265 m$^{1/2}$ and the fire results to be ventilation controlled, being the fire load significant as can be seen below. In the FDS model, the presence of structural elements is not important for the evaluation of the fire development, but it allows to compute the heat transfer model.

2 FIRE AND HEAT TRANSFER MODEL

2.1 Identification of the fire scenarios

The identification of the appropriate fire scenarios is essential to the design of a building that fulfils the fire safety performance objectives (ISO 13387, 1999). Fire scenarios define the ignition and fire growth process, the fully developed stage and the decay stage. In this case the fire triggered by the ignition of wood pallets has been considered. Conceptually, a wood pallet is a similar arrangement to a wood crib (Drysdale, 1999). The geometry, however, is different. Instead of being composed of identical rows of square-section sticks, pallets are made up of rectangular elements, whose typical setup is shown in Fig. 2.
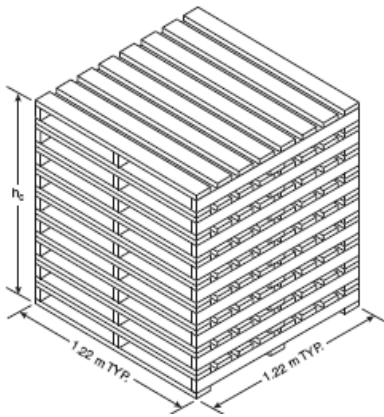
Height	3.05m
Size	1.2m x 1.2m
Weight of one pallet	15 kg
Weight of one stack of pallets	300 kg
Weight of all stacks	5400 kg
HRR$_{S,max}$	6810 MW/m^2
t$_g$	80 s
Where HRR$_{S,max}$ the maximum of heat-release-rate per unit area, t$_g$ the characteristic time of fire	

Fig. 2 Wood pallets   Tab. 1 Properties of pallets

A typical experimental Heat-Release-Rate (HRR) curve shows that a constant plateau can be seen if the stack is reasonably high (Krasner, 1968). The burning of 18 stacks of pallets has been considered as a fire scenario. Tab. 1 shows the most important characteristics of considered pallets.

2.2 Optimization and validation of the model

The reliability of the fluid dynamic prediction of events is influenced by the size of the grid. In the Fire Dynamic Simulator there is a parameter that should always be considered, which is called characteristic fire diameter D* and whose value is given in Eq. (1), (McGrattan et al, 2009):

$$D* = \left(\frac{\dot{Q}}{\rho_\infty \cdot c_p \cdot T_\infty \cdot \sqrt{g}} \right)^{2/5} \tag{1}$$

where: $\dot{Q}$ is the heat release rate, ρ_∞ is the ambient density, T_∞ is the ambient temperature, c_p is the specific heat, and g is the acceleration of gravity.

The description of the fire depends on the quality of this parameter, since it affects the combustion model by acting in the calculation of the fraction mixture, which describes the stoichiometric reaction that takes place. FDS employs a numerical technique known as Large Eddy Simulation (LES) to model the irresolvable or "sub-grid" motion of the hot gases. The effectiveness of the technique is largely a function of the ratio between the fire characteristic diameter $D*$, the size of a grid cell δx. In a few words, the greater the ratio $D*/\delta x$, more the simulation is accurate, due to the fact that the fire dynamics is resolved more directly. A ratio of 4 to 16 usually produces favorable

results at a moderate computational cost (McGrattan et al, 2009). According to other studies on the LES (Baum and McCaffrey, 1989), a good representation is obtained by using values of δx within $0.1 \cdot D^*$ and $0.3 \cdot D^*$. Tab. 2 synthesizes the studied models. In order to get a simpler feedback on the model validation and to choose the correct mesh, a strong and unrealistic hypothesis of simultaneous involvement of all pallets has been initially considered in this study. Following the directions given in ISO-13387, it is possible to calculate point B and point C of heat release rate curve shown in Fig.3, according to what is reported in Tab 3.

dx	% D^*	$\dfrac{dx}{D^*}$	Number of cells
0.3	0.15	6.89	298080
0.4	0.19	5.17	126360
0.5	0.24	4.14	64512
0.6	0.29	3.45	38880

Tab. 2 Models with different mesh sizes

Fig. 3 Considered HRR curve

A size of 50 and 60 cm does not provide an adequate simulation of the phenomenon in terms of the heat release rate (Fig. 4), maximum temperature (Fig. 5) and height of the smoke (Fig. 6). With a discretization of 40 cm fire is better modeled as a whole, but if a strong temperature gradient occurs, the result accuracy is still not satisfactory. For these reasons, for the investigations presented in the following paragraphs, a model with the mesh size of 30 cm has been used.

	time [min]	HRR [MW]
t_0	0	0
t_F	10	54
t_A	11	176
t_B	14	176
t_C	18	0

Tab 3 Values of the HHR

Fig. 4 Heat release rate curve

Fig. 5 Maximum temperature

Fig. 6 Height of smoke

2.3 Fire scenarios: variation of the fuel position

The fire development is greatly influenced by the position of the fuel in relation to the geometry of the compartment. In particular, a decisive factor is the proximity of the combustible material to the openings. The first scenario consists of 18 pallets on fire, which are located in the proximity of a corner near one of the windows; in the third scenario instead the pallets are in the middle of compartment; finally in the second and fourth scenario the pallets are positioned along one long wall: the difference between the last two cases is that in the second scenario the fuel is near to a door, while in the fourth, the pallets are very far from the vents (Fig. 7).

SCENARIO 1 ### SCENARIO 2
SCENARIO 3 ### SCENARIO 4
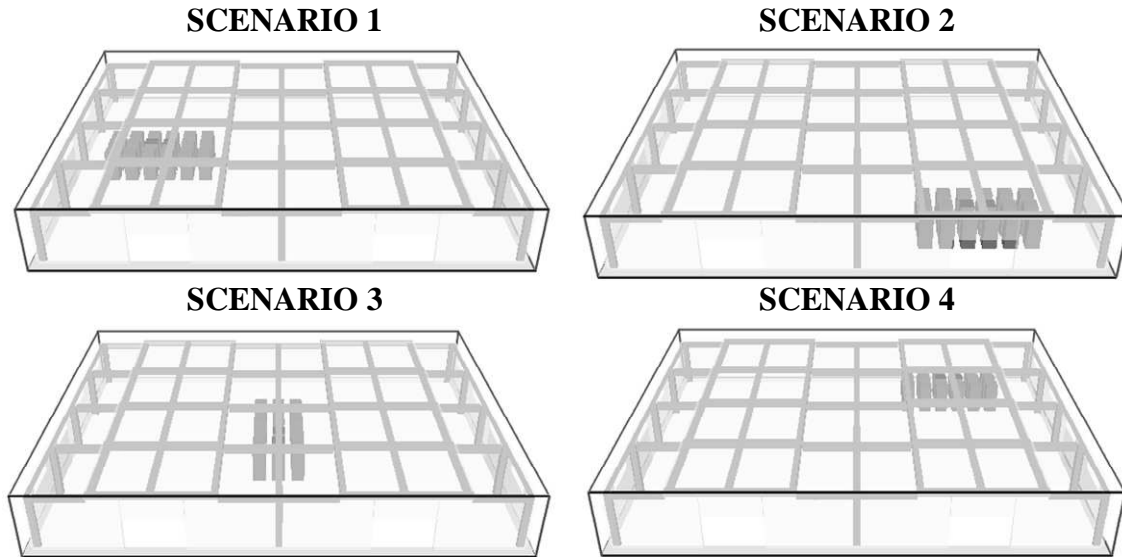
Fig. 7 Fire Scenarios: variation of the fuel position

NFPA 555 (2009), indicates an expression for estimating the minimum values of thermal power that can lead only to radiant heat ignition of combustible materials. This calculation determines whether the ignition of a material is able to determine the spread to others. The equation used is Eq. (2).

$$HRR_{min} = 30 \cdot \frac{(d + 0.02)}{0.0092} \qquad (2)$$

where: HRR_{min} is the minimum heat release rate necessary for the ignition;

d distance between materials

In Fig. 8 a possible subsequent involvement of group of pallets is shown with respect to the first fire scenario. For the second and the fourth scenario, a similar sequence has been assumed; while some differences are present in the third scenario due to the presence of a column between the pallets. The different hypotheses concerning the diffusion of fire ignition are visible in Fig. 9. The heat release rate measured in FDS for all scenarios is shown in Fig. 10, while in Fig. 11 the highest temperatures of the structural elements are reported for each scenario. The fire development in scenarios 1, 2 and 3 determinates a quite similar heating in elements. In the fourth scenario instead the heating is slower, as shown in Fig. 11.
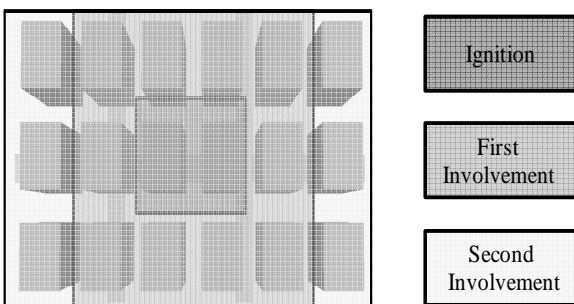

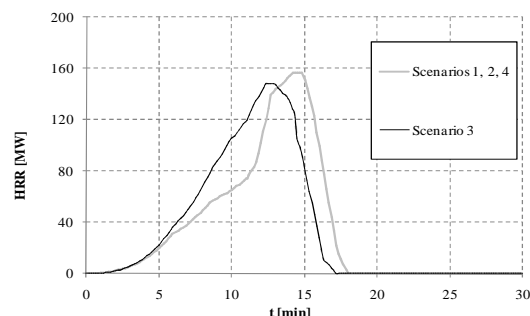Fig. 8 Involvement of pallets in the first scenario
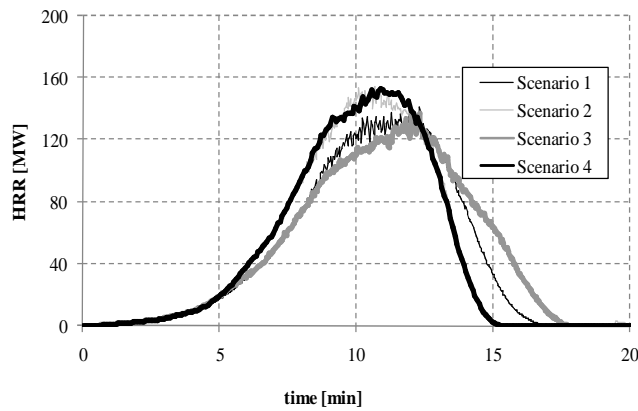
Fig. 9 Calculated heat release rate
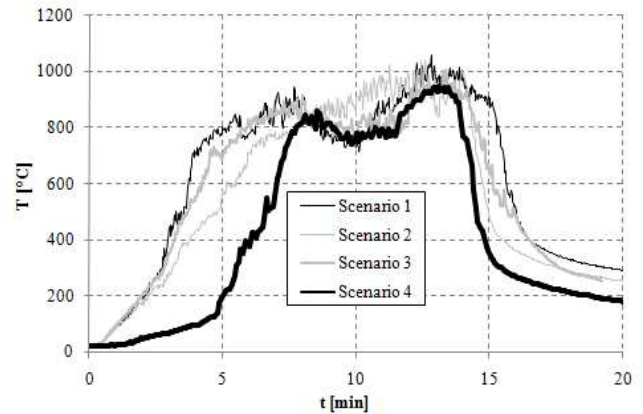
Fig. 10 Registered HRR in FDS

Fig. 11 Maximum temperature

2.4 Fire scenarios: variation of the ventilation

The development of the fire is determined by the opening factor. In particular, with reference to position 3 of the fuel (Fig. 7), the evolution of the fire has been studied in the following cases:

1. openings all closed;
2. breaking of the windows;
3. doors opening after 600 s;
4. smoke extractors activated at 68°C.

The sudden variation of the ventilation conditions determinates a strong change in development of fire, as Fig. 12 shows. The highest temperatures (Fig. 13) are reached when doors are open from the beginning. When all openings are closed instead, the fire extinguishes at an early stage by lack of oxygen. The sudden opening of the doors leads to a resumption of the fire and in an increment of the temperatures, which at a later stage reach the values of the first case, where the doors were open since the beginning. The smoke extractors lead to a change in the height of the gas, in the visibility and in the toxicity, but do not cause a big change for the purposes of structural analysis.
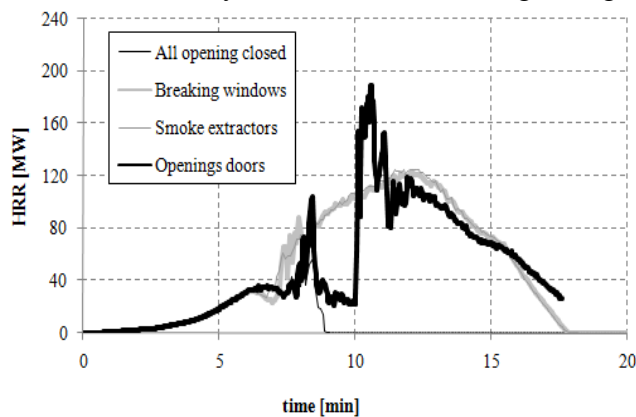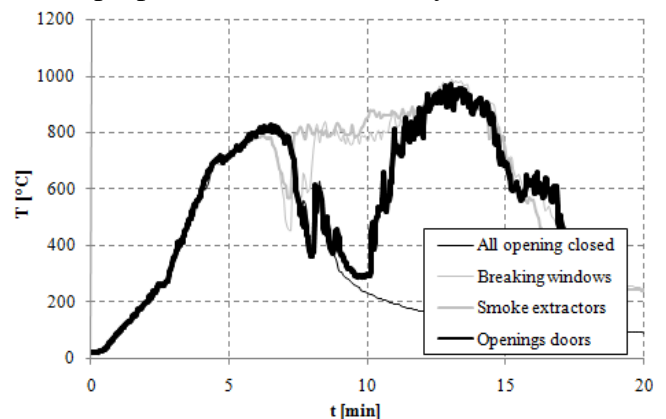

Fig. 12 Heat release rate

Fig. 13 Maximum temperature

2.5 Comparison between experimental and analytical heat release rate curve

The setting of the HRR value is a crucial point in CFD analyses finalized to assessing the fire development. For this reason, with reference to a fire of 30 stacks of pallets (dimensions 1.30m x 1.00m x 0.90), an experimental heat release rate curve (Averill et al, 2010) is compared with an analytical curve (Babrauskas, 2002), as shown in Fig. 14. The formula (3) proposed by Babrauskas is taken from Krasner (1968).

$$HRR_{s,max} = 919 \cdot \left(1 + 2.14 h_p\right) \cdot \left(1 - 0.03M\right) \qquad (3)$$

where: h_p is stack height (m) and M is moisture (%).

The experimental test was conducted by NIST in 2010. In Fig. 15 the highest temperatures of structural elements are shown. The possibility of referring to the experimental data rather than analytical assessments leads to a stronger validation.
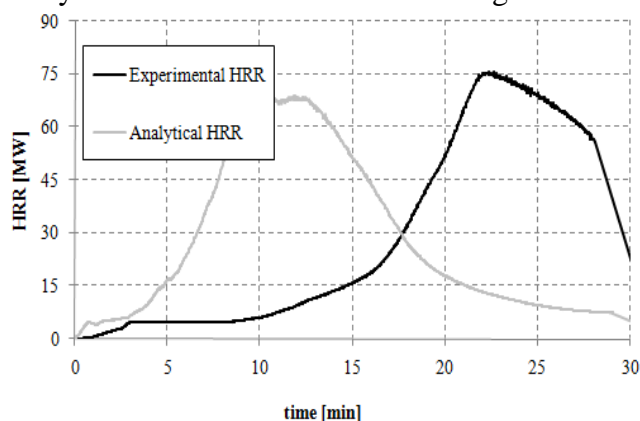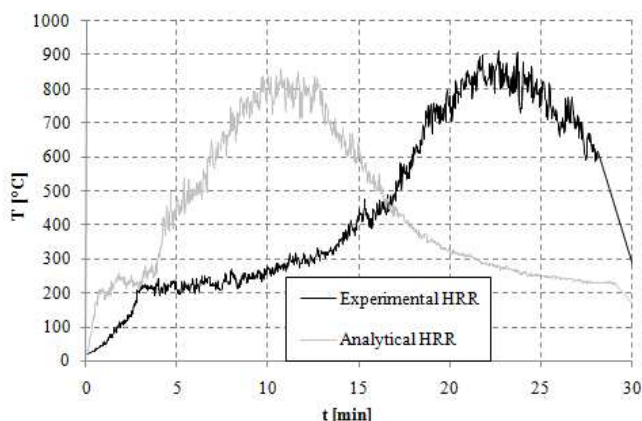

Fig. 14 Heat release rate curves

Fig. 15 Maximum temperature curves

3   CONCLUSION

In this study, aspects concerning the role of CFD analyses in the quantitative assessment of the structural performance in fire scenarios have been inquired. An application on a steel structure shows that CFD allows a more refined representation of the fire compared to an analytical evaluation. It can consider issues relevant to the development of the fire (e.g. ventilation, fuel location) and take into account significant variations of the boundary conditions in time.

REFERENCES

Buchanan A. H., Structural Design for Fire Safety, Wiley, 2002.

Yeoh G. H., Yuen K. K., Computational Fluid Dynamics in Fire Engineering, Butterworth Heinemann, 2009.

Vassart O. et al., 3D simulation of Industrial Hall in case of fire. Benchmark between ABAQUS, ANSYS and SAFIR, 10th International Fire Science & Engineering Conference, Interflam, Edinburgh, 2004.

ISO/TR 13387-1:1999 (E) Fire Safety Engineering - Part 1: Application of fire performance concepts to design objectives. Technical Report. Geneva: International Organization for Standardization.

Krasner L.M., Burning Characteristics of Wooden Pallets as a Test Fuel, *Serial 16437,* Factory Mutual Research Corp., Norwood, MA, 1968.

Babrauskas V., Heat release rate. In: SFPE handbook of fire protection engineering, 3rd edn. National Fire Protection Association, Quincy, MA, 2002.

Baum H. R., McCaffrey B.J., Fire-Induced Flow – Theory and Experiment, Fire Safety Science, 2nd International Symposium, ed. T. Wakamatsa et al., 129-148, Hemisphere, Washington, 1989.

NFPA 555: Guide on Methods for Evaluating Potential for Room Flashover, 2009.

McGrattan K., Klein B., Hostikka S., Floyd J., Fire Dynamics Simulator (Version 5) – User guide, NIST, Special Publication 1019 – 5, Washington, USA, 2009.

Averill et al, Report on Residential Fireground Field Experiments, NIST, Washington, 2010.

Drysdale D., An Introduction to Fire Dynamics, Second Edition, Wiley, 1999

Duthinh D., McGrattan K. B., Khashkia A., 2008, Recent advances in fire-structure analysis, Fire Safety Journal, Vol. 43, No. 2, 161-167.

EVALUATION OF THE FIRE RESISTANCE OF THE STEEL STRUCTURE OF A WASTE TREATMENT PLANT USING STRUCTURAL FIRE SAFETY ENGINEERING

Paulo Vila Real [a], Nuno Lopes [b]

[a] Professor, University of Aveiro, LABEST - Department of Civil Engineering, Portugal
[b] Assistant professor, University of Aveiro, LABEST - Department of Civil Engineering, Portugal

INTRODUCTION

It is the purpose of this paper to present a study performed on the fire resistance of the steel structure of a waste treatment plant.

In the Portuguese Technical Regulations for Buildings Fire Safety, on the Decree No. 1532/2008 (MAI, 2008), which is now implemented, two approaches are recommended for assessing the safety of structures exposed to fire: a prescriptive approach using the standard fire curve ISO 834; and a performance based design using the natural fire development concept.

The natural fire curve definition takes into account the size of the fire compartment, the ventilation conditions and the surrounding walls coatings, in opposition to the standard fire curve that does not depend on any of these parameters.

In addition, in the last decade several European projects (EC, 1999a,b, RFCS, 2008) have shown that in large compartments, the prescriptive regulation based on the standard fire curve is too conservative and unrealistic.

According to Part 1-2 of Eurocode 3 (EC3) (CEN, 2005a), the stability verification can be made verifying that:

a)   with the standard fire, the structure collapse does not occur before the fire resistance time defined by the regulation; or

b)   with the natural fire and advanced calculation methods the structure collapse does not occur during the complete duration of the fire, including the decay phase or during a required period of time, which may coincide with the fire resistance time defined by the regulation.

In this work, the studies, performed to assess the needs of passive protection in the steel structure of a waste treatment plant in Gaia (Portugal), are presented.

Advanced calculation methods were used (Franssen, & Vila Real, 2010), both for the natural fire characterization (programme Ozone (Cadorin 2003, Cadorin et al., 2006), developed at the University of Liege and Arcelor Profil Luxembourg Research Centre) and to simulate the thermo-mechanical behaviour (finite element program SAFIR (Franssen, 2005, 2008) also developed at the University of Liege).

It was also considered the occurrence of possible localized fires, in accordance with Part 1-2 of Eurocode 1 (EC1) (CEN, 2005b). This methodology from Eurocode was implemented in the program Elefir-EN (Vila Real et al., 2010) (developed at the Universities of Aveiro and Liege).

The fire compartment temperature definition was determined, as defined in Part 1-2 of EC1, with each of the following fire models: the localise fire and 1 or 2 zone models, according to whichever is more appropriate. These models correspond to different types of fire and different phases of the same fire.

The waste treatment plant is composed of 3 main units, one building dedicated to the reception (being this the central building), another to the post-composting and finally one dedicated to the storage. The structures have steel trusses as their primary structural elements, and self-supporting roofs composed of thin-walled cold formed steel sheeting, which had to be analysed through shell finite elements. This last structural system incorporates as well a tie rod connecting both supports.

This study, on the steel structure fire behaviour, aimed at determines the fire resistance for each of the building structures.
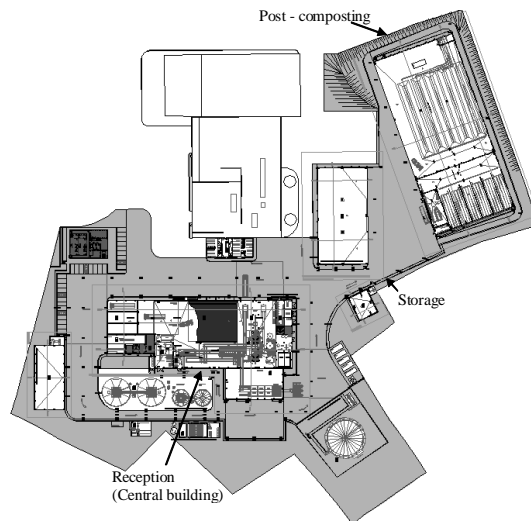
Fig. 1 Waste treatment plant.

1   FIRE SCENARIOS

The temperature evolutions were determined using the calculation software Ozone V2.2 (Cadorin 2003, Cadorin et al., 2006).

Although, as it will be shown, in all studied fire scenarios occurred flashover, on the localized fires, the maximum flame height Lf was evaluated according to EC1 and based on the Heskestad model (Heskestad, 1983, CEN, 2005b, Vila Real et al., 2010). In these analyses the rate of heat release was $RHR_f = 500$ kW/m^2, it was also considered a high fire growth rate (CEN, 2005b), and a combustion factor with the value of 1 was considered. The openings were completely open during the all fire.

1.1   Compartment fires

The considered compartment fire scenarios were:

Scenario 1 - Fire in the reception unit (central building). This compartment as an height of 12.1 m. The considered maximum area was $A_{f,max} = 4992$ m^2, and the fire area $A_{fi} = 4992$ m^2. It was considered an openings area of 68 m^2, and the fire load density was $q_{f,k} = 4960$ MJ/m^2.

Scenario 2 - Fire in the Post - composting unit. This compartment as an height of 7.8 m. The considered maximum area was $A_{f,max} = 2688$ m^2, and the fire area $A_{fi} = 2688$ m^2. It was considered an openings area of 283.5 m^2, and the fire load density was $q_{f,k} = 45753$ MJ/m^2.

Scenario 3 - Fire in the storage unit. This compartment as an height of 7.8 m. The considered maximum area was $A_{f,max} = 1250$ m^2, and the fire area $A_{fi} = 1250$ m^2. It was considered an openings area of 220.5 m^2, and the fire load density was $q_{f,k} = 13888$ MJ/m^2.

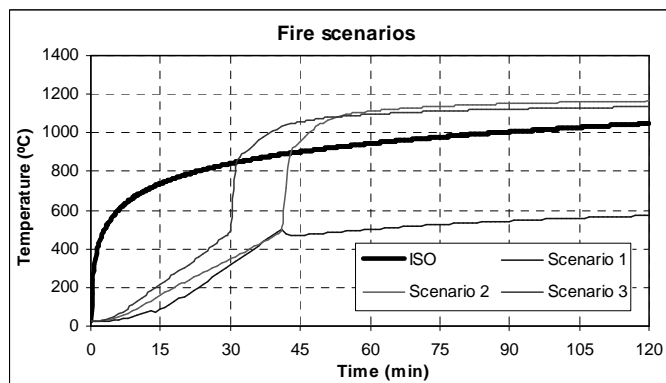The temperature evolutions of all the compartment fire scenarios are plotted in Figure 2.

Fig. 2 Temperatures evolution in the compartments.

1.2 Localised fires

A localised fire with a $A_{fi} = 78.5\,m^2$ (EC, 1999b, Heskestad, 1983) was considered. The fire load density was $q_{f,k} = 45753$ MJ/m². As the maximum temperature reached in this fire at the level of the roof was only 400 ºC at 15.67 min, being the maximum flame length 5.94 m (see figure 3), this fire scenario was not considered on the mechanical analysis.
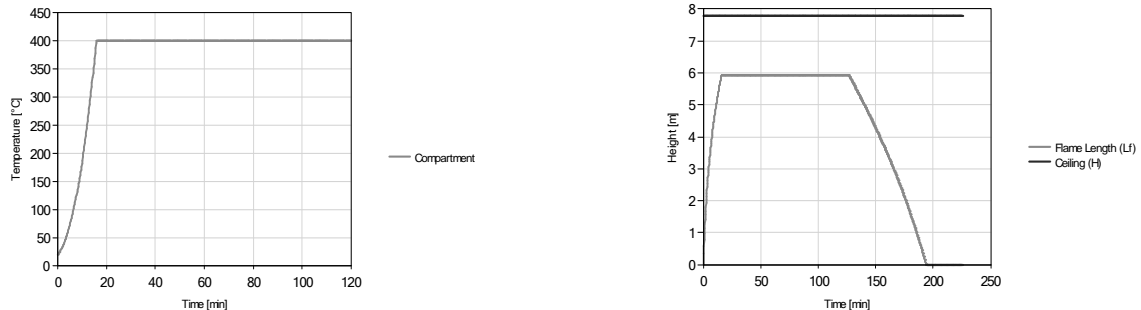

Fig. 3 Localised fire: fire compartment temperature evolution; flame length.

2 MECHANICAL ANALYSIS

A 3D mechanical analysis using the software SAFIR (Franssen, 2005, 2008), with beam and shell finite elements was used.

2.1 Mechanical actions

The fire is considered an accidental action, which means that the design value of the action effects in fire situation, should be obtained using an accidental combination as defined in EN 1990 (CEN, 2005c) and in accordance with the Portuguese National Annex of the EN 1991-1-2 (CEN, 2005a):

$$\sum G_k + \psi_{1,1} \cdot Q_{k,1} + \sum \psi_{2,i} \cdot Q_{k,i} + \sum A_d \qquad (1)$$

The roof loads were determined, in accordance with Annex A1 of the EN 1990 (CEN, 2005c), adopting the category H for roofs, which corresponds to the accidental combination:

$$1.0G_k + \psi_{1,1}Q_{k,1} = 1.0G_k + 0.0Q_{k,1} = G_k \qquad (2)$$

where G_k refers to the permanent loading and Q_k to the variable action.

2.2 Cross-sections analysis

The thermal analyses of the cross sections were performed with the program SAFIR. From these analyses it was obtained the temperature field of the cross sections for each of the considered fire scenarios, which was later applied to the mechanical analysis. No fire protection was considered in the thermal analysis.

In the main structural elements was considered that the cross sections were subjected to fire in all their four sides. Commercial sections such as SHS100x100x40 and HEA200 were used on these structural systems. In the roof it was considered fire on one side only (the underside). Figure 3 shows one of the sections analyzed (BNTA700) (Blocotelha, 2010).
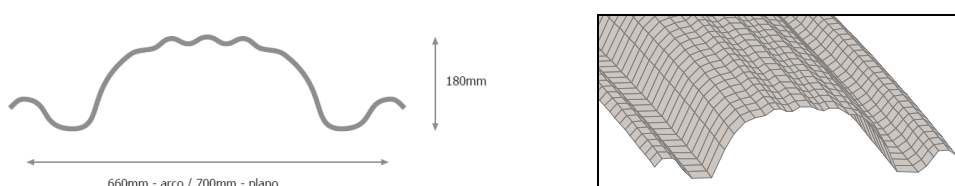

Fig. 3 Cross-section of the roof plate.

259

Three different roof plate sections (corresponding to the three units) were analysed. Their thickness varies between 0.8 and 1.5 mm, their geometry are also slightly different in each of the cross-sections.

2.3 Analyzed structural system

The main structural systems studied correspond to three-dimensional lattice girders. These truss structures were modelled with beam finite elements. Some of the truss structures were simply supported an others were continuous beams. Each unit of the waste treatment plant had a different truss structure as main structural system and different cold formed cross section for the roof sheeting, additionally the unit Post – composting had a continuous beam supporting the roof sheeting.

Several analyses were performed, being the structural elements subjected to the natural fire curves obtained from:

   a) Widespread fire in the reception unit (scenario 1 as defined in Section 1).
   b) Widespread fire in the post-composting unit (scenario 2 as defined in Section 1).
   c) Widespread fire in the storage unit (scenario 3 as defined in Section 1).

The following figure 4 shows the deformed beam lattice of the storage unit, subjected to the natural fire scenario 3, just before collapse (on 31 minutes).
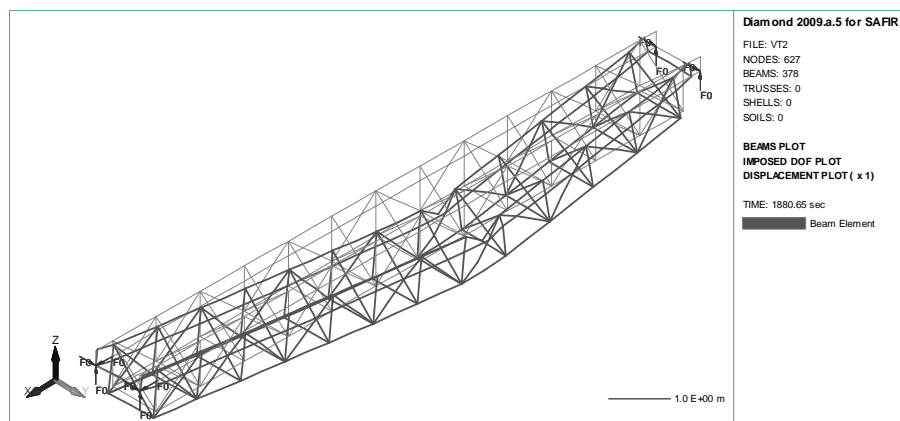

Fig. 4 Deformed shape of the truss structure of the storage unit, just before collapse (x1).

The self-supporting roof cold formed steel sheeting was analyzed using shell finite elements. This structural system was also composed of a tie rod connecting both extremities. Simplification of symmetry was used, thus considering only half of the coverage and a double support at one end and a "slide" at middle span. It were analysed the self-supporting roof sheeting with and without a tie rod with a diameter of 12 mm, also subjected to natural fire curve, and modelled using beam finite elements. Higher steel strengths on the steel sheeting due to the cold formed fabrication process (folding) were neglected.

The figures 5 and 6 show the deformed shape of the self-supporting roof of the composting unit, subjected to the natural fire scenario 2, just before collapse (43 minutes). Figure 5 illustrates the behaviour of the roof sheeting without the tie rod, while figure 6 presents the deformed shape when considering the tie rod. The time for collapse with and without the tie rod was the same
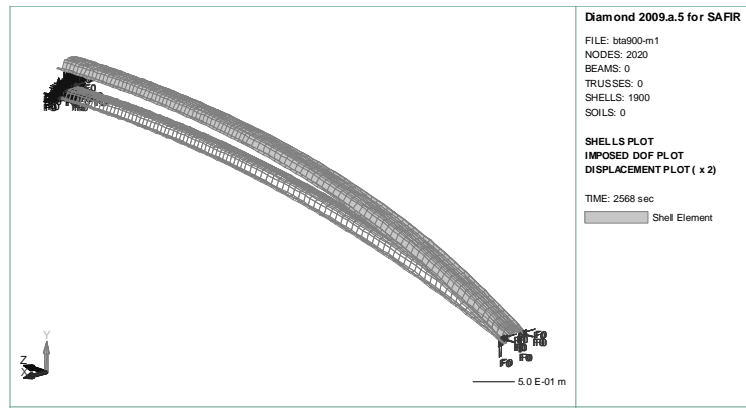
Fig. 5 Deformed shape of the roof sheeting of the composting unit, just before collapse (x2).
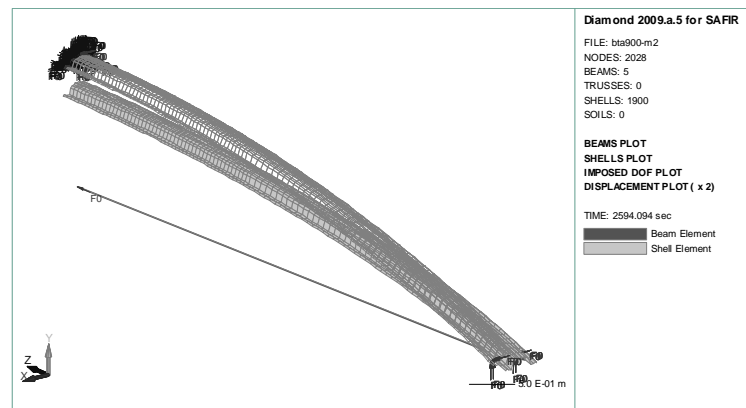

Fig. 6 Deformed shape of the roof sheeting with a tie rod, just before collapse (x2).

From the studies it was concluded that the steel structures of the various units comprising the waste treatment plant have, in the absence of passive fire protection, the resistance shown in tables 1 and 2.

Table 1 provides the fire resistance obtained for the main structures when subjected to the standard curve ISO 834 and to the fire scenarios obtained with the natural fire modeling.

Tab. 1 Fire resistance of the main structures

	ISO 834 (min)	Natural fire (min)
Reception truss structure	10	70
Post - composting truss structure	14	43
Post - composting continuous beam	37	47
Storage truss structure	9	31

Table 2 presents the fire resistance obtained for the cold formed self-supporting roof sheeting when subjected to natural fire scenarios.

Tab. 2 Fire resistance of the steel roof sheeting

	Natural fire (min)
Reception self-supporting roof sheeting (700x1.12)	> 120
Reception self-supporting roof sheeting (700x1.12) with a tie rod	> 120
Post - composting self-supporting roof sheeting (900x1.5)	43
Post - composting self-supporting roof sheeting (900x1.5) with a tie rod	43
Storage self-supporting roof sheeting (700x0.8)	30
Storage self-supporting roof sheeting (700x0.8) with a tie rod	30

As it can be observed, the instant of collapse with and without the tie rod is the same, meaning that the collapse is due to the sheeting and not due to the tie rode..

It can be also concluded that, according to the deformed shape of all the analyzed structural systems, the collapse, when it occurs, is towards the inside of the building, thus resulting in no danger to fire-fighters intervention.

3   CONCLUSION

In this work it was presented a case study to the fire resistance of the steel structure of a waste treatment plant using simplified and advanced calculation methods.

Based on studies conducted within European projects (EC, 1999a,b, RFCS, 2008), the steel structure temperatures development, resulted from a fire in a waste treatment plant, in Gaia Portugal, was analysed, in which the several compartments fit the classification of a large compartments.

The temperatures obtained with this analysis are relatively high, when compared to a prescriptive assessment following the standard ISO 834 fire curve.

The use of finite element models, on the mechanical analysis, has also revealed to be decisive, on better predict the actual behaviour of these structures in case of fire.

REFERENCES

Blocotelha, Catálogos de chapas metálicas autoportantes de coberturas, (in portuguese), 2010.

Cadorin, J.-F., Compartment Fire Models for Structural Engineering, Thèse de doctorat, University of Liege, Belgium, 2003.

Cadorin, J.-F., Franssen, J.-M., Pintea, D., Cajot, L. G., Haller, M., Schleich J. B., Software Ozone V2.2. University of Liege, Belgium and Arcelor Profil Luxembourg Research Centre, Luxembourg, 2006.

CEN (European Committee for Standardization), EN 1991-1-2, Eurocode 1 – Basis of design and actions on structures – Part 1-2: General rules – Structural fire design, 2005a.

CEN (European Committee for Standardization), EN 1993-1-2, Eurocode 3 – Design of steel structures – Part 1-2: Actions on structures exposed to fire, 2005b.

CEN (European Committee for Standardization), EN 1990, Eurocode – Basis of structural design, 2005c.

EC (European Commission), Development of Design Rules for Steel Structures Subjected to Natural Fires in Closed Car Parks, EUR 18867 EN, 1999a.

EC (European Commission), Development of Design Rules for Steel Structures Subjected to Natural Fires in Large Compartments, EUR 18868 EN, 1999b.

Franssen J.-M., SAFIR. A Thermal/Structural Program Modelling Structures under Fire, Engineering Journal, A.I.S.C., Vol 42, No. 3, 143-158, 2005.

Franssen, J.-M., User's manual for SAFIR 2007a, a computer program for analysis of structures subjected to fire, Structural Engineering, ArGEnCO, University of Liege, Belgium, 2008.

Franssen, J.-M. & Vila Real, P., Fire Design of Steel Structures. Eurocode 1: Actions on Structures. Part 1-2 – Actions on Structures Exposed to Fire. Eurocode 3: Design of Steel Structures. Part 1-2 – Structural Fire Design, ECCS, Ernst & Sohn, 2010.

Heskestad, G., "Luminous heights of turbulent diffusion flames", Fire Safety Journal, Elsevier, 1983.

MAI (Ministério da Administração Interna), Portaria n.º 1532/2008 (in portuguese), 2008.

RFCS (Research Fund for Coal and Steel), DIFISEK+ - Dissemination of Structural Fire Safety Engineering Knowledge, 2008.

Vila Real, P., Franssen, J.-M., Software Elefir-EN – Fire design of steel structural members according to Eurocode 3. http://elefiren.web.ua.pt, 2010.

FIRE RESISTANCE OF STEEL TRUSSES WITH OPENSEES

Panagiotis Kotsovinos [a], Asif Usmani [a]

[a] University of Edinburgh, School of Engineering and Electronics, Edinburgh, United Kingdom

INTRODUCTION

Steel trusses are an efficient structural system, widely used in practice in order to support loads over long spans. Hence, a structural failure of a truss can have enormous consequences. Steel truss sections can be especially vulnerable to fire because of typically high surface area to volume ratios and lots room for exposure from all sides. Fire resistance of trusses is therefore a very important research topic.

Many finite element codes, both commercial or research based, have been developed and are commonly used for modelling structures in fire. However most of these do not offer sufficient flexibility for adding new capabilities and are also not normally accessible to users or researchers for modification. The object oriented nonlinear finite element framework (OpenSees), primarily designed for earthquake engineering simulations, offers the necessary flexibility and access needed to further expand its capabilities.

Element formulations have been implemented within the OpenSees framework to model the behaviour of truss structures subjected to fire. The geometric nonlinearity caused by large displacements and material nonlinearity due to the stiffness and strength reduction experienced in a real fire have been accounted for.

It should be also noted that this extension allows for fire following earthquake analyses in a combined framework. The implementation includes modules for temperature dependent material properties according to the Eurocode and the effects of thermal expansion of structural members. Hence, the inelastic effects are accounted for by utilizing appropriate constitutive relationships. Although the implementation procedure is similar for different types of structures, this paper focuses on trusses. Several numerical examples are presented to demonstrate the accuracy of the proposed numerical procedure.

Different finite element formulations for truss elements are used based on the Total Lagrangian and Co-rotational formulation.

Excluding the strain due to creep effect the total strain is equal to the mechanical strain and the thermal strain:

$$\varepsilon_t = \varepsilon_m + \varepsilon_{th}$$

Where the thermal strain for a truss element, which considers only thermal expansion of the member, will be

$$\varepsilon_{th} = \alpha \, \Delta T = \alpha \, (T_{heated} - T_{ambient})$$

The total strain varies for different formulations. For the TL formulation the total strain will be equal the Green-Lagrange strain, while for the co-rotational formulation it will be equal to the engineering strain.

Furthermore, for elastoplastic problems the mechanical strain includes both the elastic and plastic strain

$$\varepsilon_m = \varepsilon_e + \varepsilon_p$$

The thermal strain does not produce any stress, therefore

$$\sigma = \sigma(\varepsilon_m)$$

Stress has to be work conjugate with strain, so for the total Lagrangian formulation the stress measure will be the second Piola-Kirchoff stress (S) while for the co-rotational formulation it will be the simple engineering stress.

For elastoplastic problems the stress in an element will be equal to

$$\sigma = E(T) \, \varepsilon_e = E(T) \, (\varepsilon_t - \varepsilon_{th} - \varepsilon_p)$$

The axial force in the element is given by
$$N = \sigma\, A$$

While the internal resisting force of the element is given by
$$P = \sigma\, A\, L_0\, B^T$$

Where B is the classical strain-displacement matrix

1   LOAD CONTROLLED STEP BY STEP NUMERICAL ANALYSIS

Analysis of structures in fire is usually performed into two load steps. The mechanical load is first applied as the first load step and remains constant for the second thermal load step. Such an analysis often involves the use of a step by step numerical method. The most used step by step method is the load controlled Newton-Raphson method. The temperature of the element is provided as an input. The temperature is multiplied by the load factor, as in mechanical analysis, to give the first temperature increment. During that increment, the material tangent and the thermal strain are queried from the material class in order to obtain a guess for the thermal force in the element for the first iteration which will be equal to $EA\varepsilon_{th}$. Then, further iterations follow until the equilibrium conditions are satisfied inside a convergence limit and the next increment is then applied. During each iteration the tangent stiffness matrix of the element gets updated as well as the material stress gets calculated. At the end of the iterations and before the next increment, the resisting force gets updated by removing the thermal force found in that increment from the load resulting from the material stress in order to find the actual force in the element.

For each load step during the analysis an incremental displacement is found out according to equation below.
$$\{\Delta F\} = [K]\,\{\Delta u\}$$

where ΔF is the Vector of Incremental forces
        K is the Stiffness Matrix
        Δu is the Vector of Incremental Displacements

Furthermore to remove the residual or unbalanced forces (R), iterations are included inside an increment to determine the converged displacement. The unbalanced forces are computed as the difference between total applied loads (P) and the internal resisting forces of the structure (F) as shown in the equation below for the jth iteration of the ith incremental step

$$\{R^i_{j-1}\} = \{P^i_{j-1}\} - \{F^i_{j-1}\}$$

The drawback of this load controlled procedure is that it cannot follow the equilibrium path beyond the limit points. This is the point where failure of the element takes place or a temporary loss of stability is experienced and then a post buckling path is followed. This drawback is not important for some simple or determinate structures, but for redundant structures local failure does not imply global failure of the whole structure which may be able to continue to carry the loads, without the contribution from the failed member. This is because redundant structures can find different load paths by which to support additional load when its local strength is reached at a single location (Rotter et al, 1999). Hence, alternative step by step procedures have also to be employed to check if the structure will continue to be stable or collapse. For this reason a dynamic procedure (Franssen & Gens, 2004) has been developed to make to analyse structures in fire in the OpenSees framework. An example of such an analysis is given in example 3.3.

In case of a dynamic analysis, the residual equation provided before becomes
$$R = P - Ma - Cv - F$$

Where P is the external force, Ma is the inertia force, Cv is the damping force and F is the internal force due to deformation.

2 MATERIAL MODELS OF STEEL

Several fire resistance tests of structural steel members have shown that high temperature causes material degradation so the reduction of material properties like Young's modulus and Yield Stress have to be accounted for by utilizing appropriate constitutive relationships. Hence, new uniaxial elastic plastic material models have been developed by modifying appropriately the existing ones under the OpenSees framework that take into account the material degradation under elevated temperatures, the bilinear material model (Steel01Thermal) and the elliptic material model (Steel02Thermal) (Usmani et al, 2010).

2.1 Bilinear Material

Steel01Thermal is a uniaxial bilinear steel material with kinematic hardening. The information required for this material are yield strength (F_y), Young's modulus (E_0) and strain hardening parameter (b). This material is approximate but computationally efficient at the same time. It should be noted that this material is allowed to have both constant strain hardening and temperature dependent strain hardening as suggested by Shen and Zhao (1995).

2.2 Elliptic Material

Steel02Thermal is a uniaxial Giuffre-Menegotto-Pinto steel material with isotropic strain hardening. Here the material depends on the young modulus and the strain hardening parameter as before but also from the yield stress at the start of the elliptic curve as well the yield stress at the end of the elliptic curve. Compared to the Steel01Thermal material it is considered to provide more realistic results.
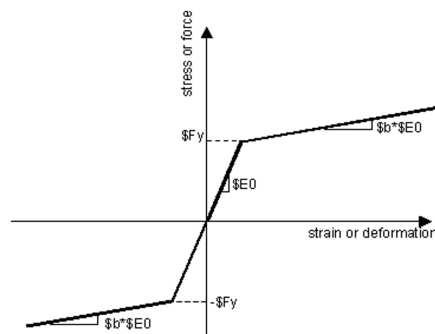
Fig. 1 Bilinear Material   Fig. 2 Elliptic Material
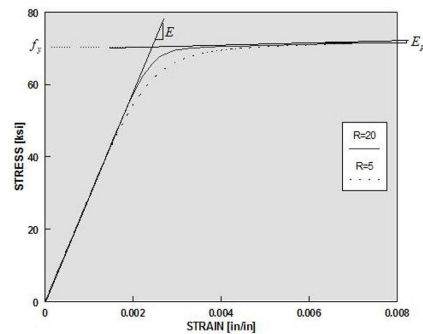
3 NUMERICAL MODELLING

Some numerical examples are presented to validate the procedures developed.

3.1 Restrained truss

The first example is a restrained truss which is restrained against thermal expansion and half of it is heated. This truss is modelled using two elements but only the left one is heated (Figure 3). The aim of this example is to demonstrate that the developed procedure captures both geometrical (thermal expansion) and material (yielding) effects. The length of each element is 1000mm. The area of the elements was selected as 100mm^2. The boundary conditions of the truss were restrained both horizontally and vertically. The example was solved by both Total Lagrangian and Co-rotational formulations and for constant strain hardening equal to 0.1 as well as temperature dependent properties using the values suggested by Shen and Zhao (1995). The results of the analyses are shown in Figure 4.
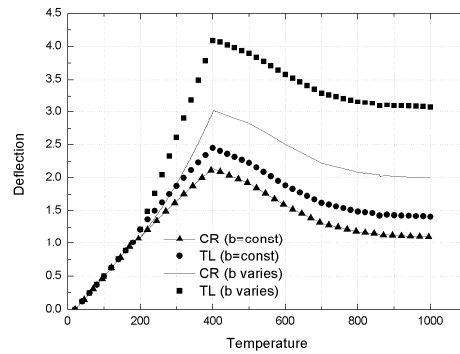
Fig. 3 Restrained truss   Fig. 4 Load-deflection curve

The results show that the model can capture both geometric and material phenomena. In the case of the formulations with constant strain hardening it can be seen that although the members yield early (at a temperature of about 200^0C), they continue to expand almost linearly until the temperature reaches about 400^0C when the yield stress of the material drops. Then the members deform towards the opposite direction.

For the case of temperature dependent strain hardening it can be seen that the curve shows a similar behaviour. The difference with the previous case is that because the strain hardening changes here the members have different behaviour after the yield point.

3.2 One member truss

The example selected is the benchmark provided by Lin et al (2010) which was solved analytically by the authors using a Total Lagrangian approach. For comparison purposes both Total Lagrangian and Co-rotational procedures developed are examined here. The temperature increments for the OpenSees modelling were applied in 10^oC steps.
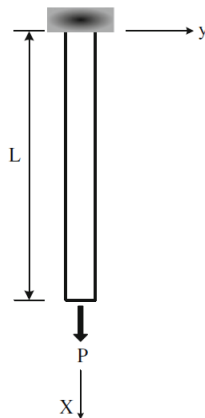
Fig. 5 One member truss   Fig. 6 Load-deflection curve
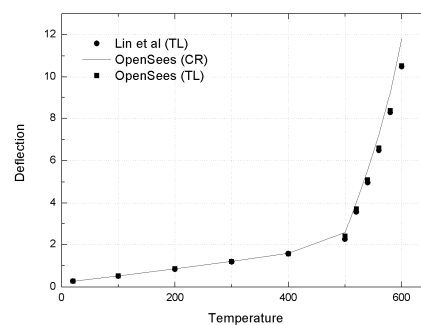
The comparison between the authors and OpenSees results shows very good agreement. Furthermore, as expected the OpenSees TL solution is almost identical to the analytical one as it is also based in a TL formulation. The CR solution finds a slightly higher result by 1mm.

3.3 Two Member Truss

This example was also solved by Lin et al (2010) using a Generalised Displacement Control (GDC) method and loses stability through snap-through buckling. In order to analyse this example a

266

dynamic procedure was followed. Further details of the dynamic approach for modelling the post-buckling behaviour will not be discussed here as it is outside the scope of the present paper.
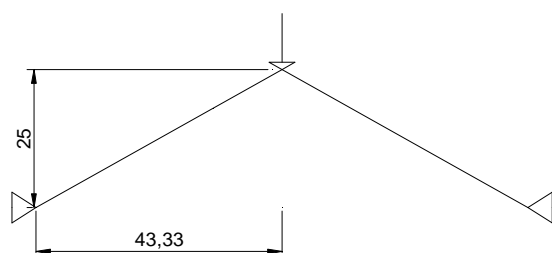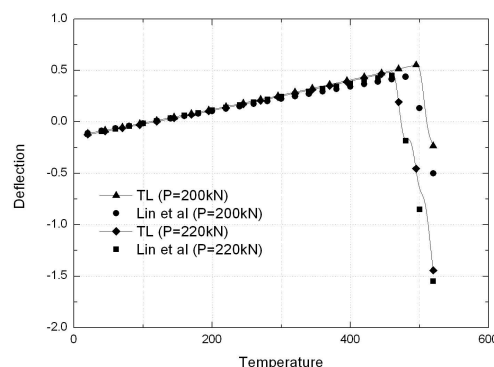

Fig. 7 Two member truss   Fig. 8 Load-deflection curve

The results of the dynamic analysis agree well with those obtained from Lin et al (2010) using Generalised Displacement Control (GDC). The slight difference between the results is attributed to the different analysis technique. A static analysis using the GDC method will show convergence for most problems (except when snap-back problems are involved) but does not take into account the inertia forces that are developed.

For the particular example it is also of interest to note that as the temperature increases the truss deflects upwards but when the members have yielded, the deflection of the truss changes direction towards the other side. Moreover, the differences of the final deflection for the 200kN and 220kN cases show that the effect of preloading plays a role in the behaviour of the truss.

4   SUMMARY

This paper presented the procedures developed for modelling the fire resistance of trusses in the object oriented and open source framework OpenSees. More specifically Total Lagrangian and Co-rotational formulation based elements to account for the nonlinear effects. Several numerical examples have been presented to demonstrate the procedures developed. A dynamic approach was also followed to examine the postbuckling response of a truss that loses stability through snap-through buckling.

5   ACKNOWLEDGMENTS

REFERENCES

Franssen J.M., Gens F., Dynamic analysis used to cope with partial and temporary failures, Proceedings of International Workshop on Structures in Fire, Ottawa, 2004, 1089-94

Lin T.J., Yang Y.B., Huang C.W., Inelastic nonlinear behaviour of steel trusses cooled down from a heating stage, International Journal of Mechanical Sciences 52 (2010) 982-992.

J.M.Rotter, A.M.Sanad, A.S.Usmani, and M.A.O'Connor. Structural performance of redundant

structures under local fires. In *Proceedings of Interflam'99*, Edinburgh, Scotland, June-July 1999.

Usmani A. S. , Rotter J. M., Lamont S., Sanad A. M., GIllie M., Fundamental principles of structural behaviour under thermal effects, *Fire Safety Journal*, 36(8), 721-744 (2001).

Usmani A., Zhang J., Jiang J., Jiang Y., Kotsovinos P., May I., Zhang J., Using OpenSees for Structures in Fire, Proceedings of International Conference on Structures in Fire, Michigan, 2010, 1089-94

Shen J.Y., Zhao J.C., Modelling fire resistance behaviour of multi-storey steel frames, Proceedings of International Conference on Computing in Civil and Building Engineering, Berlin, 1995, 1089-94

Wang P., Li G., Guo S., Effects of the cooling phase of a fire on steel structures, Fire Safety Journal 43 (2008) 451-458.

TEMPERATURE OF STEEL COLUMNS EXPOSED TO LOCALISED FIRE

Zdeněk Sokol [a]

[a] Czech Technical University Prague, Faculty of Civil Engineering, Prague, Czech Republic

INTRODUCTION

Temperature of steel structures exposed to fire is the critical factor influencing the resistance. The temperature depends on the fire behaviour, position of the element with respect to the fire and fire protection. There are simple models for prediction of temperature of both unprotected and protected steel elements. These models can be easily used for compartment fires and for beams exposed to localised fires.

Fig. 1. Column exposed to localised fire, fire test Mittal Steel, Ostrava, June 2006

1. STEEL STRUCTURES EXPOSED TO LOCALISED FIRE

Gas temperature at localised fire depends on distance from the fire. The highest temperature can be observed in the plume and in the hot zone directly above the fire. The temperature in far from the fire is quite low.

As a result, the temperature of elements exposed to localised fire is variable along their length. The highest temperature of beams is observed above the fire, but it is decreasing at larger distances. There are two models for beams: the Heskestad model applicable at situation when the beam is not engulfed in flames and Hasemi model for beams engulfed in flames. These models are included in standard EN 1993-1-2.

The standard does not give any rules for evaluation the column temperature. Application of step-by-step method in combination with Heskestad model for localised fire is given in this paper.

2. MODEL OF LOCALISED FIRE

The model for localised fires in situation when the flames do not impact the ceiling gives the length of the flames and temperature along the vertical axis of the fire. The model is given in Annex C of EN 1991-1-2.

The input parameters include:

- Fire growth rate given as time t_α to reach the rate of heat release 1 MW,
- Fire load in MJ,
- Maximum rate of heat release for fuel-controlled fire RHR_f produced by 1 m^2 of the fire, depending on type of combustible materials,
- Maximum fire diameter D.

These input data are used to derive the rate of heat release Q. The concept of t-square fires is included in EN 1991-1-2, Annex E, see Fig. 2. The picture indicates the rate of heat release at any time of the fire and consists of three phases: the growing phase of the fire, steady state represented by horizontal plateau and the decay phase. It is assumed the fire is fuel-controlled. In case when the fire is ventilation-controlled, the maximum rate of heat release needs to be reduced according to amount of oxygen available in the fire compartment, see Fig. 3, where H_u is net calorific value of combustible materials, m is combustion factor, ($m = 0,8$), A_v is opening factor and h_{eq} is height of the opening. The details are given in EN 1991-1-2.
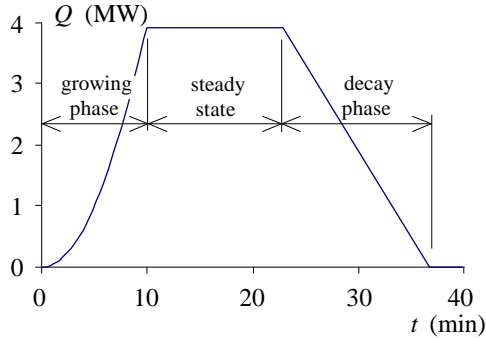
Fig. 2. Model of rate of heat release according to EN 1991-1-2
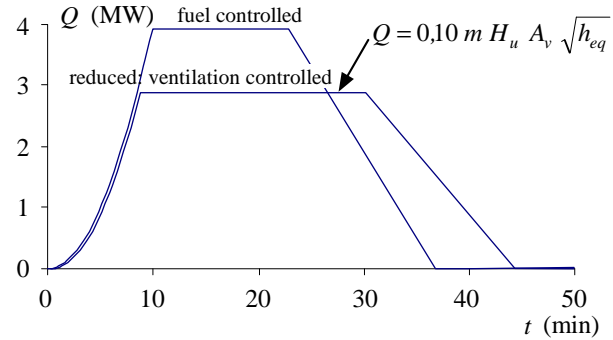
Fig. 3. Model of rate of heat release for fuel-controlled fire

The gas temperature along the vertical axis of the fire is given by:

$$\theta_g = 20 + 0,25\, Q_c^{2/5} (z - z_0)^{-5/3} \tag{1}$$

where Q_c is the convective part of the rate of heat release

$$Q_c = 0,8\, Q \tag{2}$$

and the virtual origin z_0 is

$$z_0 = -1,02\, D + 0,00524\, Q^{2/5}. \tag{3}$$

The length of the flame L_f as function of time t (depending on rate of heat release Q) is given by

$$L_f = -1,02\, D + 0,0148\, Q^{2/5} \tag{4}$$

where the fire diameter D at time t can be obtained from

$$D = \sqrt{\frac{4\, Q}{\pi\, RHR_f}}\,. \tag{5}$$

3. TEMPERATURE OF COLUMN NOT ENGULFED IN FLAMES

The prediction of column temperature is not described in the standard EN 1993-1-2. In cases when the flames impact the ceiling the Hasemi model can be used also for columns giving their temperature of the upper part. As an alternative, zone model can be used and the column temperature can be derived from the hot zone temperature. This approach can be used for relatively small compartments and compartments with low height where the hot zone temperature is high and the column temperature is significant.

However, for columns in large and high compartments, the above method does not give satisfactory results as the hot zone spreads to large area, therefore its depth and temperature is low. The column temperature in the upper part is not significant, but the lower part might be heated by radiation from the localised fire and the column temperature can be much higher than temperature at the top.

The column temperature can be calculated when the effect heat gained from radiation and heat „loses" by convection and surrounding space is taken into account, see Fig. 4. Standard step-by-step method as in EN 1993-1-2 can be used and is described in the paper with these assumptions:

- The fire temperature is calculated according to model described above (EN 1991-1-2, Annex C), flames do not impact the ceiling,
- the localised fire is replaced by cylindrical surface with diameter equal to diameter of the fire. The position of the column with respect to the fire, see Fig. 4,
- the column is not engulfed in the flames, the heat is transferred to the column by radiation only,
- the emisivity of the fire is 1,0,
- the column is surrounded by cold air, the ambient temperature is 20°C,
- the temperature is variable along the column height,
- non-uniform temperature of the cross-section is neglected,
- the effect of heat conduction along the column length is neglected, this is conservative assumption leading to higher column temperature.
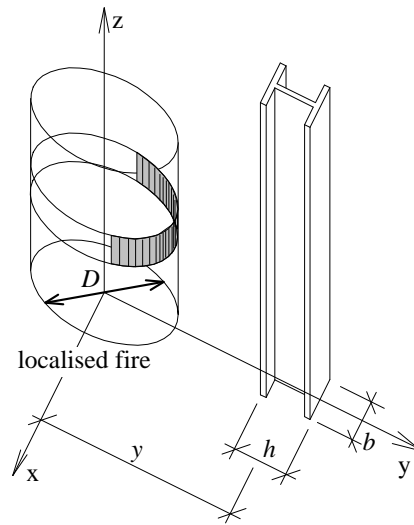
Fig. 4. Model of column exposed to localised fire

The heat gained by the column can be calculated from the heat flux received from any point of the flames (cylindrical surface) as

$$h_{net,gain} = \Phi \, \varepsilon_{res} \, \sigma \left(\left(\theta_g(z) + 273 \right)^4 - \left(\theta_m + 273 \right)^4 \right), \tag{6}$$

where the flame temperature (temperature of the radiating surface) $\theta_g(z)$ is variable with respect to distance from the floor of the compartment z.

The heat which is lost from the column because of convection and radiation to surrounding space is obtained from the corresponding heat flux given by

$$h_{net,loss} = (1-\Phi)\varepsilon_m \, \varepsilon_f \, \sigma \left(\left(\theta_m + 273 \right)^4 - \left(20 + 273 \right)^4 \right) + \alpha_c \left(\theta_m - 20 \right), \tag{7}$$

where the heat transfer coefficient $\alpha_c = 25$ W/m^{2}K.

As the flame temperature depends on height, the radiating surface needs to be divided to rings according to Fig. 4. Temperature of the ring is assumed to be uniform, and the total heat flux to any location on the column is obtained as sum of the fluxes from all the rings (including the heat loss) as

$$h_{net} = \sum h_{net,gain} - h_{net,loss} \tag{8}$$

The column is exposed to radiation on three sides only, Fig. 5, and the shadow effect is taken into account by considering the envelope of the column cross-section.

4. CONFIGURATION FACTOR

The effect of radiation include the configuration factor Φ. General formula for its evaluation is

$$\Phi = \int_{A_1} \frac{\cos \varphi_1 \, \cos \varphi_2}{\pi \, r^2} \, dA_1 \,, \tag{9}$$

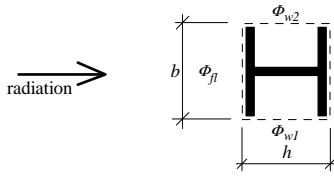where the angles of source area A_1 and target area A_2 are shown on Fig. 6.

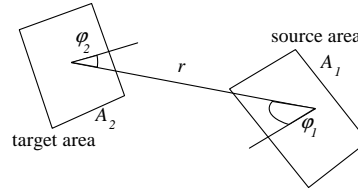Fig. 5. Envelope of the column cross-section and surfaces exposed to radiation

Fig. 6 Configuration factor Φ

The configuration factor is evaluated for each rectangle comprising the ring of the radiating surface. Only the visible part of the ring is taken into account, see Fig. 4. The total heat flux from that ring is therefore given as sum of the heat fluxes from these small rectangles at equal temperature.
The configuration factor was calculated numerically using the equation above. It is calculated separately for the front surface of the column (column flange, Φ_{fl}) and for both side surfaces (column webs, Φ_{w1} and Φ_{w2}).
The resulting configuration factor from the single ring to any location on the column is given by

$$\Phi = \frac{b \, \Phi_{pas} + h \, (\Phi_{st1} + \Phi_{st2})}{b + 2 \, h} \,. \tag{10}$$

5. RESULTS

The method described above was used to evaluate the column temperature of single storey industrial building sized 60×150 m with height 7 m. The building is used for metal forming and assembling of final products. Only non-combustible materials are presented in the building and the assumption of localised fire fits to the nature of the building. The next pictures show results from two fire scenarios: localised fire of metal-forming machine and localised fire of a fork lift. Fire resistance 15 minutes is required.

5.1 Localised fire of metal-forming machine

Exact evaluation of the fire load is difficult as there are no data available. The fire load is based on estimation of amount of combustible material and its calorific value (electric components, cables, switches, covers, oil fill). The characteristic value of fire load is

$$Q_{f,k} = \sum m \, H_u = 10 \cdot 40 + 5 \cdot 43{,}2 = 616 \text{ MJ} \,.$$

and the design value of fire load (based on compartment size and danger of fire activation)

$$Q_{f,d} = \delta_{q1} \, \delta_{q2} \prod \delta_{n,i} \, m \, Q_{f,k} = 2{,}2 \cdot 1{,}22 \cdot 1{,}0 \cdot 0{,}8 \cdot 616 = 1326 \text{ MJ} \,.$$

Medium fire growth rate with $t_\alpha = 300$ s, maximum fire diameter $D = 2$ m and maximum rate of heat release $RHR_f = 500$ kW/m^2 were chosen as the parameters for the localised fire. The maximum rate of heat release RHR_f and fire growth rate t_α were chosen in such way the end of the steady state is the same as the required fire resistance, i.e.15 minutes.
The rate of heat release derived from the parameters above is shown on Fig. 7.
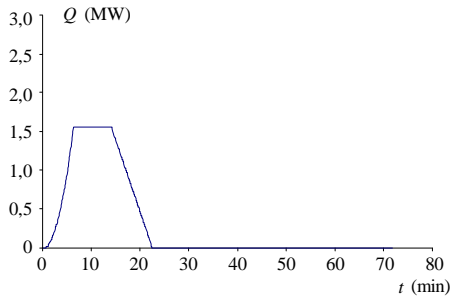The length of the flame is shown on Fig. 8.
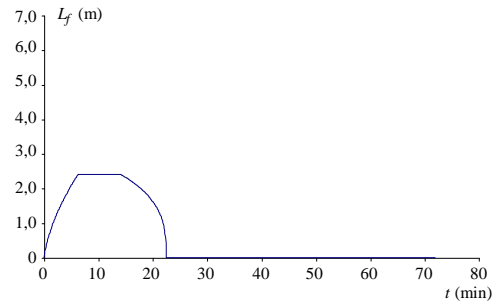
Fig. 7 Rate of heat release

Fig. 8 Flame length

The maximum flame length is 2,41 m, the flame does not impact the ceiling.

Temperature of the hot zone below the ceiling was calculated using zone model (Ozone software). Because the maximum gas temperature is only 60°C, the temperature of the upper part of the column does not to be considered as significant for the column resistance.
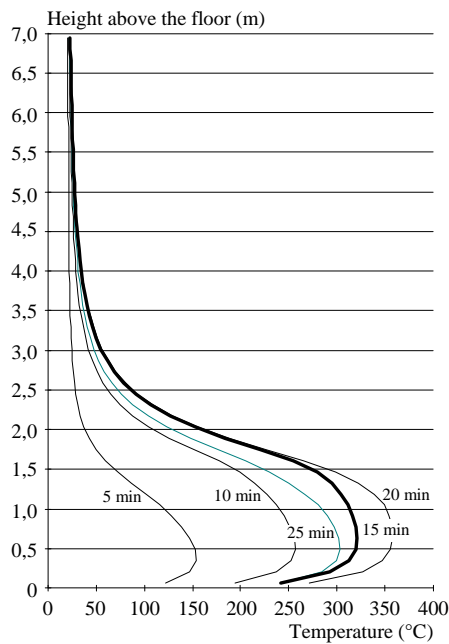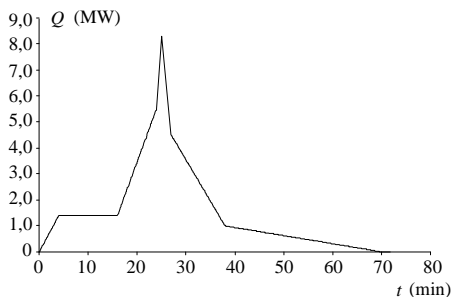

Fig. 9 Temperature of column section HEA 260 along the height

The maximum column temperature 320°C at time 15 minutes is reached 0,65 m above the floor.

5.2 Localised fire of forklift

The parameters of localised fire were of the forklift were adopted from research focused on fires in car parks, as rate of heat release of the forklift is not available. Diameter of the fire was chosen to be the same as length of the forklift, i.e. $D = 2,70$ m. Rate of heat release is shown on Fig. 10.

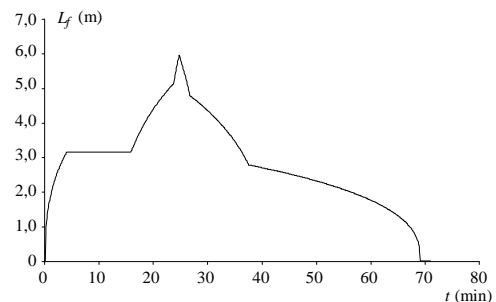
Fig. 10 Rate of heat release

Fig. 11 Flame length

The maximum flame length is 5,91 m, the flames do not impact the ceiling.

The gas temperature of the hot zone is only 90°C, therefore the temperature of the upper part of the column is not significant for the column resistance.

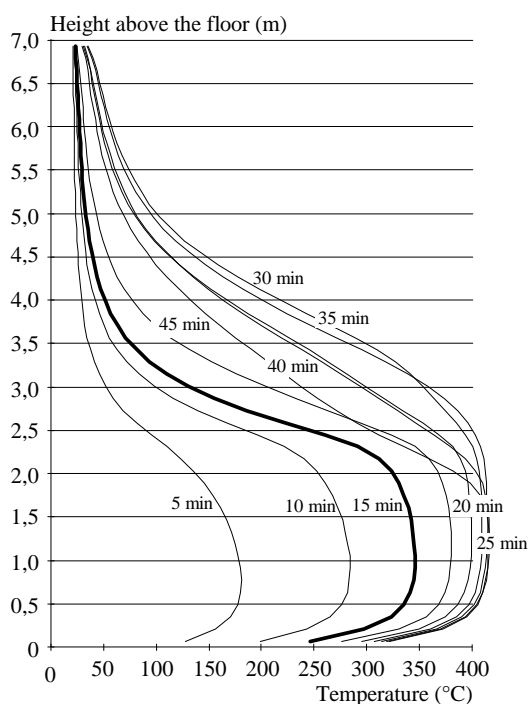The maximum column temperature 345°C at time 15 minutes is reached 1,10 m above the floor.

Fig. 12. Temperature of column section HEA 260 along the height

6. SUMMARY

The method described in this paper can be used to evaluate temperature of steel columns exposed to localised fire which is not dealt in European standards. It is compatible with EN 1991-1-2 and EN 1993-1-2. It is necessary to use numerical calculation of configuration factor and step-by-step method. Results from practical application are included.

ACKNOWLEDGEMENT

REFERENCES

EN 1991-1-2, Eurocode 1:Actions on structures – Part 1-2: General actions – Actions on structures exposed to fire, Brussels: CEN, November 2002.

EN 1993-1-2, Eurocode 3: Design of steel structures – Part 1-2: General rules – Structural fire design, Brussels: CEN, December 2003.

Buchanan A.H., Structural design for fire safety, Wiley, New Zealand, 2002.

Franssen J.M., Zaharia R., Design of Steel Structures Subjected to Fire, Background and Design Guide to Eurocode 3, University Liège, 2005.

Development of design rules for steel structures subjected to natural fires in closed car parks, CEC Agreements 7210-SA/211/318/518/620/933: Validation of the method & Measured rate of heat release of burning cars.

Sokol, Z. - Wald, F.: Prediction of Column Temperature Exposed to Localised Fire. In Technical Sheets 2008 - Part 3. Praha: CIDEAS-Centrum integrovaného navrhování progresivních stavebních konstrukcí, 2009, vol. 3, p. 59-60.

Sokol, Z. - Wald, F. - Kallerová, P. - Bonnet, N.: Column Behaviour during Localised Fire Test. In Proceedings of the Fifth International Conference Structures in Fire. Singapore: Nanyang Technological University, 2008, p. 256-263.

BEHAVIOUR OF FRAME COLUMNS IN LOCALISED FIRES

Ruirui Sun [a], Ian Burgess [a], Zhaohui Huang [a]

[a] University of Sheffield, Department of Civil and Structural Engineering, Sheffield,UK

INTRODUCTION

Column behaviour plays a key role in the robustness of framed structures in fire, and a key research topic in recent years [1-4] has been the effect of axial restraint from superstructure on column buckling. As a result of these studies, the limiting (initial buckling) temperature of a column can now be predicted with reasonable accuracy. However, most studies have concentrated on isolated columns with clearly defined boundary and loading conditions. It is well recognised that the behaviour of a column in a complete building differs from that of an isolated column, because of the effects of structural continuity. In a frame, both the critical temperature of a column and its capacity to re-stabilize after initial buckling are important aspects of preventing a progressive collapse mechanism from developing. A conventional static analysis is terminated when a local instability takes place. To evaluate frame behaviour after initial instability the analysis should be continued beyond this instability until total collapse or re-stabilisation happens. In this paper, a simplified method to predict the behaviour of an individual column as a result of its interactions with other frame members is described and tested against a newly-developed static/dynamic analysis.

1   STATIC/DYNAMIC PROCEDURE AND FRAME ANALYSIS

In order to overcome the propensity of conventional static analysis to fail at the first singularity and to enable the analysis to continue through its unstable stage, a combined static and dynamic procedure has been developed for *Vulcan*. With this extended capability, it has been possible to trace the structural behaviour of single members or whole frames from initial static response, through local failure or instability, to stable post-buckling behaviour. The dynamic analysis is carried out by an explicit scheme. It has the benefit of avoiding convergence checking, and is therefore less time-consuming within each time step. The explicit scheme has been widely used for structural progressive collapse analysis. This particular implementation has been validated [5] using several practical cases. In this study, it is used to carry out structural analysis of steel frame under localised fire conditions. A planar frame shown in Fig.1 has been tested under localised fire conditions. The central column at ground floor level is assumed to be heated by an IS0834 fire curve.
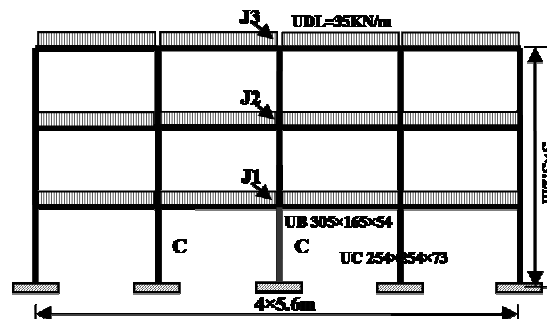

Fig. 1: The test frame.

Failure of the frame develops through three stages, as shown in Fig.2. In Stage I the column is heated progressively, and its thermal expansion against restraint provided by its superstructure increases its compressive force. When this force rises to the level of the capacity of the column, degraded by its increased temperature, the column will buckle. In Stage II, the ends of the beams attached to the column and its upper storeys move downwards with the vertical buckling deflection of the heated column. Moments then develop at the ends of these beams as this deformation

increases. If these moments exceed the beams' plastic moment capacity, plastic hinges will be generated at their ends. During this stage, catenary action is gradually activated. The catenary force is highest in the beams directly connected to the failed column. The axial forces in these beams will pull the adjacent columns inwards; the forces in the upper-storey beams are much lower since the upper storeys of these columns stay vertical. If the lateral restraint from the outer bays is not stiff and strong enough to stabilise this deformation, Failure Stage III is initiated. Plastic hinges are generated in the neighbouring columns, and the total collapse of the frame happens.
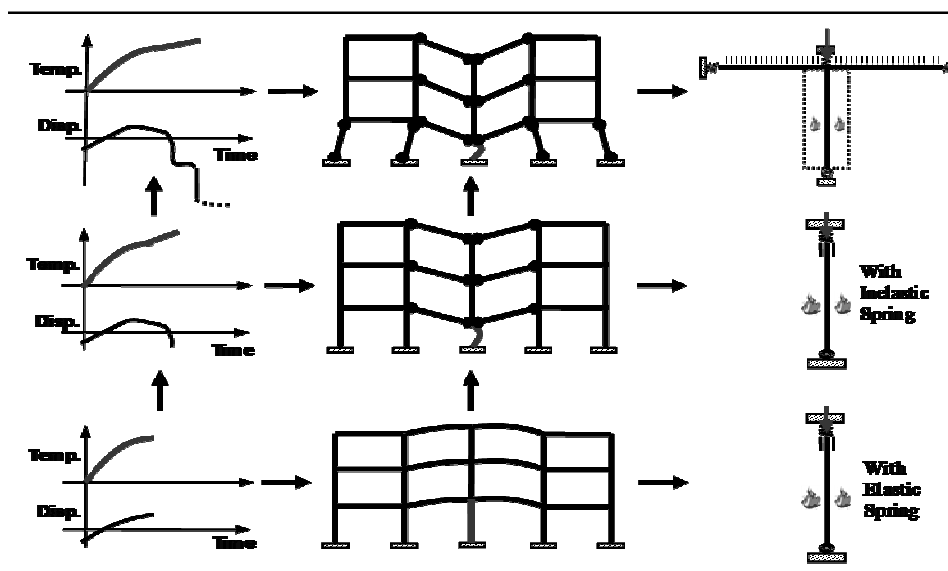
Fig. 2: Failure process and proposed simplified model.

On the basis of these three stages, the simplified model has been proposed. The key to Stage I is the buckling, or critical, temperature of the heated column, which depends on the stiffness of the axial restraint provided by the upper-storey beams above the column. This can be simulated by a simple model containing a single column with an axial elastic spring at the top end. For Stage II, the simultaneous yielding of the beam directly attached the column's upper storeys can be considered implicitly in the force-displacement characteristic of the spring. In order to take into account catenary action, the beams connected to the heated column are included in an extended simplified model, and the lateral restraint provided by surrounding bays are also simulated by horizontal springs. Several terms are clarified as follow:

Initial critical temperature of column: the temperature at which the column initially buckles.

Collapse temperature of column: the temperature beyond which the column restrained by inelastic restraints cannot achieve any re-stabilisation.

Collapse temperature of frame: the temperature beyond which no re-stabilisation position can be achieved by model with column and beams.

2   SIMPLIFIED MODEL

2.1 Restrained column model

The column model with elastic axial restraint has been studied by other researchers such as Poh and Bennetts [6], Shepherd [1] and Ali *et al.* [3]. As discussed above, these researches mainly focus on studying the buckling temperatures of restrained columns. The post-buckling behaviour of columns and their interaction with other members of the frame are outside their scope. Recently, a simplified spreadsheet calculation to predict the column behaviour from pre-buckling, through the buckling stage, and then in the post-buckling stage, has been proposed by one of the authors on the basis of the simplified model described previously. In this study, the simplified restrained column model, analysed by the static/dynamic version of *Vulcan* will be used to validate this calculation method, and this model will also be extended later to study the column behaviour considering the interaction

with other members of the frame. The comparison of results from the *Vulcan* analysis and the spreadsheet calculation method is shown in Fig.3.
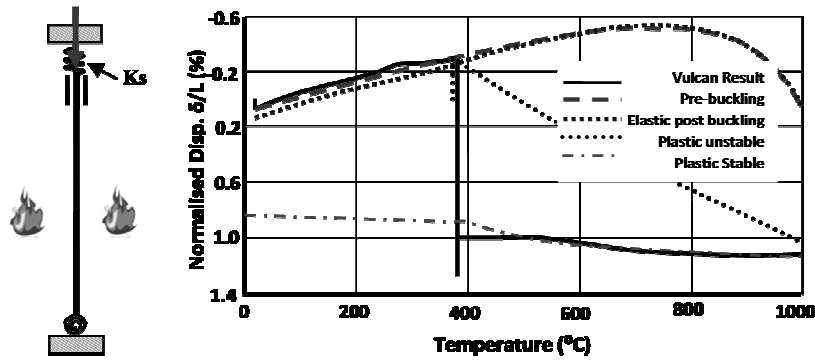

Fig. 3: Comparison of results from different simplified models.

2.2 Restrained column model considering beam yielding effects

In Stage I the restraint stiffness from beams above the heated column (Fig. 4) is:

$$K_s = \frac{12E\sum I_s}{L_s^3} \tag{1}$$

This calculation of lateral beam stiffness assumes that both ends of the beams are completely fixed against rotation, but this is not the case in a real structure. If the rotational stiffness of connections is considered, the lateral stiffness of a beam can be modified to:

$$Ks = \frac{1}{\frac{L^2}{2K_\theta}+\frac{L^3}{12EI}} \tag{2}$$

where K_θ is the initial rotational stiffness of the semi-rigid connections.

A purely elastic spring cannot represent the restraint conditions realistically if beam yielding takes place. When the beams above the affected column yield the restraint stiffness provided by these beams to the column will be lost, and the restraint condition of the column changes. When the plastic hinges are formed at the ends of a beam, the vertical shear force carried by the beam can be calculated as strength (see Fig. 5):

$$F_{pb} = 2 \times \frac{M_p}{L} \tag{3}$$

The restraint strength provided by the other beams above the column is determined as:

$$F_p = \sum F_{pb} \tag{4}$$

If taking connections into consideration and assuming that the plastic hinge forms in connections, this restraint strength can be estimated as:

$$F = \sum F_p = \sum \frac{2M_\theta}{L} \tag{5}$$

where M_θ is the aggregated moment capacity of the connections.

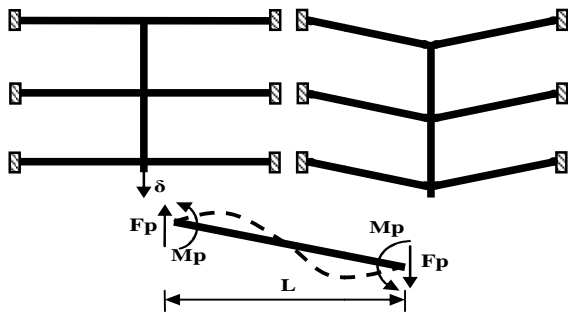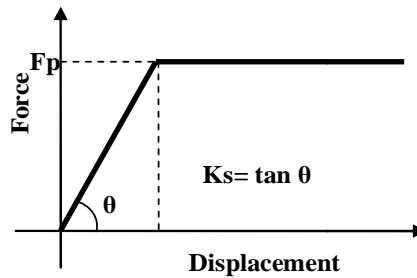Fig. 4: Beam yielding effects.   Fig. 5: Force-Displacement Curve.

2.3 Extended model

After the column has initially failed, large deformations develop in the attached beams. The force shed by the failed column transfers to the adjoining members through catenary action. To investigate the effect of this catenary action, a sub-frame with column and beam members is shown in Fig.6. The top of column and the outer ends of the beams are restrained by springs. As discussed above, the spring at the top of the column is inelastic, while the lateral stiffness provided by the adjoining columns is represented by elastic springs. The stiffness of the lateral restraint springs at the ends of the beams provided by neighbouring column bays, and is calculated as:

$$K_C = \frac{12E \sum I_s}{L_s^3} \qquad (6)$$

In order to test the ability of the extended model to predict the column behaviour in a frame, the results from this model have been compared with those from full-frame analysis. As can be seen from Fig.7, the extended model can predict very well not only the initial failure temperature of the column but also the re-stabilisation of the frame.
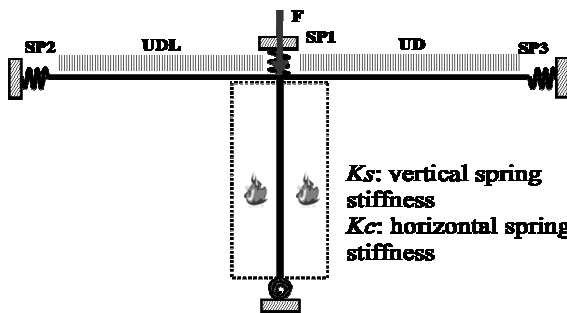

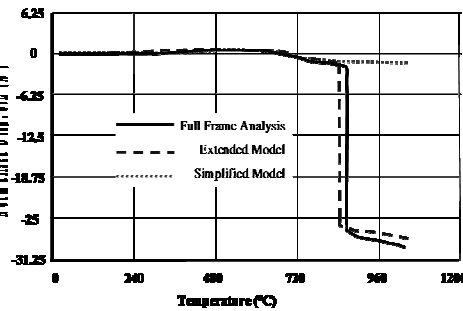Fig. 6: Simplified model.   Fig. 7: Comparison of results.

3   PRELIMINARY PARAMETRIC STUDIES

With the simplified model, the key behaviour of frame can be predicted rather than carrying out complex full frame analysis. Three stages of failure have been described above. The restraints from above beams and lateral supports significantly affect the structural behaviour during these three stages. In first stage, the axial restraint of column influents the critical temperature of column buckling; in second stage, the strength of restraints determines whether the beam above yields or not; in last stage, the centenary force develops in beam and connections and lateral restraints would be important for re-stabilisation of frame. Several parameters have been studied to identify their influence on the behaviour of column considering the interaction with surrounding members.

3.1 Strength and stiffness of restraints from superstructure

When the heated column has buckled, the beams will support an increased proportion of the super-imposed load. If the beams are strong enough, the column will not necessarily collapse completely. The ultimate collapse temperature will relate not only to the stiffness of restraints but also to their strength. Columns with restraints of different stiffnesses and strengths have been tested. The change of strength and stiffness are indicated by the strength ratio Fp/Fb, and the stiffness ratio K_s/K_c, respectively. K_s is the restraint stiffness and K_c is the axial stiffness of the column; F_p is the aggregate strength of restraints, and F_c is the axial resistance of the column (based on Eurocode 3 values). As shown in Fig.8, for cases with restraints of low strength, the model is effectively a simply supported column under axial force, so the collapse temperatures for different restraint stiffness are identified. As the strength of restraints increases, the collapse temperatures of columns increase and vary with different stiffness ratio of restraints. With the same strength of restraints, the higher stiffness achieves higher collapse temperatures. This is shown in by Fig.9. There are two points during a fire at which the beams may yield. The first occurs during the initial column heating, when the beams resist the thermal expansion of the column and reverse moments increase at the ends of beams. It is possible for the beams to yield under this scenario. The second occurs

when the heated column has buckled, and the beams cannot support enough of the superimposed load. Two lines, "Pre-buckling yield" and "Post-buckling yield" locate these two conditions. Each has two intersection points with the axial force curve for the column with elastic restraint. The first intersection point with the "Pre-buckling yield" indicates beam yielding before column buckling, while the second intersection with "Post-buckling yield" indicates beam yielding after initial column buckling. The axial force curve for columns with inelastic restraint should be obtained as shown in this figure. The results shown in Fig. 8 are only for stocky columns (slenderness ratios 30 and 60); for slender columns the results could differ, but the rationale implied by Fig. 9 can also be used for slender columns.

(a) Load ratio of column--0.3

(b) Load ratio of column--0.7

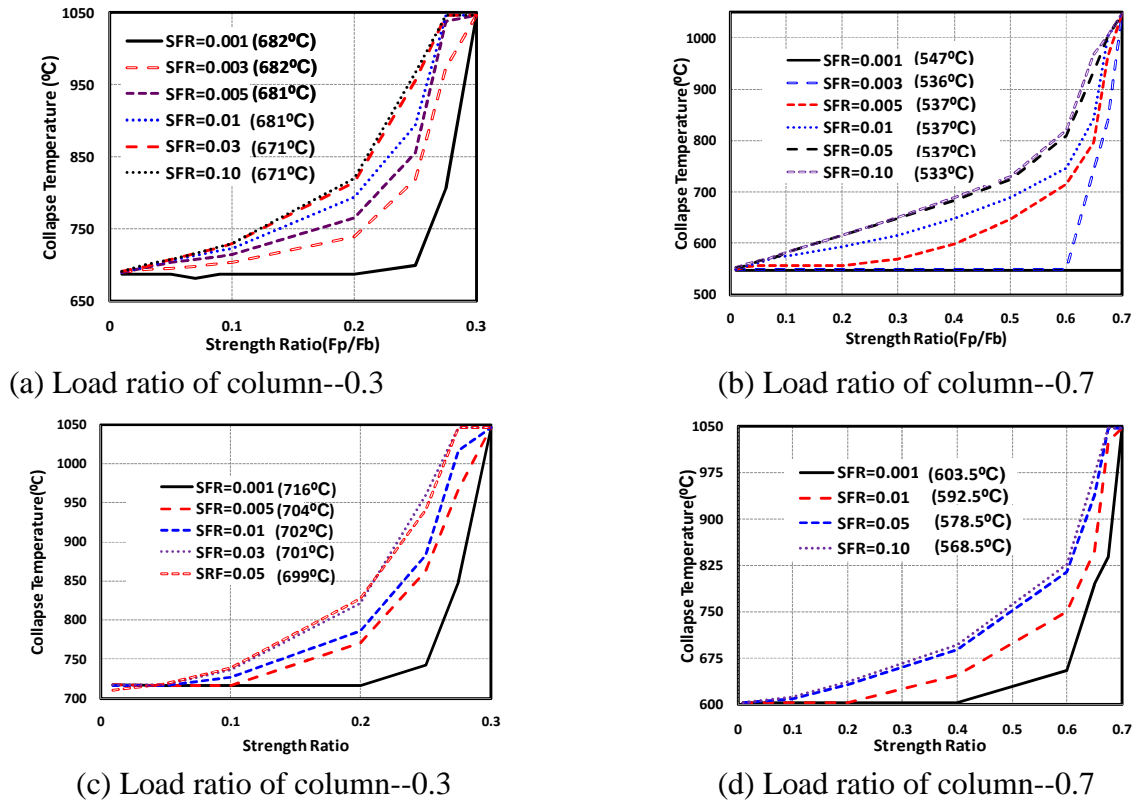(c) Load ratio of column--0.3

(d) Load ratio of column--0.7

Fig.8: Collapse temperatures of column: (a), (b) for slenderness 30; (c), (d) for slenderness 60.

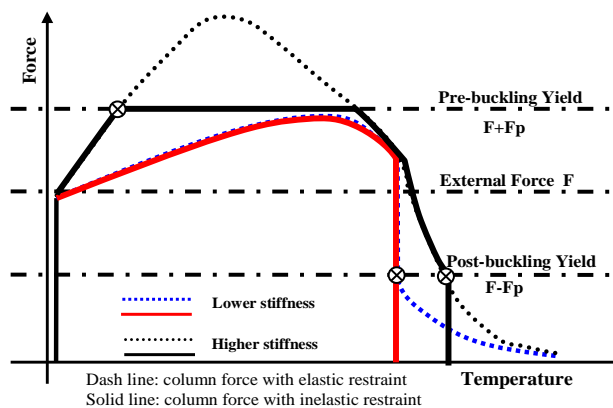
Fig. 9: Axial force development in column with rising temperature.

3.2 Stiffness of lateral restraints and connection rigidity

After the collapse of column, lateral restraint becomes the most important factor to determine whether (or when) re-stabilisation occurs. The three failure stages are indicated in Fig.10. Stiffer lateral stiffness provides a lower displacement at re-stabilisation, but a smaller axial force in the beams. Connections are vulnerable, and may fracture, at this stage. As mentioned previously, the model can take rotational stiffness of connections into consideration. As indicated in Fig.11,

different connection rotational stiffnesses do not change the failure temperature or re-stabilisation displacements significantly.
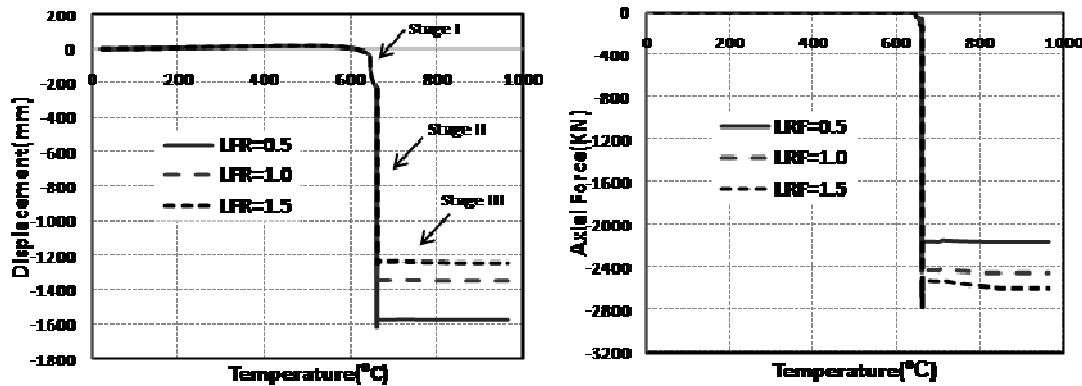

Fig. 10: Displacement of column top and axial force in beam with different lateral restraint stiffnesses (LFR=K_s/K_c).
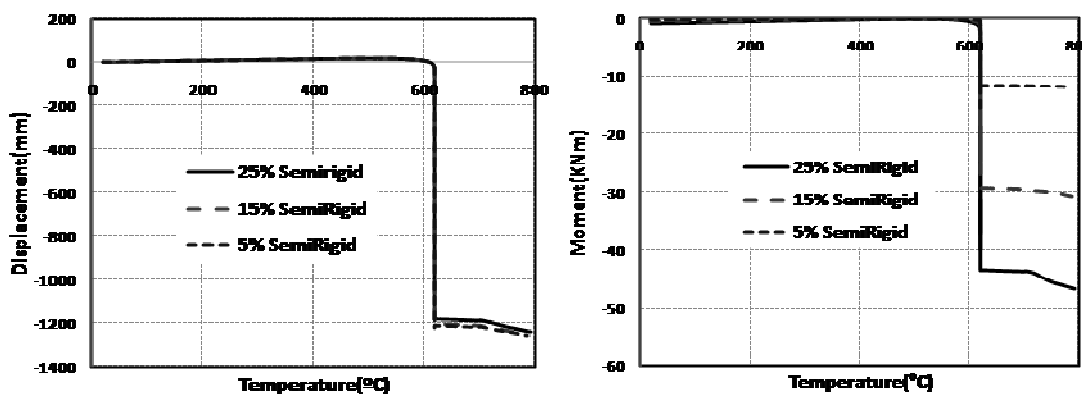

Fig. 11: Displacement of column top and moment with semi-rigid connections.

4   CONCLUSION

A simplified model has been proposed to study the column behaviour in framed structures based on the collapse mechanism of frame under localised fire. The boundary restraints from surrounding members are modelled by springs. The influence of stiffness and strength of restraints on the collapse temperature of column, and the effect of lateral restraints and connection rigidity on the behaviour of frame after column fails have been studied. It is an effective way to predict the structural behaviour under fire without carrying out complex detailed analysis. This method can be adopted to propose different simplified models for different frame under various fire scenarios. This model is based on 2D frame containing beam, column and connections. It is also feasible to include slabs into simplified models to investigate behaviour of composite frame under fire scenarios.

REFERENCES

Shepherd P., The Performance in Fire of Restrained Columns in Steel-framed Construction, Phd Thesis, University of Sheffield, 1999.

Y.C. Wang, Post-buckling behaviour of Axially Restrained and Axially Loaded Steel Columns under Fire Conditions, Journal of structural Engineering, March 2004.

Franssen, J. M., Failure temperature of a system comprising a restrained column submitted to fire. Fire Safety Journal, 34, 191-207, 2000.

Ali F., Nadjai A., Effect of Rotational Restraint on Performance of Steel Column in Fire, Journal of Applied Fire Science, 21-34, Volume 13, Number 1/2004-2005.

RR Sun, ZH Huang, IW Burgess, A Static/dynamic Procedure for Collapse Analysis of Structure in Fire, Fireseat, Edinburgh, 2010.

Poh K W, Bennetts I D. Analysis of structural members under elevated temperature conditions. J Struct Eng, 1995, 121(4): 664–675.

THE ROLE OF ACTIVE FIRE PROTECTION MEASURES IN A NATIONAL FIRE SAFETY CONCEPT IN GERMANY

Christoph Klinzmann[a]

[a]hhpberlin - Ingenieure für Brandschutz GmbH, Hamburg, Germany

INTRODUCTION

At the moment the building codes in Germany that regulate the fire protection of structural elements are prescriptive. This means that these codes contain requirements regarding the necessary fire resistance class of structural members which depend on the usage of the building.

With the implementation of the fire parts of the Eurocodes in 2011, realistic natural fire models are allowed for to be applied in structural fire design. The Eurocodes will make it possible that the structural members can be designed economically according to the boundary conditions like fire load, ventilation conditions and the geometry of the building. The application of the Eurocodes must be embedded within a holistic safety concept that ensures that the overall safety level is not reduced to an unacceptable level due to reduced design requirements. For the application in Germany a new safety concept was developed, which replaces the informative Annex E of Eurocode 1 part 1-2 (DIN EN 1991-1-2, 2010).

In this paper the main focus lies on the effect of the interaction of different safety measures, the resulting overall safety level and their consideration in the safety concept.

1 ACTIVE FIRE PROTECTION MEASURES

In Germany, the main focus of fire protection lies on structural fire protection measures. They have the advantage to be very effective in means of performance. Other countries like Great Britain follow different philosophies with a reduced amount of structural protection measures and more active fire protection measures like fire alarm systems or sprinklers in some cases. Active protection measures are usually composed of more or less complex technical systems. This means that they are at least subjected to potential failures or malfunctions under certain conditions. More complex and possibly less redundant systems lead to a higher probability of failure of a measure.

The aim of all active fire protection measures is to control the fire in one way or another. In the ideal case the fire can be extinguished, in some cases the fire size can only be reduced or the fire can be controlled to prevent it to spread beyond the compartment of origin. The measures can be considered as barriers preventing the starting fire from becoming a fully developed fire that affects the rest of the building concerned.

Active protection measures can be classified by their type and their influence on the fire. Direct measures, like the fire brigade or a sprinkler system affect the fire directly, e. g. by its extinction. Indirect measures like fire alarm systems only have impacts on the direct fire protection measures or on the consequences of a fire.

One of the main targets of the investigation described in this article was to quantify the safety benefit of active fire protection measures in structural design. This was achieved using the methods of probabilistic system analysis.

2 EFFECT OF ACTIVE PROTECTION MEASURES IN DESIGN FIRES

The definition of the design fire is the starting point of a performance-based fire safety design. In most applications, a design fire usually consists of the so called heat release rate (HRR) that describes the release of energy due to the fire over a period of time. Figure 1 exemplarily shows the different stages of a design fire for different types of fires. The fire starts with the ignition and is followed by the fire spread. It is widely assumed that the energy release during the fire spread follows a quadratic law (α-t² approach, ISO/CD 13388). After reaching the maximum heat release

rate (ventilation or fuel controlled), the energy release is assumed to remain constant until a decaying phase starts which leads to a subsequent extinction of the fire when all available fire load has been burnt.
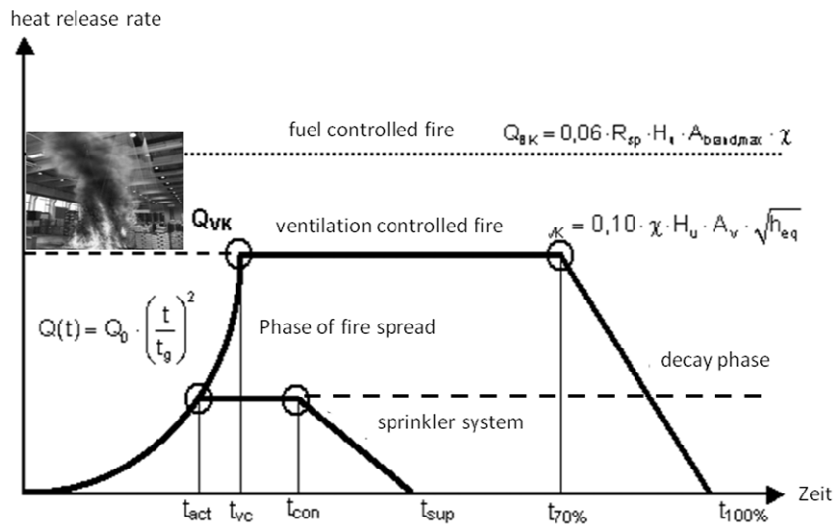

Figure 1: Heat release rates for different types of fires

Active fire protection measures can affect the release of energy during a fire, but some measures are only able to affect the consequences of the fire (e. g. temperature or toxic combustion products).

A sprinkler system is usually able to control or even to extinguish the fire at an early stage. In this case, the energy release into the room is reduced significantly. This is shown in figure 1, the sprinkler system is activated at the time t_{act} and controls the fire at t_{con} and is able to extinguish the fire at t_{sup}.

The work of the fire brigade can be considered in a similar way, with the difference that due to a longer response time of the plant or the public fire brigade, the fire spread takes longer, leading to a higher amount of energy release compared to a fire controlled by sprinklers. Plant fire brigades with better knowledge of the premises and significant shorter driving times usually have significant shorter response times.

A fire alarm system is an example for an indirect measure. In most cases a fire alarm system shortens the time of detection of the fire, leading to an earlier response of the fire brigade and lower energy releases.

Smoke and heat exhausts usually do not affect the heat release rate fuel controlled fires that are most relevant for structural fire design. For that reason, the consideration of smoke and heat exhausts was omitted in the safety concept for the moment.

It was already mentioned that every technical system can malfunction, active fire protection measures are no exception. Apart from their effect on the fire, the quantification of a safety benefit of a measure requires knowledge about its reliability. The available information will be discussed in the following chapter. A deeper discussion can be found in Klinzmann and Hosser, 2009.

3   RELIABILITY OF ACTIVE FIRE PROTECTION MEASURES

In Germany statistics about fire events are not collected systematically, at the moment no centralised fire database or statistics are available for the public. For that reason the data used for the analysis described here was based on literature studies (e.g of VDS, 1990).

It was found that the probability of failure of a fire alarm system is likely to lie between $p_{f,fa} = 0,05$ and $p_{f,fa} = 0,10$. Analogous to fire alarm systems, sprinkler systems must be serviced well to achieve to relatively low probability of failure of $p_{f,sprinkler}=0,02$ that was found in the studies.

The determination of a probability of failure of fire fighting is more complicated. It is common knowledge that fire fighting measures can fail as well. For the analyses it was assumed that this is

the case when the fire is able to spread beyond a size that cannot be controlled anymore. It was assumed that this is the case if the fire has reached an area of 200 m².

The benefit of fire alarm systems in terms of the increased reliability of fire fighting measures was modelled by a gain of time in the overall response time of the fire brigade of 5 minutes.

The reliability data acquired is required to quantify the overall safety benefit of the different measures and their combinations or interactions. This is the basis for the determination of safety factors that can be applied on the parameters of design fires in order to consider positive effects of installed active fire protection measures. In the following, the probabilistic system analyses carried out to quantify the safety levels and safety benefits in the different scenariis as well as some exemplary results are explained.

4 PROBABILISTIC SYSTEM ANALYSES

The effect of the different active fire protection measures on the reliability of a structural member in a fire was investigated in a research project during which the safety mentioned concept was developed (Hosser et al., 2009).

The probabilistic system analyses that were carried out had to consider all possible outcomes of fire scenarios evolving from of functional and not working active fire protection measures. This can be seen in figure 2, where a system consisting of an automatic and a manual fire alarm system, a sprinkler system, an on-site plant fire brigade as well as a public fire brigade is illustrated via an event-tree.
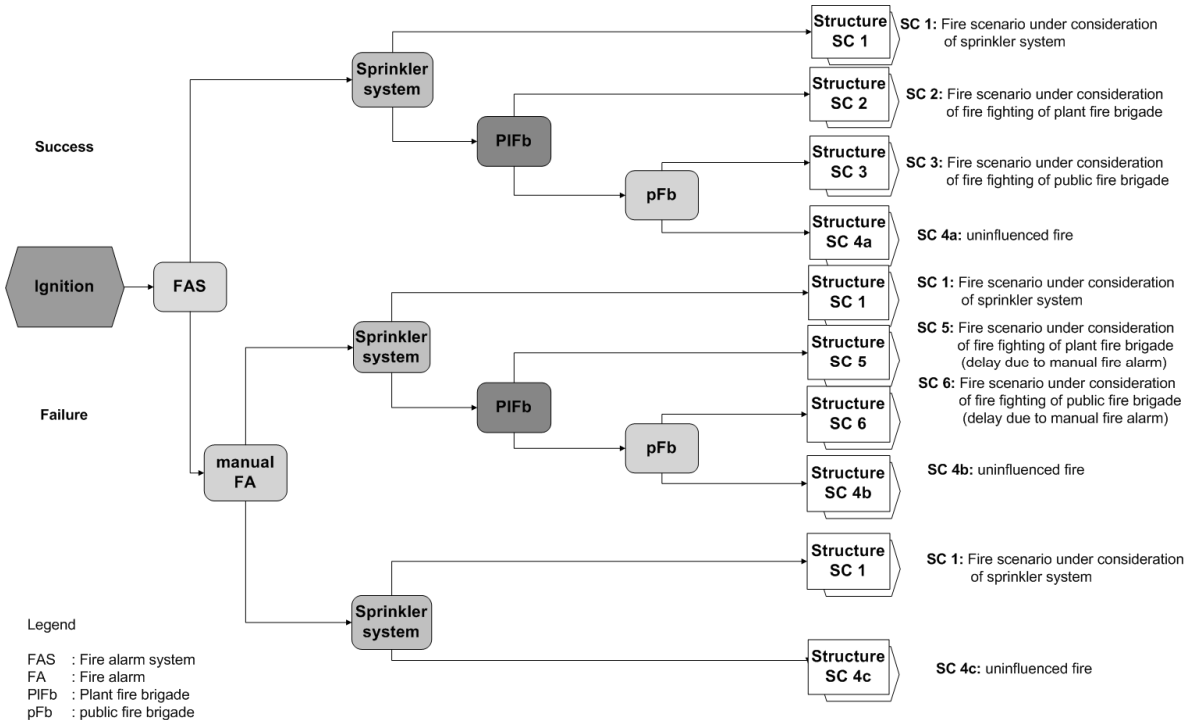

Figure 2: Event-tree for the system of active fire protection measures

Event tree analyses help to investigate how the different measures (barriers) affect the development of the fire in the compartment, the size of the fire and its consequences starting from the event "ignition of a fire in the compartment". Each failure of a barrier increases the probability that the fire becomes a fully developed fire that can spread beyond the compartment of origin and stresses the structural members with higher temperatures.

The probabilistic system analysis computes the probability of failure of a structural member due to the different scenarios at discrete time intervals. The overall probability of failure p_{fi} or the reliability index β_{fi} respectively of the whole system of active fire protection measures and the structural element is computed in a subsequent step via the logical relations determined with the help of the event-tree. The boundary conditions of the different scenarios and the stochastic models that were analysed and the models used can be found in [Klinzmann, 2009 and Hosser et al., 2009].

In many cases more than a single type of active fire protection measures has to be considered. Especially buildings like high-rise towers, shopping malls, stadiums and large atria are equipped with different types of measures that interact with each other. The problem is that the effects of the protection measures are not necessarily independent.

The interaction of plant and public fire brigades that are called to the same fire scene can be taken as an example. Usually the plant fire brigade responds to the fire earlier than the public fire brigade due to longer distances and less knowledge of the premises. This means that the additionally called public fire brigade is not able to increase the reliability of the structural members in the burning room significantly in case a well working plant fire brigade is present. The safety concept must ensure that the actual safety level is not overestimated because of the interaction of non-independent active fire protection measures. For that reason the additional consideration of a public fire brigade in case a plant fire brigade is present is not allowed according to the safety concept.

5   RESULTS

In the system reliability analyses carried out the following protection measures and combinations of active fire protection measures were investigated in addition to the uninfluenced fire:

- a fire brigade with an overall response time of 20 minutes
- a fire brigade with an overall response time of 20 minutes and a well serviced sprinkler system
- a fire brigade and a fire alarm system (FAS)

The analyses were carried out on the basis of the event tree in figure 3 that was simplified according to the measures considered, leading to four different design fires for the structural member. The results of the analyses are shown in figure 3.
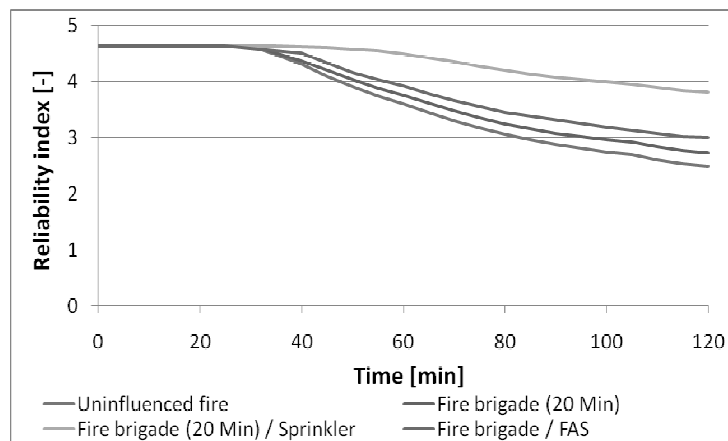

Figure 3: System reliability index under consideration of different active fire protection measures

The graphs show the development of the reliability index at discrete points in time for the 4 different scenarios. It can be seen that in all solutions the reliability starts to decrease after a time span of approximately 30 minutes. This means that up to this time the structural member under no circumstance reaches a critical temperature. The structural member used in this case is an insulated steel beam, which shows a performance similar to members made of concrete. Unprotected steel beams would reach lower reliability indexes earlier due to the quicker heating.

It can be seen that the active fire protection measures have different impacts on the overall reliability level. The blue line represents the uninfluenced fire and is taken as reference solution. Its minimum is obtained after 120 minutes and lies around a value of β=2.50 for the reliability index. The scenario with the next higher reliability is the one with the consideration of fire fighting by a fire brigade with an overall response time of 20 minutes. The probability of failure of the fire fighting lies around $p_{f,fw} = 0,50$. The minimum reliability index of this scenario after 120 minutes is approximately β=2.75. In the next scenario a fire alarm system that provides a gain in response time of the fire brigade of 5 minutes is considered, leading to a minimum reliability index of approximately β=3.00. In an earlier study [10] it was found out, that a fire alarm system is able to

reduce the probability of failure of the fire fighting by a factor of around 0.5, depending on the overall response time. The scenario with the highest reliability considers a sprinkler system with a probability of failure $p_{f,sprinkler}=0.02$ in addition to the fire fighters. The minimum reliability index in this scenario lies at around $\beta=3.85$.

The investigations described were able to quantify the reliability benefit of the different measures. Additionally, it was found out that the scenario of the uninfluenced fire, occurring if all active fire protection measures fail, is the representative scenario. This phenomenon is independent of the active fire protection measure and the complexity of the event-tree. This is shown in table 3. The table compares the reliability index computed within the system analysis with a reliability index computed based on the reliability index calculated from the reliability index of the uninfluenced fire. The probability of failure can be computed from the reliability index via the relation $p_f=\Phi(-\beta)$ and vice versa via the relation $\beta=-\Phi^{-1}(p_f)$, being Φ the Gaussian distribution and Φ^{-1} its inverse.

Table 3: Comparison of reliability indexes

Scenario	Reliability index (System analysis)	Reliability index (calculated with probability of failure)
Uninfluenced fire	~2.50 (p_f=6.2E-3)	$-\Phi^{-1}$(6.2E-3)=2.5
Fire fighters	~2.75	$-\Phi^{-1}$(6.2E-3*0.5)=2.74
Fire fighters and fire alarm system	~3.00	$-\Phi^{-1}$(6.2E-3*0.5*0.5)=2.96
Fire fighters and sprinkler system	~3.85	$-\Phi^{-1}$(6.2E-3*0.5*0.02)=3.84

The safety concept developed for Eurocode 1 that is published in DIN EN 1991-1-2, 2010 makes use of the described results. It provides representative data for the probability of failure of different active fire protection measures and formulas to consider this information in the calculation of the required reliability level. A higher amount of active fire protection measures leads to a lower required reliability. This influences the values of the partial safety factors for the maximum heat release rate and the fire load density. A lower required reliability leads to lower partial safety factors. This shows that active fire protection measures can be used to reduce the requirements demanded of structural members. More details can be found in Klinzmann, 2009.

6   IMPLEMATION INTO SOFTWARE

With the introduction in 2011, the described safety concept will applicable in Germany. The partial safety factors that are required for the leading input parameters are either tabulated or can be programmed easily. They will be available in the relevant software packages within short time.

7   CONCLUSION

The first part of this article briefly analysed different active fire protection measures and their effect on natural fires. In a subsequent step, the available data regarding the probability of failure of these measures was discussed. In Germany, no centralised statistics regarding the availability of such data exists. This leads to the problem that all analyses must rely on eventually biased information from manufactures or not in all cases representative data from different countries.

In the second part of this article, the probabilistic analyses carried out for the development of a safety concept for German National Annex of Eurocode 1 were explained. The main focus lays on the consideration of the active fire protection measures in the design fires for structural fire design. It was shown that a fire uninfluenced by active fire protection measures is the representative scenario that should be used as a basis of the design fire. The safety concept developed provides a methodology to consider the rareness of such an event positively via the probability of failure of the active fire protection measures available.

The probability of occurrence of the mentioned scenario of an uninfluenced fire in the building of concern must be analysed. Especially in large buildings with separations with a determined fire

resistance an uninfluenced fire in a whole storey of the building is unlikely and usually not representative. In these cases, a different fire, e. g. under consideration of active fire protection measures can be representative.

It must be mentioned, that these facts apply only for the fire design of structural members. The simulation of the egress of people from the building and of the smoke distribution in the building usually requires different design fires. The uninfluenced fire usually is representative due to the fact, that the egress of people from the building takes place during the phase of fire spread and should be finished long before the fire becomes a fully developed fire. In Germany, the safe egress of all people in the building is guaranteed by short escape routes. In most cases, the verification of a minimum smoke height, e. g. in convention centres, shall ensure safe and effective fire fighting measures. The representative scenario in this case must include the consideration of the effects for fire fighting.

REFERENCES:

DIN EN 1991-1-2/NA: Nationaler Anhang - National festgelegte Parameter — Eurocode 1 - Einwirkungen auf Tragwerke — Teil 1-2/NA: Allgemeine Einwirkungen – Brandeinwirkungen auf Tragwerke; December 2010

DIN EN 1991-1-2: 2003-09. Eurocode 1 - Einwirkungen auf Tragwerke - Teil 1-2: Allgemeine Einwirkungen; Brandeinwirkungen auf Tragwerke, Beuth Verlag, Berlin, Germany

Hosser, D.; Weilert, A.; Klinzmann, C.; Schnetgöke, R.; Albrecht, C.: Erarbeitung eines Sicherheitskonzeptes für die brandschutztechnische Bemessung unter Anwendung von Ingenieurmethoden gemäß Eurocode 1 Teil 1-2" (Sicherheitskonzept zur Brandschutzbemessung). Abschlussbericht zum DIBT-Forschungsvorhaben ZP 52-5-4.168-1239/07. Institut für Baustoffe, Massivbau und Brandschutz (iBMB), Technische Universität Braunschweig, November 2008

ISO/CD 13388 Committee Document, *Fire Safety Engineering. Design Fire Scenarios and Design Fires,* ISO/TC92/SC4, 1997.

Klinzmann, C.; Hosser, D.: Berücksichtigung abwehrender und anlagentechnischer Maßnahmen beim brandschutztechnischen Nachweis von Bauteilen, vfdb-Zeitschrift (2), April 2009, Kortlepel Verlag Zweigniederlassung der Ebner Verlag, GmbH & Co. KG, Bremen, Germany

VdS Schadenverhütung, Jahresbericht 1990 / 91, Köln, Germany

COMPUTATIONAL MODELLING FOR PERFORMANCE BASED FIRE ENGINEERING (PBFE)

Francesco Petrini, Konstantinos Gkoumas

Sapienza University of Rome, School of Engineering, Rome, Italy

INTRODUCTION

Modern codes endorse two different methods for the design of structures subjected to fire: either by means of a prescriptive approach or with a performance-based approach. A prescriptive-based code provides for fire safety by prescribing some combination of specific requirements, without referring to the desired safety level or how it is achieved. In comparison, a performance-based code allows any solution that can lead to an *a priori* imposed safety level. In some cases, for example when dealing with complex structures where it is impossible to comply with all the architectonical prescriptions specified by a prescriptive approach, a prescriptive-based code proves to be inadequate, and a performance-based approach is more appropriate in obtaining the optimal structural behaviour under fire.

On the basis of the above premises, this paper focuses on the application of the performance-based approach (in the context commonly referred as PBFE – Performance Based Fire Engineering) to an exhibition pavilion with a relatively complex geometry subject to fire. The structure is of interest since, due to its occupancy, it is prone to elevated fire risk.

Conceptually the paper is organized as follows: chapter one describes the case study and the fire scenarios considered under a performance based approach. Chapter two deals with the determination of the fire load using a computational fluid dynamic code (FDS - Fire Dynamics Simulator). Finally, chapter three reports the performed structural analysis, accounting for the non linearity of materials and the decay of their mechanical characteristics with the temperature

1 THE PERFORMANCE BASED FIRE DESIGN APPROACH

The performance based fire design (PBFD) in the last years gained a lot of ground mostly for facilities prone to elevated fire risk. The focus is on the structural performance in the presence of fire and includes requirements of fire resistance both for the structural elements (e.g. beams, slabs, columns) or for the structural system as a whole (avoidance of excessive vibrations, of progressive collapse, etc.). A very important step to guarantee an assigned level of safety is to verify that the resistance of the structure under fire is higher than the fire severity (fire resistance > fire severity). In general, there are three techniques for checking the fire resistance: in the time, temperature or strength domain. An outline of the performance based approach implemented in this study is synthesized in the following paragraphs.

1.1 Design goals

It is necessary to predict not only the structural resistance, but also the level of damage in case of fire in order to assure an appropriate performance. In this study, the design goal set is that the structure has to resist to fire, withstanding the total combustion of any combustible material, within the whole building or in a specific zone, without intervention from the fire-fighters.

1.2 Structural collapse and performance metrics

The definition of structural collapse is delicate, especially when considering a strongly redundant structure. In fact, the failure of a single steel member does not lead to the collapse of the entire structure. In that case, it is possible to consider a limited deformability for a group of elements, so that the vertical displacement of some key points can be assumed as performance metrics.

1.3 Fire scenarios

In accordance with ISO/TS 16733 (2006), for a comprehensive description of the fire scenarios, the following aspects need to be specified:

- the fire source;
- the nature and physical characteristics of the combustible;
- the growth rate of the fire and the peak of rate of the released heat.

In the specific case, the structure is a strongly redundant rectangular building with sides of 144m and 72m (Fig. 1). It consists in 24 concrete columns. The horizontal elements consist in 3 steel reticular beams in the principal direction and 11 in the minor direction. The structure has two openings of 36x6 m in the centre of the smaller sides.

Given the structure's occupancy (exposition pavilion), it is realistic to consider inside the presence of stands. Each of these is assumed formed by a wooden table on top of which some paper is deposited, surrounded by three plastic shelves and two sofas.

In order to estimate the fire evolution in the structure, six scenarios have been considered. The source of ignition is considered to be the paper on the table. The position of the fire ignition according to the six scenarios is shown in Fig. 2.

In accordance with what is prescribed by EN 1991-1-2 (2002), the value for the Rate of Heat Release (RHR) has been defined on the basis of the occupancy of the structure. From table E.5 (EN 1991-1-2, 2002), the RHR considered is the one for a shopping centre. In this context the development of fire is fast. The following values have been considered to describe the fire development: α=0.04444 kW/s^2 (fire growth factor), RHR$_f$=250 kW/m^2, t$_a$=150 s (time needed to reach a rate of heat release of 1 MW).
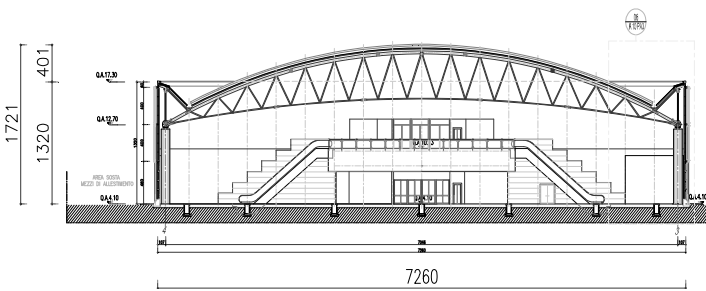
Fig. 1 Cross Section of the structure   Fig. 2 Location of the six scenarios
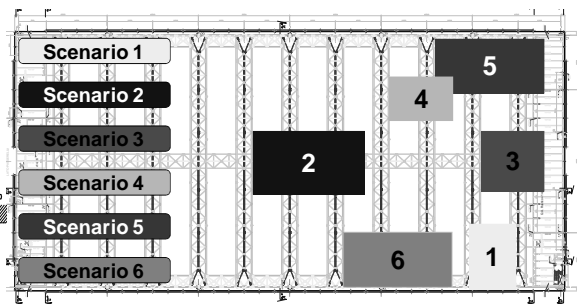
In order to obtain the corresponding natural fire curves, standard procedures have been implemented (see for example, Karlsson and Quintiere, 2000). After the flashover, the RHR remains constant until the beginning of the decay that at this stage occurs according to a linear law.

Following prescriptions from the ISO/TR 13387-1, 1999 and considering a fire load density of q$_{f,k}$=600 MJ/m^2, taken from table E.4 of EN 1991-1-2, 2002, the characteristics of the RHR curve for the six scenarios are those indicated in Table 1.

Tab. 1 Values of the RHR curve in specific time points

Scenario	Area [m^2]	RHR$_{max}$	t$_A$ [s]	t$_B$ [s]	t$_C$ [s]
1-3-4	216	54000	1102	1552	2512
2-5-6	432	108000	1559	2959	3919

Fig. 3 shows the two RHR-time curves used in all six scenarios.

The analysis is divided in two steps:

- the determination of fire load (Joyeux et al, 2002);
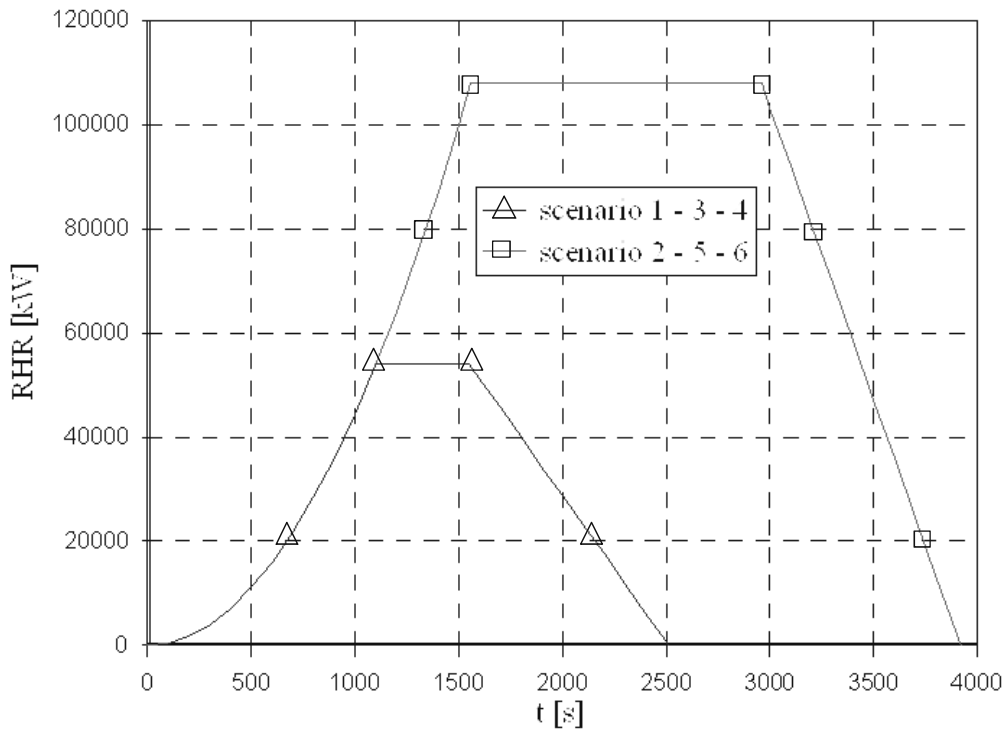- the characterization of the fire effects on the structure (Buchanan, 2008).

Fig. 3 RHR-time curves for the six scenarios

2   DETERMINATION OF THE FIRE LOAD

Three different analyses have been performed by means of a computational fluid dynamic (CFD) code (McGrattan et al, 2009) in order to determine the fire action in the structure:

- analysis of the sensitivity to the mesh;
- study of the boundary conditions;
- determination of the thermal map for each of the considered scenarios.

In the first analysis, the external environment has been considered as a solid at 20°C. Consequently, a sensitivity analysis has been carried out in order to establish the accuracy of the mesh.
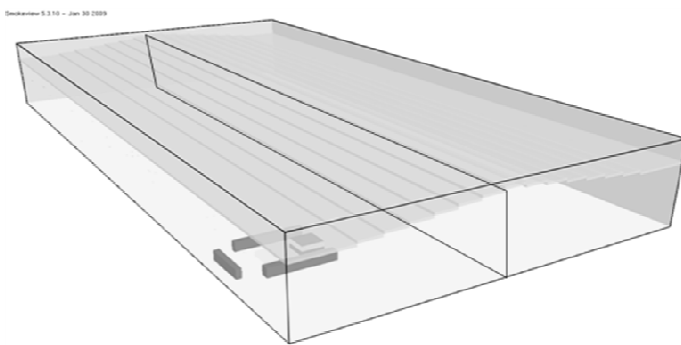
Fig. 4 Tridimensional model without external environment
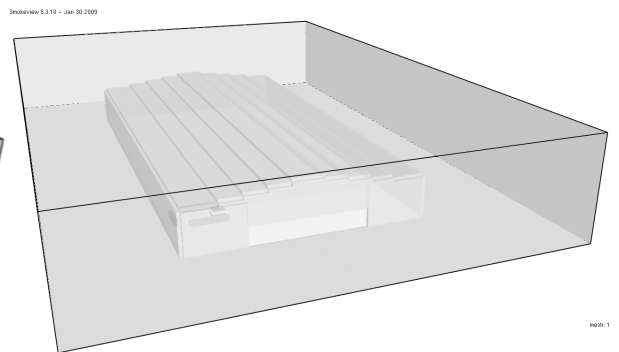
Fig. 5 Tridimensional model with external environment

In the analysis (Fig. 4), rectangular parallelepiped elements are used with base dimensions between 1.5 m and 0.5 m and height 1 m, or elements with a square base of 1 m and a variable height between 1.5 m and 0.5 m. Due to the lack of convergence of the phenomenon, a finer model has been realized. This model is composed by concentric cubic elements. As a consequence, a large amount of elements (about 440060) has been used, with a very high computational load (corresponding to analyses lasting about 70 hours).

In this model, scenario 1 has been analyzed, and the flashover occurs after 930 seconds.

The computation of temperature is strongly influenced by the boundary conditions. Thus, the model has been included in a larger environment in order to verify the role of the boundary conditions (Fig. 5). In a first place, the initial volume has been extended 4 m beyond the structure in the minor direction, 8 m in the major one, and 4 m in vertical direction. In the final configuration of the model, it extends respectively of 28 m, 36 m and 8 m.

This model is characterized by a great amount of elements (more than 1 million) and by a huge computational load (with analyses running up to 10 days on a multi core PC).

In both cases, the validation of the model is based on the:

- qualitative analysis of the propagation of flames;
- global analysis by means of the RHR curve;
- local analysis applying temperature-time curves on the structural elements and the significant sections.

Once the model has been validated, a thermal map of the structure is realized by applying it to the six scenarios. Fig. 6 shows the modelling of scenario 2 in FDS. Fig. 7 illustrates the heat release distribution at the flashover development. The significant difference between the application of the ISO 834 nominal curve and the application of the natural curves obtained with the FDS software is highlighted in Fig. 8.
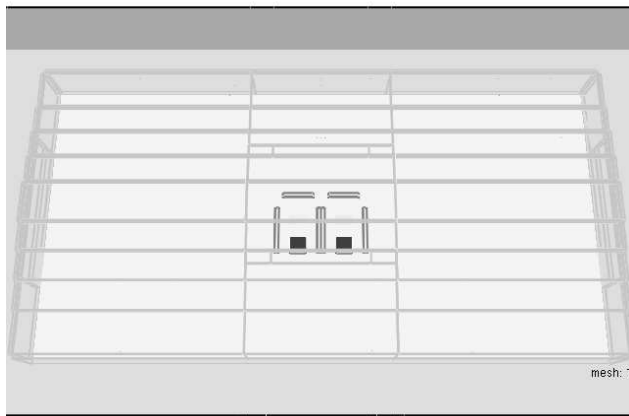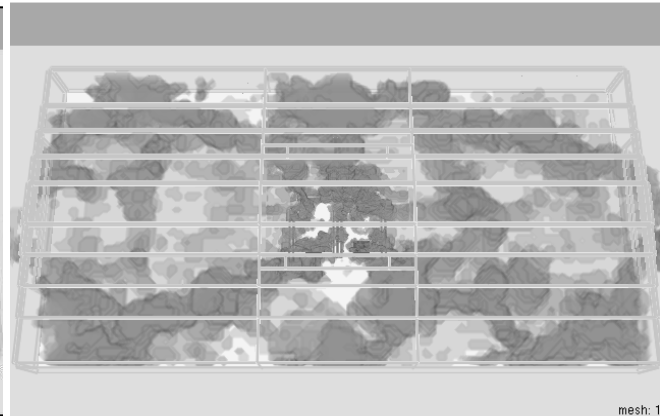
Fig. 6 Scenario 2 modelled in FDS

Fig. 7 Fire peak (flashover development)
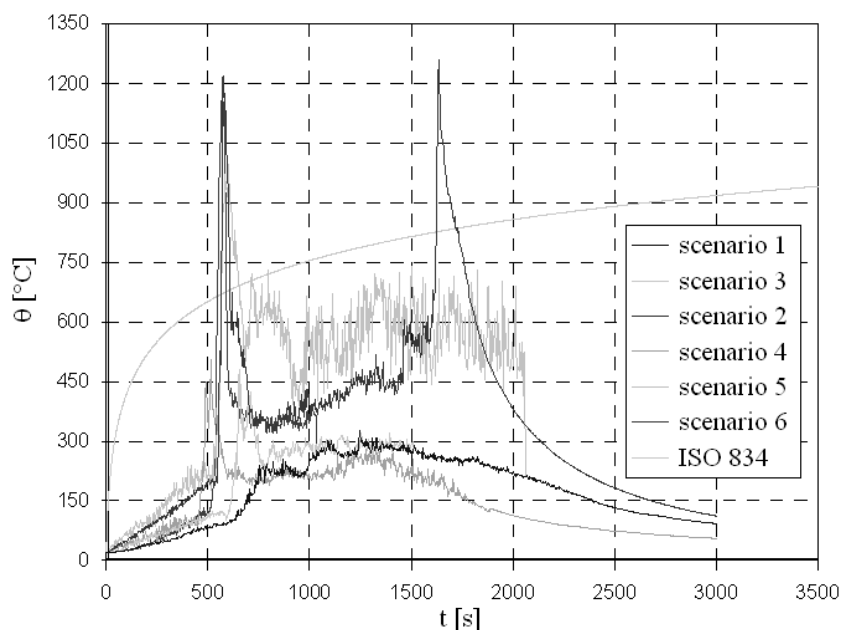
Fig. 8 Temperatures registered during the fire peak

3   STRUCTURAL ANALYSIS

The obtained fire load has been applied using the finite element code Straus7/Strand7 in order to inquire on the structural response (Usmani et al, 2001, Crosti et al, 2009). Figs. 9 and 10 show the vertical displacements corresponding to scenario 2 after the application of the nominal and the natural curves.
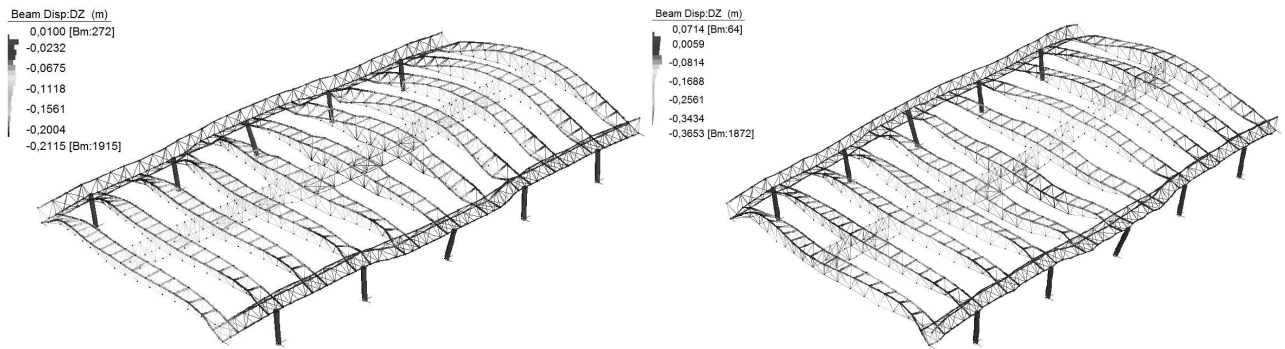

Fig. 9 Global displacements for scenario 2 with the nominal curve

Fig. 10 Global displacements for scenario 2 with a natural curve

For the same load scenario, considering the critical node 322 (Figs. 11 and 12), Figs. 13 and 14 illustrate the vertical displacement. This analysis accounts for the non linearity of the materials and the decay of their mechanical characteristics due to the temperature variation (Crosti et al, 2009, Petrini and Bontempi, 2009).
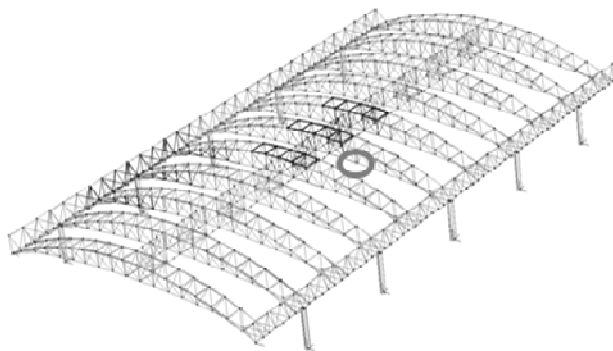
Fig. 11 Position of node 322
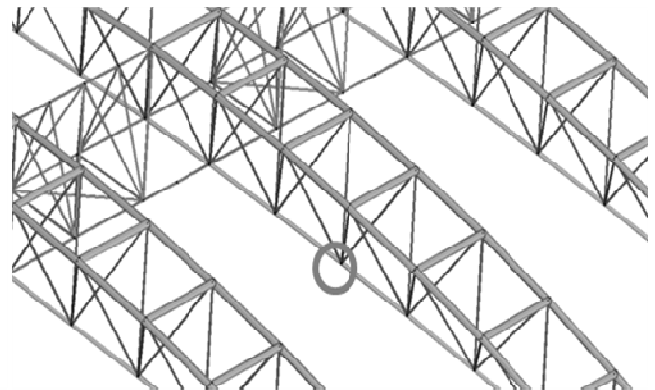
Fig. 12 Position of node 322 (detail)
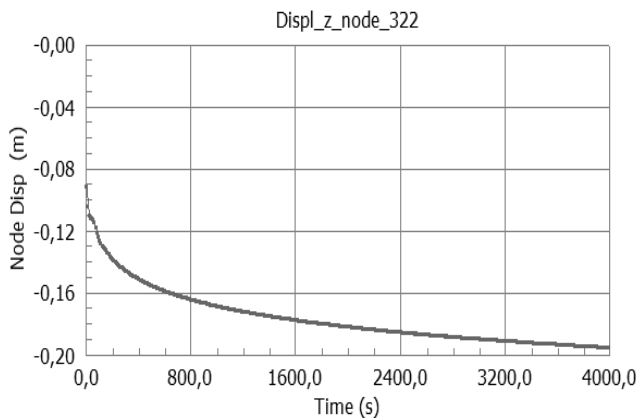
Fig. 13 Vertical displacements for scenario 2 with the nominal curve
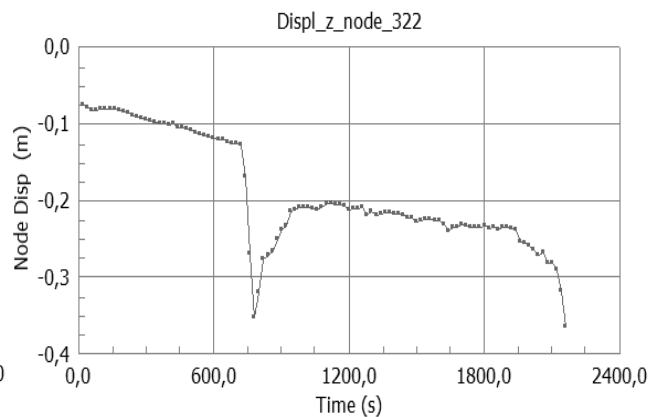
Fig. 14 Vertical displacements for scenario 2 with a natural curve

The difference between the two curves can be explained considering the differences between the temperature distributions obtained in two cases. In fact, whereas a thermic load can be applied outside the nominal area of the scenario using natural curves, it is not realistic to consider the nominal curve outside the scenario area.

The adequate behavior of the structure under fire, leads to the accomplishment of the prescribed performance. Moreover, the alternative load paths among the elements emerge. Conclusively, it is important to highlight the local collapse in some fire scenarios.

4   CONCLUSION

In the present paper, aspects concerning the numerical analyses for the performance based fire design of complex structures has been inquired. An application on a complex steel structure has been presented, where both computational fluid dynamic analyses for the assessment of the fire development and structural analyses for the structural response investigation are developed. The analyses show that use of advanced methods for the numerical simulation of fire is fundamental in order to obtain reliable results in assessing the structural behaviour.

Even though simplified methods for the fire modelling, using nominal fire curves, apparently conduct to similar results (in terms of the deformed shape under fire), using more advanced methods with CFD, a detailed description of the structural response (e.g. the detail on the vertical displacement time history for critical nodes) highlights the great difference of the two methods in obtaining the structural response. Considering the above, the use of advanced numerical simulations is recommended, especially for complex structures.

ACKNOWLEDGMENTS

REFERENCES

Buchanan A. H., Structural Design for Fire Safety, Wiley, 2008.

Crosti C., Giuliani L., Gkoumas K., Bontempi F., Structural analysis of steel structures under fire loading, Applications of Structural Fire Engineering, Prague 19-20 February 2009.

EN 1991-1-2, Eurocode 1: Actions on structures – Part 1-2: General actions – Actions on structures exposed to fire, European standard, 2002, CEN, Brussels.

ISO/TR 13387-1:1999 (E) Fire Safety Engineering - Part 1: Application of fire performance concepts to design objectives. Technical Report. Geneva: International Organization for Standardization.

ISO/TS 16733: Fire safety engineering – Selection of design fire scenarios and design fires, Technical Committee ISO/TC 92, 2006.

Joyeux D., Kruppa, J., Cajot L., Schleich J., Van de Leur P., Twilt L., Demonstration of Real Fire Tests in Car Parks and High Buildings, Final Report, Contract No. 7215 PP 025, CTICM, Metz, France, 2002.

Karlsson B., Quintiere J.G., Enclosure Fire Dynamics, CRC Press, 2000.

McGrattan K., Klein B., Hostikka S., Floyd J., Fire Dynamics Simulator (Version 5) – User guide, NIST, Special Publication 1019 – 5, Washington, USA, 2009.

Petrini F., Bontempi F., Performance-Based Fire Engineering, Atti del XXII Convegno Collegio dei Tecnici dell'Acciaio (CTA), Padua, Italy, 28-30 September 2009, (in Italian).

Straus7/Strand7, www.strand7.com.

Usmani A.S., Rotter J.M. , Lamont S., A.M.Sanad, Gillie M., 2001, Fundamental principles of structural behavior under thermal effects, Fire Safety Journal, 36, 721-744.

LOADING-BEARING CAPACITY METHOD FOR STRUCTURAL FIRE SAFETY DESIGN – A CASE STUDY

Du Yong[a], Li Gou-qiang[b]

[a] Nanjing University of Technology, School of Civil Engineering, China
[b] Tongji University, School of Civil Engineering, China

INTRODUCTION

Since the Cardington frame fire tests in UK in the 1990s, structural design for fire safety based on single element behavior in the standard fire resistance test has been negated. A great deal of work on the behavior of steel structures in large space buildings fire has been developed since 2000s in China [1]~[3]. It is revealed that the temperature during a large space fire is different from that in compartment fire described schematically by the Fig.1 and Fig.2 which show the non-uniform temperature field for the horizontal plane at a given height of large space and the typical temperature history of growth and full development phase. The non-uniform temperature field remains some parts of the structure at relatively low temperature. These cooler parts adjacent can provide adequate restrain and stiffness to the heated area, and restrained thermal expansion will lead to thermal stress in the heated area during fire period. Structural collapse will occur if load sharing exceeds the structural loading capacity, although the maximum temperature shown in Fig.2 is lower than the standard test. On the other hand temperature histories in large space fire should be gotten instead of ISO-834 and other standard temperature curves for large space structural fire safety design. The behavior of single structural element heated in a furnace with a standard fire exposure dose not consider the real boundary and load situation, the result from standard test can't represent of the real structural element response in whole structure in large space fire. These are proved by centenary action in beams and tensile member action in slabs found in the behavior of real structure [4]. However calculation methods are developed in advanced fire-resistance design.
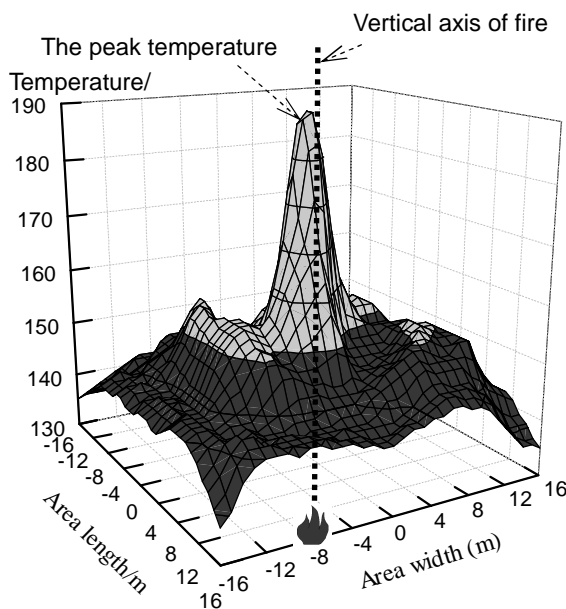

Fig. 1 FDS simulated temperature distribution in the horizontal plane at 6m height from fire
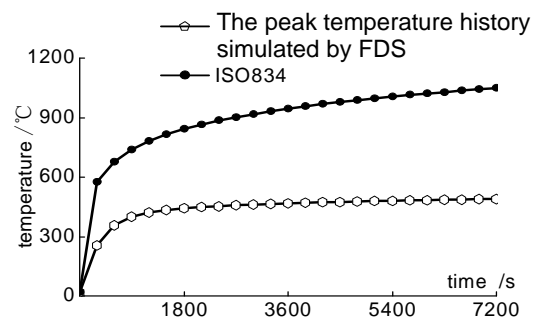
Fig. 2 Comparison of FDS simulated the maximum temperature history and ISO834 curve

1   LOADING-BEARING CAPACITY METHOD

Experimental and analytical methods are suitable for evaluating the performance of structural fire resistant if the boundaries fit to the real structure. Whereas it is difficult to simulate the boundary

conditions of elements in real structures and natural fires, the standard fire test bears very little resemblance to the behaviour of any but the simplest of real structure. The whole structure fire test isn't widely employed in routine structural design for its expensive and complex.

Some fire design codes have now been introduced for designing structures to resist fire by calculation. In principle fire loading can be treated as any other form of load. However, the structural behaviour in fire in all but the simplest case is much more complex than normal temperature for the material characteristics varied with temperature. Computer-based finite element methods are employed which include the non-linear material properties temperature dependent and the effects of thermal expansion. The loading-bearing capacity method carries out a structural analysis for the fire situation with the method discussed above, and check structures loading-bearing capacity in fire ultimate limit stat. The basic steps in loading-bearing capacity method for structural fire safety design are:

(1) design fire scenarios based on fire performance and determine the fire temperature distribution,

(2) determine critical temperature based on FE calculated,

(3) guess the thickness of fire protection for members (without fire protection is permitted),

(4) calculate the maximum temperature in members,

(5) if the maximum temperature in member is lower than critical temperature, come back step (3).

2   THE BUILDING

As a part of the complex cultural center, the auditorium covers 896m^2 with 1100 seats shown in Fig. 3~Fig.5. Because of the long span a steel grid structure roof was chosen, which is supported on the concrete columns above 13.965m high from the auditorium ground. The two rows of columns have 30m span and are space at 9m. The active fire protections are set in the auditorium to prevent the spread of fire and structural collapse during natural fire.

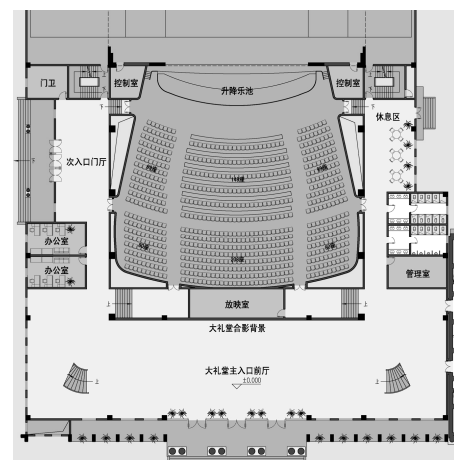

Fig. 3 Air photo of the auditorium
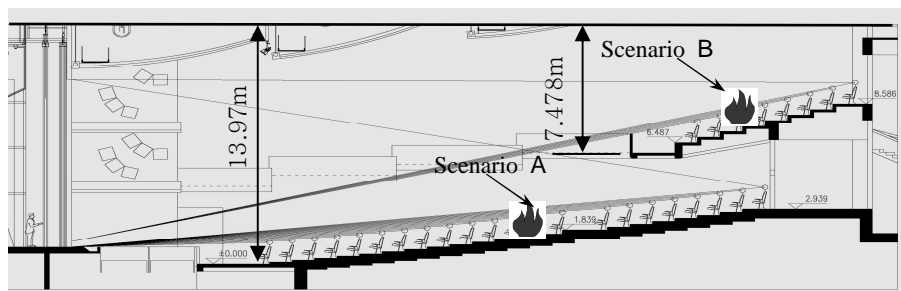

Fig. 4 Plan of the auditorium

Fig. 5 Fire scenario in the auditorium

3   DESIGN FIRE

3.1. Fire scenarios

Scenario A– the auditorium covers 32m×28m=896m^2 and with the height of 13.965m. The localized fire is in the middle of the compartment shown in Figure 5.
Scenario B – the balcony covers 32m×10m=320m^2 and with the height of 7.478m. The localized fire is in the middle of the balcony shown in Figure 5.

3.2. Estimating rate of heat release

Stackable sofas are most commonly used in auditorium and are regarded as the main fire resource. The heat release rate of the fire must be known for calculation of fire behavior in auditorium. The test on HRR for real products have been run by Babrauskas and colleagues since 1980s at NIST. The highest HRR is 3MW recorded in Fig. 6 and the whole fire last 20min.
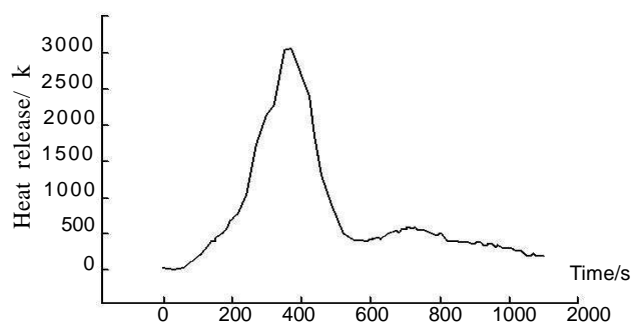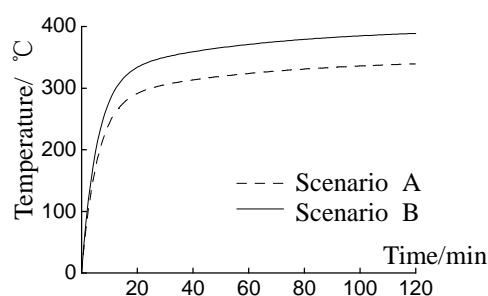
Fig. 6 Heat release history

Fig. 7 The maximum temperature history for scenario A and B

The fire grows as the t-squared fire and fire growth coefficient for the fast fire is 0.04689kW/s^2. Taking account of the fire duration of members and fire traveling it has been considered as the most critical fire load that four sets of stackable sofa covered 3m×3m combust in the meantime, and the highest HRR is 12MW during fire course 1.5h.

3.3. Smoke temperature distribution

Due to the large dimension of the auditorium, a prescriptive rule using the standard fire curve ISO 834 isn't available and quite unrealistic. Temperature distribution in large space fires obtained from the parameter equation (1), which bases on the computational fluid dynamics [5].

$$T(x, z, t) = T_g(0) + T_g^{max} \cdot f(t) \cdot k_{sm} \tag{1}$$

where $T(x, z, t)$ the smoke temperature at the point above floor and from the vertical axis of fire through the whole fire

$T_g(0)$ ambient temperature

x, z the horizontal distance from the vertical axis of fire, and the height above the floor

t the time in the temperature history

T_g^{max} the maximum temperature of smoke, given by Eq.(2)

$$T_g^{max} = (20Q + 80) - (0.4Q + 3)H + (52Q + 598) \times 10^2 / A_{sp} \tag{2}$$

where A_{sp}, H the floor area, and the height of the internal space respectively
     Q the fire power

$$f(t) = 1 - 0.8e^{(-\beta t)} - 0.2e^{(-0.1\beta t)} \tag{3}$$

where β the regression parameter dependent on the fire growth types listed in table 1

$$k_{sm} = \eta + (1-\eta) e^{(D/2-x)/7}, \quad \text{if} \ \ x \le D/2, \ \ \text{then} \ \ x = D/2 \tag{4}$$

$$D = 2\sqrt{A_q/\pi} \tag{5}$$

Where η the shape factor dependent on the floor area, A_{sp}, and the height of the internal space, H, listed in table 2

D the effective diameter of fire source

A_q the area of the fire.

Input each coefficient into Eq.2 and the maximum temperatures can be got as 347℃and 398℃in the scenario A and B respectively, and decrease from the vertical axis as the Eq.4. As large shape coefficient of chords, the temperatures in steel chords is the same as these hot smoke temperature.

Tab. 1 Factor β with fire growth types

	Fire growth type			
	Slow	Medium	Fast	Ulter
β	0.001	0.002	0.003	0.004

Tab.2 Factor η with volumes of large space building

A_{sp} (m²)	H (m)				
	6	9	12	15	20
500	0.60	0.65	0.70	0.80	0.85
1000	0.50	0.55	0.60	0.70	0.75
3000	0.40	0.45	0.50	0.55	0.60
6000	0.25	0.30	0.40	0.45	0.50

4 STRUCTURAL FIRE ANALYSIS

4.1 Loading combination rule

For each load case, design value for the effects of actions shall be determined from accidental combination rule given as[5]

$$S_m = \gamma_{0T}(S_{Gk} + S_{Tk} + \phi_f S_{Qk}) \tag{6}$$

$$S_m = \gamma_{0T}(S_{Gk} + S_{Tk} + \phi_q S_{Qk} + 0.4S_{Wk}) \tag{7}$$

where S_m the design value of the accidental actions

S_{GK}, S_{Tk}, S_{Qk}, S_{Wk} the characteristic value of permanent actions, thermal actions in fire situation, occupational variable actions and wind action respectively

ϕ_f, ϕ_q the frequent and the quasi-permanent coefficient of the occupational variable actions respectively

γ_{0T} the safety coefficient of buildings in fire.

The more serious action between Eq.6 and Eq.7 will be employed.

4.2 Global FE model

The finite element model was developed using commercial software ANSYS to analysis the behavior of the space truss above auditorium during the design fire. Fig. 8 graphically shows a half of globe structure. The material properties assumed in FE model are given in Tab. 3, and the stress-strain curves at elevated temperature was shown in Fig. 9. The supports provide restraint in the horizontal directions and fixed in the vertical direction, but rotationally free. 3D axial elements were used to represent the steel tubes in space truss shown in Fig.10. Each element is associated with its appropriate section properties and material characteristics at elevated temperature. In the meantime the model elements were fully geometrically nonlinear. The temperature distribution as the result of Eq. 4 is loaded on each element node according to the maximum temperature, T_g^{max}, in Eq.2. The heat transfer model of ANSYS software was used to establish the gradient through the longitudinal of the 3D Link8 element in response to Eq.1.
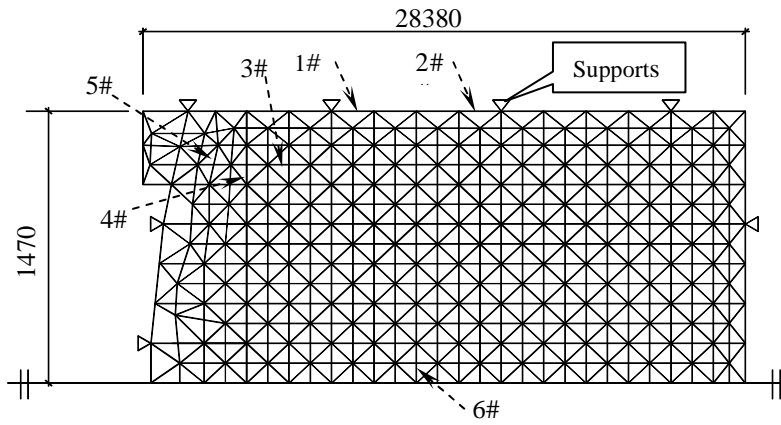
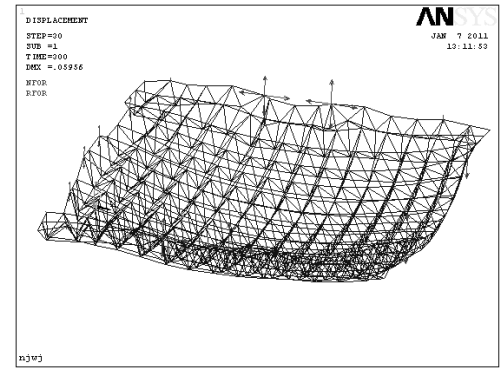Fig.8 The space truss global model

Fig.9 Deformation of FE model

Tab. 3 Material properties at elevated temperature

Parameter Name	symbol	value	unit
Thermal expansion coefficient	α_s	1.4×10^{-5}	m/(m · ℃)
Thermal conductivity	λ_s	45	W/(m· ℃)
Specific heat	c_s	600	J/(kg · ℃)
Density	ρ_s	7850	kg/m^3
Poisson ' s ratio	υ_s	0.3	—
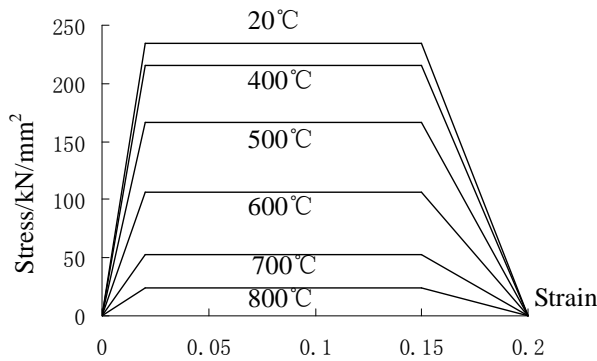
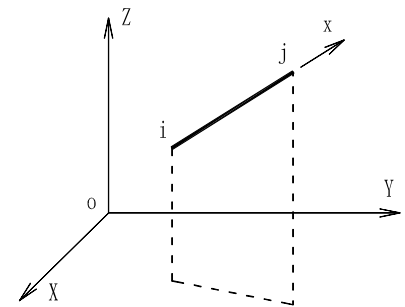Fig.9 Stress-strain relation for steel at elevated temperatures

Fig.10 3D element for FE analysis

4.3 Failure criteria

To assess the result obtained from the FEA, 'failure' rule must be established. At ultimate limit state, stability of the structure would be maintained throughout the design fire. This is primarily assessed by checking in the rate of deflections during the fire. Runway deflections (a rapid increase in the rate of deflection) are assumed to indicate incipient failure of the structure. On the basis of the accidental combination rule, the following verification condition must be satisfied.

$$T_d \leq T_m \tag{8}$$

where T_d the maximum temperature of structures (or elements) subjected to design fire

T_m the critical temperature of structures (or elements) given by structural fire analysis as follow.

4.4. Thermo-mechanical analysis

In Fig. 11, the top chord 1# failed at 90°C for the strong restraint along the longitudinal axis, which connects the support directly, then bottom chord 3# and the web chord 4# failed at 410°C and 520°C respectively, finally the top chord 6# in the midspan of the space truss failed at 770°C. The sharp variations shown as Fig.11 reflect the internal forces redistributed performance as other member

failure, and the compress forces increased due to axial restrain. These thermo-mechanical coupling effects caused the chords failure. When one element lost its loading capacity, high redundant structures can redistribute to other stiffer and stronger elements. In Fig. 12 the greatest downward displacement in the midspan of the space truss increases with the maximum temperature elevated during fire history. At 770°C, the displacement increased rapidly and the global structure lost its loading capacity. The analysis indicated that the critical temperature, 770°C, at accidental load combination is higher than the maximum temperature, 398°C, in structure caused by the design fire scenario B. The space truss covered the auditorium design is fitted to the fire limit state without fire protection measures.
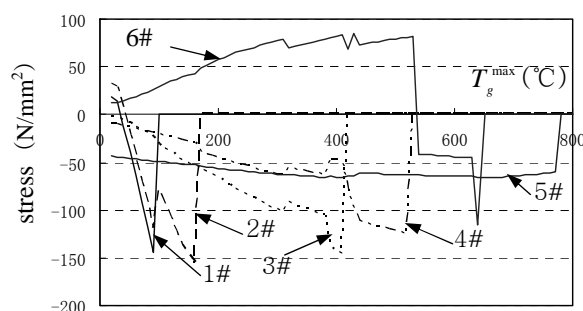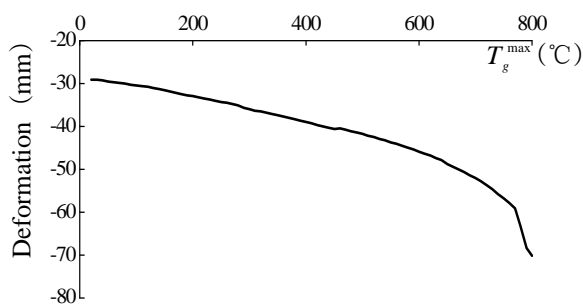

Fig. 11 Stress history curves

Fig.12 The great displacement history curve

5   CONCLUSIONS

This paper provides a snapshot of information and analysis to demonstrate the loading-bearing capacity method is sufficient for fire safety design.

A detailed FEA of the space truss with a credible design fire was carried out to determine the deflections and forces in the space truss.

The performance- based structural fire safety design showed that the space truss above the auditorium can maintain its structural loading capacity without fire protection while the active fire protection is out of work in design fire scenario.

REFERENCES

Li G. Q., Du Y., Analyses the parameters of fire temperature elevation at the top of large space buildings, Fire Science and Technology, 2005, 1, pp.19-21(in chinese)

Du Y., Li G. Q., Fire radiation effect on steel member at elevated temperature in large space fire, Fire Safety Science, 2006, 4, pp.189-199(in chinese)

Du Y., Li G. Q., Utility temperature elevation empirical formula in large space fire, Fire Science and Technology, 2005, 3, pp,283-287(in chinese)

Izzuddin B. A., Song L., Elnashai A. S. and Dowing P. J., An integrated adaptive environment for the fire and explosion analysis of steel frames—Part II: verification and application, Journal of Constructional Steel Research, 2000, 3, pp,87-111.

National Institute of Standards for Engineering, Technical code for fire safety of steel structures in buildings, CECS 200: 2006 China

Kevin B., Grattan M. C., Glenn P. Forney, Kuldeep P., Fire Dynamics Simulator(Version3)— User's Guide, NISTIR 6784,2002 Ed.: 2002 U.S.

RC FRAME EXPOSED TO FIRE AFTER EARTHQUAKE

Ljupco Lazarov [a], Koce Todorov [a], Meri Cvetkovska [a]

[a] University "Ss. Cyril and Methodius", Faculty of Civil Engineering, Skopje, Macedonia

INTRODUCTION

Earthquakes represent an extreme event causing enormous damage to buildings, infrastructure, not to mention a loss of human lives. The occurrence of a fire following an earthquake can understandably produce a disastrous effect. Although ground shaking is the major concern in most earthquakes, subsequent fire could be even more dangerous to urban infrastructure. The post earthquake fire if ignited could grow, intensify, and spread out of control in the neighborhood. Therefore, besides satisfying structural design requirements for normal loads, such as dead and live loads including the seismic hazard, buildings should also be designed to withstand the fire following earthquakes for a certain minimum duration as required for a desired level of performance. Fire resistance requirements for specific building members and structures are provided in building codes. However, much of these criteria are developed for fire exposure under normal conditions without a cumulative damage from preceding earthquake (Iding, 2003, Mousavi at all, 2008).

The behavior of a particular reinforced concrete structure exposed to fire after surviving strong earthquake is presented. The seismic response of the structure was evaluated using a nonlinear static pushover analysis.

1 BASIC THEORY

A computational procedure for nonlinear analysis of reinforced concrete frame subjected to fire loading exposed to different fire models is analyzed. For that purpose the program FIRE (Cvetkovska, 2002) is used. A coupled thermal - structural analysis approach is implemented in the program. In each time step, the fire behavior of a structural member is estimated using a complex, coupled heat transfer - strain equilibrium analysis, based on theoretical heat transfer and structural mechanics principles. The analysis is performed in three sub steps within each time step: namely, calculation of fire temperatures to which the structural members are exposed, calculation of temperatures in the structural members, and calculation of resulting deflections and internal forces including an analysis of the stress and strain distribution. The program FIRE carries out the nonlinear transient heat flow analysis (modulus FIRE-T) and nonlinear stress-strain response associated with fire (modulus FIRE-S) (Iding at all, 1977).
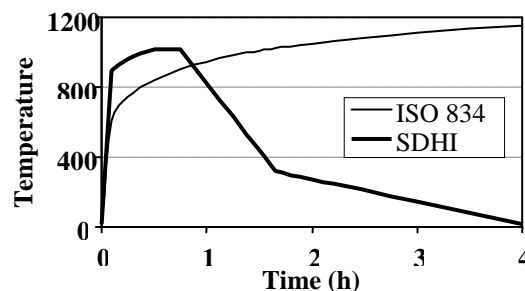

Fig. 1 ISO 834 and SDHI fire models

The solution technique used in FIRE is a finite element method coupled with time step integration. The computer modulus FIRE-T solves the governing differential equation of heat transfer in conduction and in that purpose the following assumptions are made: a fire can be modeled by a single valued gas temperature history: ASTM E119, ISO 834 or SDHI (short duration, high

intensity) fire model, Fig. 1; no contact resistance to heat transmission at the interface between the reinforcing steel and concrete occurs; the fire boundary conditions can be modeled in terms of both convective and radiating heat transfer mechanisms; the temperature dependant material properties are known (recommended in Eurocode 2, part 1.2); while cracks appear, or same parts of the element crush, the heat penetrates in the cross section easier, but in this study it is neglected. It has been assumed that the heat flow is separable from the structural analysis. The response of a reinforced concrete elements and plane frame structures exposed to fire is predicted by modulus FIRE-S. This modulus accounts for: dimensional changes caused by temperature differences, changes in mechanical properties of materials with changes in temperature, degradation of sections by cracking and/or crushing and acceleration of shrinkage and creep with an increase of temperature. To define the fire response of reinforced concrete structure is thus a complex nonlinear analysis problem in which the strength and stiffness of a structure as well as internal forces continually change due to restraints imposed by the structural system on free thermal expansion, shrinkage, or creep. Pushover analysis, representing dynamic effects of an earthquake via static nonlinear procedure, is incorporated in the program as an option that precedes the post earthquake fire analysis.

2   NUMERICAL EXAMPLE – CASE STUDY

2.1 Structural Geometry and Material Characteristics

The object of the numerical analysis is a two-story three bay planar reinforced concrete frame structure. Frame geometry, element cross-sections and reinforcement of all cross sections are schematically presented in Fig. 2. Concrete compressive strength is f=30MPa, reinforcement yield strength is f_y=400MPa. Structure self weight is included in the permanent and live loads, applied on beams as cumulate uniformly distributed, q=45kN/m'. Total weight of the structure is W=2x(45.0x15.0)=1350kN. The reinforcement of beam cross sections is taken in such a way that the stresses in steel bars due to nominal load q are approximately 60% of the yield strength. The percentage of column reinforcement is taken to be 1%.
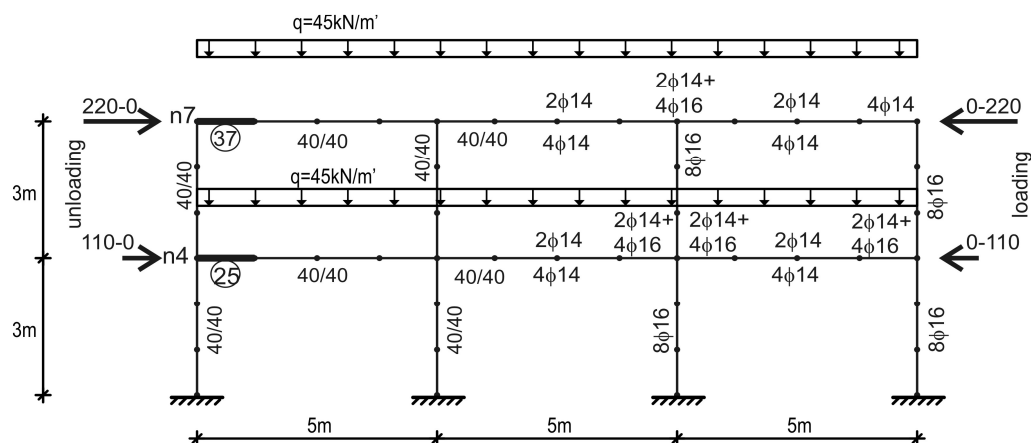

Fig. 2 Geometry and loading

2.2 Description of Analysis Cases

Thirteen different loading cases have been analyzed:
1. Gravity load (q=45kN/m'), (abbreviated as "g" in figures and tables)
2. Gravity load + ISO fire scenario 1
3. Gravity load + SDHI fire scenario 1
4. Gravity load + ISO fire scenario 2
5. Gravity load + SDHI fire scenario 2

6. Gravity load + Pushover (loading + unloading) + ISO fire scenario 1
7. Gravity load + Pushover (loading + unloading) + SDHI fire scenario 1
8. Gravity load + Pushover (loading + unloading) + ISO fire scenario 2
9. Gravity load + Pushover (loading + unloading) + SDHI fire scenario 2
10. Gravity+Pushover (loading+ unloading +opposite loading+ unloading) + ISO fire scenario 1
11. Gravity+Pushover (loading+unloading+opposite loading+ unloading)+ SDHI fire scenario 1
12. Gravity+Pushover (loading+unloading +opposite loading+ unloading)+ ISO fire scenario 2
13. Gravity+Pushover (loading+unloading +opposite loading+ unloading)+SDHI fire scenario 2

Fire scenario 1 assumes fire in the first story left compartment and fire scenario 2 assumes fire in the second story left compartment of the frame. In the pushover analysis a triangular load distribution in horizontal direction is applied, Fig. 2. In loading case 6 up to loading case 9, the horizontal forces are incrementally increased from 0 to 220kN on the second floor and from 0 to 110kN on the first floor pushing the rightmost floor nodes of the structure (applied in direction from right to left).

2.3 Results of Analysis Cases

The value for the base shear of 330kN (220kN + 110kN) corresponds to 0.244W and is chosen in such a way that the structure is pushed into nonlinear range and rather large number of plastic hinges are formed. Total base shear has been reached corresponding to top story horizontal displacement of 4.23cm, Fig. 3*a*. Once the loading phase up to corresponding base shear of 330kN is completed, unloading phase takes place. After unloading the corresponding residual plastic displacement at node 7 was 1.09cm, Fig. 3*b*.
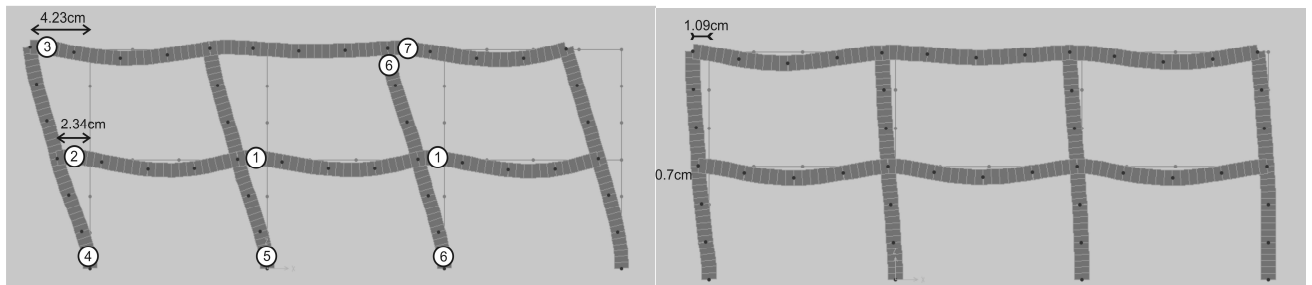

Fig. 3 *a)* Sequence of plastic hinges formation and horizontal displacements due to pushover
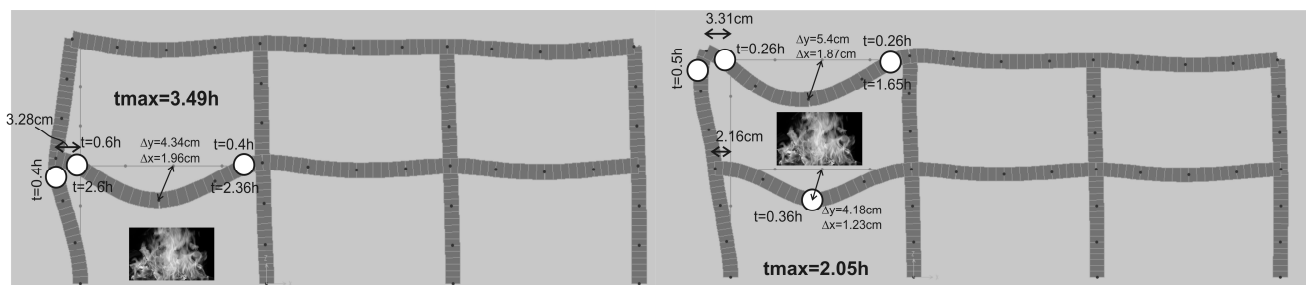*b)* Residual displacements after pushover

Fig. 4 *a)*L. case 6, sequence of hinges due to fire, *b)*L. case 8, sequence of hinges due to fire

To accomplish loading cases 6 to 9, after unloading the structure is exposed to two different fire scenarios for two different fire load models. In loading case 10 up to loading case 13, the horizontal forces are applied to the structure that is already plastically deformed in the previous cycle of pushover analysis and are incrementally increased from 0 to 220kN on the second floor and from 0 to 110kN on the first floor, pushing the leftmost floor nodes (node 7 and node 4) of the structure (applied in direction from left to right). Again, to accomplish loading cases 10 to 13, after unloading the structure from total base shear of 330kN in the opposite direction, the frame is exposed to two different fire scenarios for two different fire load models. Some of the obtained results are graphically presented.

Base shear-displacement relations from loading case 10 for nodes 7 and 4, due to ISO fire scenario 1, are presented in Fig. 5. Loading, unloading, loading in opposite direction and unloading from opposite direction are assigned as: L1PO, UL1PO, L2PO and UL2PO consequently. The sequence of formation of plastic hinges on Fig. 3*a* are shown on the L1PO branches of Fig. 5. Additional results for displacements of nodes: 4, 7, 9 and 12 for characteristic moments of the analysis in fire scenario 1 or 2 and for fire models ISO and SDHI, are presented in Tab. 1, Tab. 2 and Tab. 3.
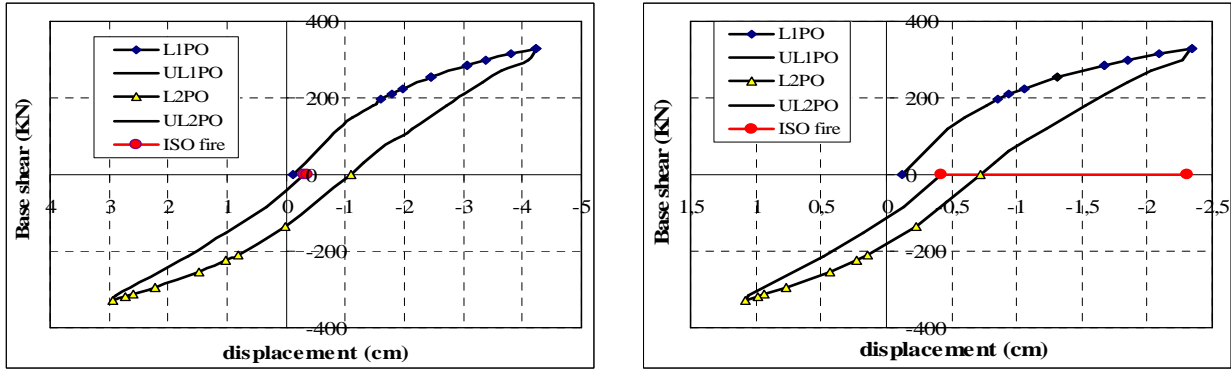

Fig. 5 Base shear-displacement relations for nodes 7 and 4, due to ISO fire scenario 1

Tab. 1 Fire scenario 1

node	Displac. (cm)	only "g" and fire action				"g"+ seismic action + fire action					
		g	g+ISO t=3.3h	g+SDHI		g	g+LPO	residual displac.	residual + ISO t=3.49h	resid.+SDHI	
				t=1.1h	t=5h					t=1.1h	t=5h
4	Δx	-0.12	-2.85	-1.83	-1.08	-0.12	-2.34	-0.72	-3.28	-2.23	-1.49
7	Δx	-0.13	-0.27	-0.20	-0.19	-0.13	-4.23	-1.09	-1.12	-1.03	-1.01
9	Δy	-0.43	-4.14	-1.27	-1.61	-0.43	-0.64	-0.78	-4.34	-1.45	-1.78

Tab. 2 Fire scenario 2

node	Displac. (cm)	only "g" and fire action				"g"+ seismic action + fire action					
		g	g+ISO t=2.0h	g+SDHI		g	g+LPO	residual displac.	residual + ISO t=2.0h	resid.+SDHI	
				t=1.1h	t=5h					t=1.1h	t=5h
4	Δx	-0.12	-1.62	-1.22	-0.70	-0.12	-2.34	-0.72	-2.16	-1.79	-1.27
7	Δx	-0.13	-2.62	-1.98	-1.89	-0.13	-4.23	-1.09	-3.31	-2.67	-2.25
9	Δy	-0.43	-3.67	-2.68	-1.53	-0.43	-0.64	-0.78	-4.18	-3.23	-2.46
12	Δy	-0.56	-5.34	-3.29	-4.26	-0.56	-0.59	-0.73	-5.41	-3.27	-4.29

Tab. 3 Fire scenario 1 and 2

node	Displac. (cm)	"g"+ seismic action in two directions+ fire action						
		g	g+L1PO	residual displac.1	g+L2PO	residual displac.2	residual + **fire 1** t=3.54h	residual + **fire 2** t=2.43h
4	Δx	-0.12	-2.34	-0.72	+1.12	-0.42	-2.31	-1.60
7	Δx	-0.13	-4.23	-1.09	+3.05	-0.30	-0.36	-1.55
9	Δy	-0.43	-0.64	-0.78	-0.87	-0.96	-3.70	-4.20

As expected, residual horizontal displacements of nodes 4 and 7 as well as the residual vertical displacements of nodes 9 and 12, are slightly higher when fire action is applied after pushover, then in the case when no seismic action was applied. This trend is observed in both fire scenarios and both fire models. Interesting results are obtained for the capacity of this reinforced concrete structure to sustain fire load. Namely, the duration of time that the structure survived the ISO fire after a pushover episode was higher then the duration of time that the structure survived the ISO fire without a seismic action in fire scenario 1, 3.49 hours against 3.3 hours (loading case 6). In fire scenario 2 the duration of time, for both cases, was almost equal, t=2.0 hours (loading case 8). That

was even more emphasized in loading cases 10 and 12, when a full cycle (loading, unloading, loading in opposite direction and unloading from opposite direction) was completed, Tab. 3.
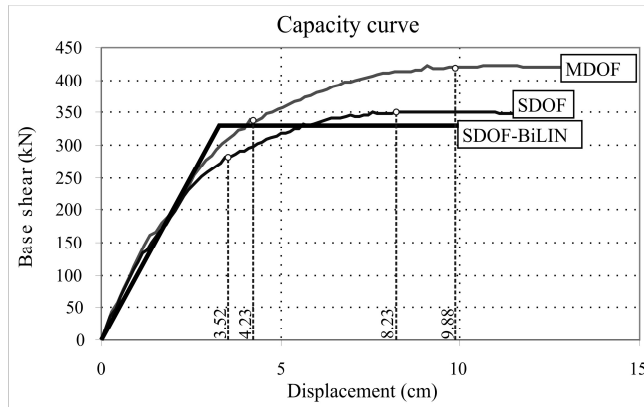

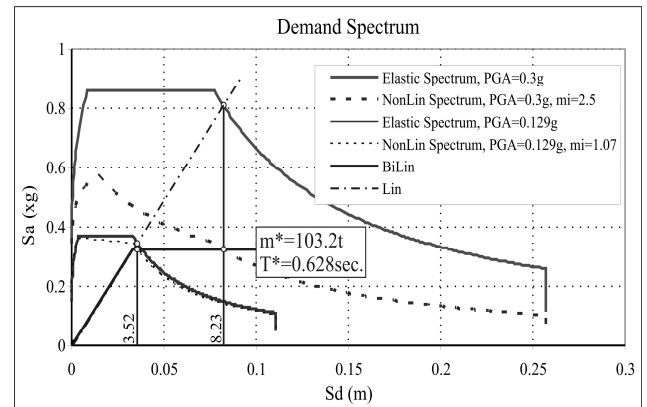Fig. 6 Pushover curve – capacity curve

Fig. 7 Elastic and demand spectra

The reinforcement of the RC frame cross sections is defined from criteria that do not take into acount seismic provisions. In order to see what is the seismic capacity of the structure and to what level of seismic demand corresponds the assumed base shear of 330kN, the N2 method was implemented (Fajfar, 2000). Final results of capacity-demand calculations are graphicaly presented in Fig. 6 and Fig. 7. Base shear of 330kN and the obtained displacement of 4.23cm at node 7 corresponds to elastic demand spectrum for PGA=0.129g. By inverse procedure, it was found that this RC frame has capacity (base shear of 420kN and target displacement of 9.88cm) to sustain elastic demand spectrum for PGA=0.3g. All loading cases were reapplied such that the horizontal forces were increased up to a base shear of 393kN (corresponding approximatelly to 94% of frame's capacity). Due to limited space only few results for displacements for nodes 4 and 7 are listed. For base shear=393kN, Δ_{x4}=4.19cm, Δ_{x7}=7.31cm. For base shear=0kN (unloading), Δ_{x4}=1.98cm, Δ_{x7}=3.04cm (residual displacements). It is worth mentioning also, that increased resistance in case of fire scenario 1 was observed. The structure has sustained fire load after earthquake in duration t=3.76 hours.
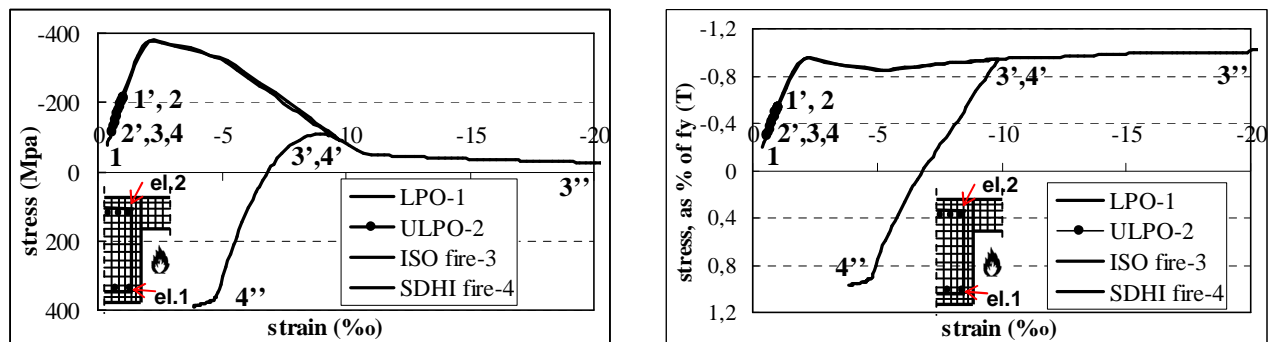

Fig. 8 Bottom bar, Node 4, fire scenario 1

Stress-strain hystories for reinforsing bars in beam cross sections of nodes 4 and 7 for applied loading cases are presented in Fig. 8 thru Fig. 11. The interpretation of the numbers next to particular stress-strain curve is such that, for example on Fig. 8 the stress-strain hystory for ISO fire-3 starts at point 3, continues thru point 3' and finishes at point3''. Also, the stress-strain relation for some reinforcement bars is doubly presented, as for example bottom bar, Node 4, fire scenario 1 on Fig. 8. The left graph presents real stress-strain relations during time history of loading and on the right graph stresses are normalized as percentage values of the reduced yield stress due to elevated temperature, $f_y(T)$.
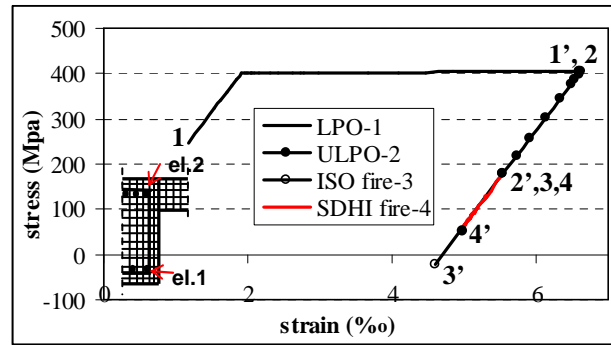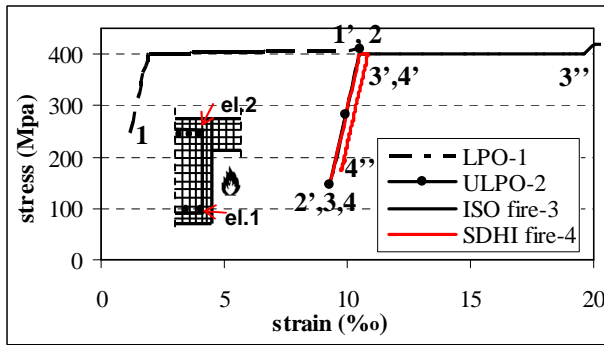
Fig. 9 *a)*Top bar, Node 4, fire scenario 1,   *b)*Top bar, Node 7, fire scenario 1
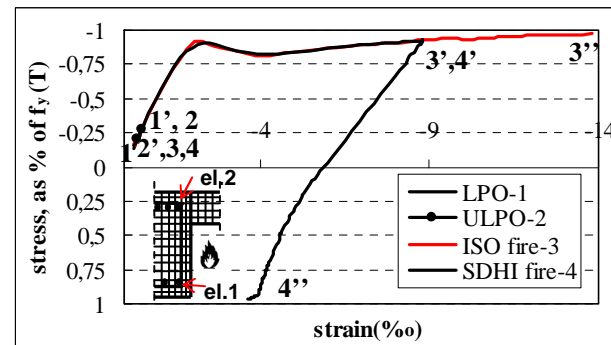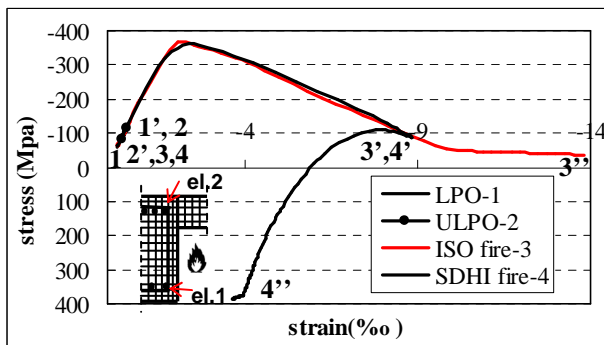

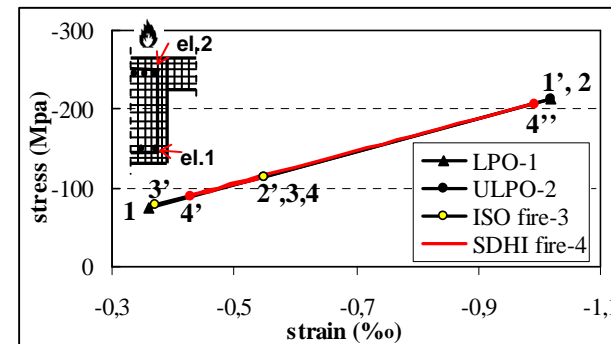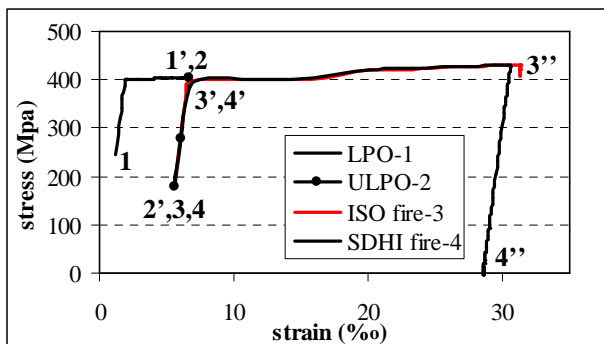Fig. 10 Bottom bar, Node 7, fire scenario 2

Fig. 11 *a)*Top bar, Node 7, fire scenario 2 ,   *b)*Bottom bar, Node 4, fire scenario 2

REFERENCES

EUROCODE 2,"Design of Concrete Structures, Part 1-2: General rules - Structural Fire Design", CEN - European Committee for Standardization, 2004.

Cvetkovska M. "Nonlinear stress strain behaviour of RC elements and RC frames exposed to fire", Phd. thesis, University St.Cyril and Methodius, Skopje, 2002 (in Macedonian).

Fajfar P., "A nonlinear analysis method for performance-based seismic design", Earthquake Spectra, 2000, 16(3): 573-92.

Iding R., Bresler B. and Nizamuddin Z.,"FIRES-RC II-A Computer Program for The Fire Response of Structures-Reinforced Concrete Frames", Report no.UCB FRG 77/8, Structural Engineering and Structural Mechanics, department of Civil Engineering, University of California, Berkeley, California 1977.

Iding R., "Calculating Structural Response to Fire", Fire Protection Engineering, 2003.

Mousavi S., Bagchi A., Kodur V., "Review of post-earthquake fire hazard to building structures", Canadian Journal of Civil Engineering, Jul. 2008.